Sede Amministrativa: Università degli Studi di Padova

Dipartimento di Biologia

SCUOLA DI DOTTORATO DI RICERCA IN BIOSCIENZE E BIOTECNOLOGIE

INDIRIZZO BIOLOGIA CELLULARE

CICLO XXVI

THE ROLE OF MITOCHONDRIA IN SHAPING THE ONCOGENIC SIGNALING

Direttore della Scuola: Ch.mo Prof. Giuseppe Zanotti

Coordinatore d'indirizzo: Ch.mo Prof. Paolo Bernardi

Supervisore: Ch.mo Prof. Paolo Bernardi

Co-supervisore: Dr. Andrea Rasola

Dottoranda: Ionica Masgras

Dicembre 2013

TABLE OF CONTENTS

ABBREVIATIONS

BSA	bovine serum albumin
CsA	cyclosporine A
CyP-D	Cyclophilin D
DMEM	Dulbecco's modified Eagle's medium
ERK	extracellular signal regulated kinase
ETC	electron transport chain
FH	fumarate hydratase
GAP	GTPase-activating protein
GRD	GAP related domain
GSK	glycogen synthase kinase
HIF	hypoxia-inducible factor
HK	hexokinase
IDH	isocitrate dehydrogenase
IMM	inner mitochondrial membrane
LOH	loss of heterozygosity
MEK	mitogen-activated protein kinase
mtDNA	mitochondrial DNA
NAC	*N*-acetyl-L-alanine
NAO	nonyl acridine orange
NF1	Neurofibromatosis type 1
OMM	outer mitochondrial membrane
OXPHOS	oxidative phosphorylation
PAGE	polyacrylamide gel electrophoresis
PBS	phosphate-buffered saline
PI	propidium iodide
PTP	permeability transition pore

RC	respiratory chain
ROS	reactive oxygen species
SDH	succinate dehydrogenase
SDS	sodium dodecyl sulphate
TCA	tricarboxylic acid
TMRM	tetramethylrhodamine methyl ester
TRAP1	tumor necrosis factor receptor-associated protein-1

Summary

Cancer cells are endowed with the capability to reprogram cell metabolism in order to support neoplastic growth and cell death escape. A key role in this process is played by signaling pathways, mainly cascades regulated by kinases. Integration of survival and death stimuli occurs on mitochondria, where many of these signals converge to the regulation of a channel, the permeability transition pore (PTP), that triggers mitochondrial depolarization and release of pro-apoptotic factors from mitochondria. PTP opening commits cells to death, and it is regulated by a variety of factors. Here I have studied how signal transduction pathways affect cell metabolism, particularly mitochondrial bioenergetics, which could eventually lead to modulation of PTP opening.

In the first part of my work, I have explored the presence of the PTP in cells depleted of mitochondrial DNA (ρ^0 cells) which lack respiration and constitute a model for the analysis of mitochondrial involvement in several pathological conditions, among which cancer. I have observed that these cells are indeed equipped with a functioning PTP, whose regulatory mechanisms are similar to those observed in cancer cells. In detail, inhibition of PTP opening is a survival mechanism achieved by two different mechanisms: the first one is the mitochondrial binding of the glycolytic enzyme hexokinase (HK) II, which is up-regulated in ρ^0 cells; the second one relies on the hyper-activation of the ERK-GSK3 signaling pathway that converge on mitochondria where it maintains the PTP regulator cyclophilin D (CyP-D) in the dephosphorylated form. I observed that mitochondria of ρ^0 cells maintain a membrane potential which is readily dissipated after displacement of HK II from the mitochondrial surface by treatment with either the drug clotrimazole or with a cell-permeant HK II peptide, or by keeping ρ^0 cells in serum and glucose starvation. The PTP inhibitor cyclosporin A (CsA) is able to decrease the mitochondrial depolarization induced by either HK II displacement or by nutrient depletion. Moreover, glucose and serum deprivation causes concomitant ERK1/2 inhibition and GSK3α/β activation with the ensuing phosphorylation of CyP-D and PTP opening. Indeed, GSK3α/β inhibition with indirubin-3'-oxime decreases PTP-induced cell death in ρ^0 cells following nutrient ablation.

In the second part of my work, I have focused my attention on a tumor predisposition syndrome, called Neurofibromatosis type 1 (NF1), caused by loss of function of neurofibromin, which acts as a negative regulator of the Ras signaling cascades. Here I have investigated whether the Ras hyper-activation induced by neurofibromin ablation can affect mitochondria bioenergetics, thus contributing to the metabolic rewiring of NF1 tumors. I observed that the absence of neurofibromin confers to mouse embryonic fibroblasts (MEFs) the capability to form colonies in an *in vitro* tumorigenesis assay, and that the use of an ERK inhibitor completely abrogates colony formation. Moreover, I injected wild-type and *Nf1*$^{-/-}$ MEFs subcutaneously into nude mice in order to test the capability of the cells to form tumors *in vivo*. I observed that the absence of *Nf1* leads to the growth of a tumor mass within a month, whereas no tumor can be formed in the same time frame by wild-type MEFs. I started the analysis of mitochondrial bioenergetics by measurements of oxygen consumption rate (OCR) performed with an extracellular flux analyzer on adherent cell monolayers. *Nf1*$^{-/-}$ MEFs display a lower OCR than wild-type MEFs both in basal condition and upon treatment with a low concentration of an uncoupler, which stimulates respiration maximally. Moreover, I found that the fraction of oxygen consumption coupled to ATP production by mitochondrial ATP synthase is lower in cells without *Nf1*, suggesting that ATP requirements are mainly supplied by glycolysis. Accordingly, upon glucose starvation or inhibition of glycolysis with 5-thioglucose *Nf1*$^{-/-}$ cells display a stronger decrease in ATP levels compared to wild-type cells. The different OCRs between wild-type and *Nf1*$^{-/-}$ cells are not related to differences in mitochondrial mass or membrane potential.

In order to establish whether a modulation of respiratory chain activity could account for the observed OCR differences, I analyzed the expression level of the respiratory chain complexes. Complex I (NADH dehydrogenase) is down-regulated by *Nf1* ablation, as a lower level of some of its subunits and of the assembled complex I was detected. Furthermore, the enzymatic activity of complex I is expectedly lower in *Nf1*$^{-/-}$ cells. Interestingly, administration of an ERK inhibitor increases the expression of complex I subunits resulting in its augmented assembly and activity; remarkably, this effect is more pronounced in *Nf1*$^{-/-}$ MEFs than in wild-type cells.

I also observed down-regulation of complex II (succinate dehydrogenase) activity in knock-out cells compared to wild-type MEFs. Interestingly, I found that complex II interacts with the mitochondrial chaperone TRAP1 and the kinase ERK, a fraction of which is mitochondrial; these interactions are stronger in *Nf1*$^{-/-}$ than in wild-type cells, as assessed by blue native gel analysis. However, silencing of TRAP1 does not change the activity of complex II; in accordance to this, the OCR of cells in which TRAP1 has been down-regulated does not vary, yet modulation of TRAP1 levels affects maximal respiration of *Nf1*$^{-/-}$ cells. Interestingly, silencing of TRAP1 in *Nf1*-deficient MEFs compromises the tumorigenic properties of these cells.

Taken together, these observations suggest that the absence of neurofibromin leads to a more glycolytic metabolism by down-modulating the activity of respiratory chain complexes. The metabolic switch observed upon *Nf1* deletion is a typical marker of cancer cells that favors tumor progression. We hypothesize that Ras-ERK signaling is upstream to the regulation of mitochondrial bioenergetics, and that the metabolic changes prompted by Ras-ERK activation can contribute to the transformed phenotype that we observe in *Nf1*$^{-/-}$ MEFs.

Sommario

Le cellule tumorali hanno la capacità di riprogrammare il metabolismo al fine di sostenere la crescita cellulare e di sfuggire ai segnali di morte. Un ruolo centrale in questo processo è a carico delle vie di segnale, principalmente regolate da chinasi. L'integrazione degli stimoli di morte e di sopravvivenza avviene nei mitocondri, dove molti di questi segnali convergono sulla regolazione di un canale, il poro di transizione di permeabilità (PTP), che è responsabile della depolarizzazione mitocondriale con il conseguente rilascio di fattori pro-apoptotici dall'organello. L'apertura del PTP porta le cellule alla morte ed è regolato da un'ampia varietà di fattori. In questo lavoro ho studiato come i meccanismi di trasduzione del segnale impattano sul metabolismo cellulare, in particolare sulla bioenergetica mitocondriale, giungendo quindi ad una modulazione dell'apertura del PTP.

Nella prima parte del mio lavoro ho indagato la presenza del PTP in cellule depletate del DNA mitocondriale (cellule ρ^0) che presentano una totale assenza della respirazione e costituiscono un buon modello per l'analisi del coinvolgimento dei mitocondri in molte condizioni patologiche tra cui il cancro. Ho osservato che queste cellule possiedono un PTP funzionale, i cui meccanismi di regolazione sono simili a quelli presenti nelle cellule tumorali. Nel dettaglio, l'inibizione dell'apertura del PTP è un meccanismo di sopravvivenza raggiunto attraverso due meccanismi: il primo riguarda la localizzazione mitocondriale dell'enzima glicolitico esochinasi (HK) II, che è over-espresso nelle cellule ρ^0; il secondo meccanismo è basato sull'iper-attivazione della via di segnale ERK-GSK3 che converge sui mitocondri dove mantiene il regolatore del poro, la ciclofilina D (CyP-D), nello stato defosforilato e quindi inattivo. Ho osservato che i mitocondri delle cellule ρ^0 mantengono un potenziale di membrane che è dissipato in seguito alla dislocazione del HK II dalla superficie mitocondriale attraverso trattamento con clotrimazolo o tramite l'uso di un peptide che permea le membrane, o, in alternativa, a seguito di deplezione di siero e glucosio. L'inibitore del poro, la ciclosporina A (CsA), è in grado di diminuire la depolarizzazione mitocondriale indotta dalla dislocazione del HK II o dalla deplezione di nutrienti. Inoltre, la deplezione di siero e glucosio causa una concomitante inibizione di ERK1/2, un'attivazione di GSK3α/β e una conseguente fosforilazione di CyP-D con

apertura del PTP. Infatti, inibendo GSK3α/β con l'indirubina, la morte cellulare causata dall'apertura del poro in seguito a deprivazione di nutrienti è diminuita.

Nella seconda parte del mio lavoro mi sono focalizzata su una sindrome che predispone i pazienti all'insorgenza di tumori, la Neurofibromatosi di tipo 1, causata da perdita di funzione della neurofibromina, un regolatore negativo della via di segnale dominata da Ras. Ho studiato la possibilità che l'iper-attivazione della via di Ras dovuta all'inattivazione della neurofibromina possa modificare la bioenergetica mitocondriale, contribuendo così a cambiamenti metabolici in tumori di pazienti con NF1. Ho osservato che l'assenza della neurofibromina in fibroblasti embrionali di topo (MEFs) conferisce la capacità di formare colonie in un saggio tumorigenico *in vitro*, mentre il trattamento con un inibitore di ERK inibisce la formazione delle colonie in modo significativo. Inoltre, ho iniettato queste cellule sotto cute in topi nudi al fine di testare il loro potenziale tumorigenico *in vivo*. Ho osservato che l'assenza di neurofibromina porta alla crescita di una massa tumorale nell'arco di un mese dall'iniezione, mentre non si osservano masse tumorali nel caso di cellule wild-type. Ho iniziato l'analisi del profilo bioenergetico mitocondriale misurando il consumo di ossigeno in cellule adese ed ho osservato che cellule senza neurofibromina presentano un diminuito tasso di respirazione basale, oltre che una minore respirazione massima raggiunta dopo trattamento con basse concentrazioni di un disaccoppiante. Inoltre, la frazione di respirazione accoppiata alla produzione di ATP da parte dell'ATP sintasi è minore nelle cellule senza neurofibromina, suggerendo che le richieste energetiche sono principalmente a carico della glicolisi. In accordo a questi dati, in seguito a deplezione di glucosio o all'inibizione della glicolisi con 5-tioglucosio le cellule assenti della neurofibromina presentano un maggiore calo nei livelli di ATP rispetto a cellule wild-type. Le differenze del consumo di ossigeno, inoltre, non sono dovute a cambiamenti nella massa mitocondriale o nel potenziale di membrana.

Al fine di determinare se possibili differenze nell'attività della catena respiratoria siano la causa di una diversa respirazione, ho analizzato l'espressione proteica di diverse subunità dei complessi respiratori. Il complesso I (NADH deidrogenasi) è diminuito in seguito alla deplezione della neurofibromina, così come la sua attività. Inoltre, la repressione farmacologica di ERK in cellule knock-out è in grado di aumentare specificatamente

l’espressione delle subunità del complesso I, e quindi la sua attività; al contrario, questo effetto è meno forte nelle cellule wild-type.

Ho osservato anche una diminuita attività del complesso II (succinato deidrogenasi) nelle cellule knock-out. Inoltre, ho trovato un’interazione tra il complesso II, lo sciaperone mitocondriale TRAP1 e la chinasi ERK, una frazione della quale è stata trovata nei mitocondri; queste interazioni sono molto più forti nelle cellule knock-out rispetto a quelle wild-type. Tuttavia, il silenziamento di TRAP1 non causa una variazione dell’attività del complesso II, bensì un’aumentata respirazione massima nelle cellule senza neurofibromina. Inoltre, la diminuita espressione di TRAP1 causa la perdita del potenziale tumorigenico delle cellule knock-out.

Questi risultati suggeriscono che l’assenza della neurofibromina porta ad un fenotipo glicolitico con una diminuzione della respirazione mitocondriale. Questo cambiamento metabolico è tipico delle cellule tumorali poiché favorisce la progressione tumorale. Abbiamo quindi ipotetizzato che i cambiamenti metabolici causati dall’iper-attivazione della via di segnale Ras-ERK possano contribuire al fenotipo trasformante che abbiamo osservato nelle cellule senza neurofibromina.

1.INTRODUCTION

1.1. The hallmarks of cancer

Cancer cells are characterized by changes in a variety of intrinsic biological processes and in environmental interactions that lead to loss of tissue homeostasis. In 2000 it has been proposed that six essential alterations in cell physiology collectively dictate malignant growth of most and perhaps all types of cancers (Hanahan and Weinberg, 2000): self-sufficiency in growth signals, insensitivity to growth-inhibitory (anti-growth) signals, evasion of programmed cell death (apoptosis), limitless replicative potential, sustained angiogenesis, and tissue invasion and metastasis (Fig. 1). Each of these physiologic changes represents the successful breaching of an anticancer defense mechanism. Indeed, cancer development requires complex heterotypic interactions among neoplastic cells and several other cell types in the tumor microenvironment which act as active participants rather than passive bystanders in tumorigenesis.

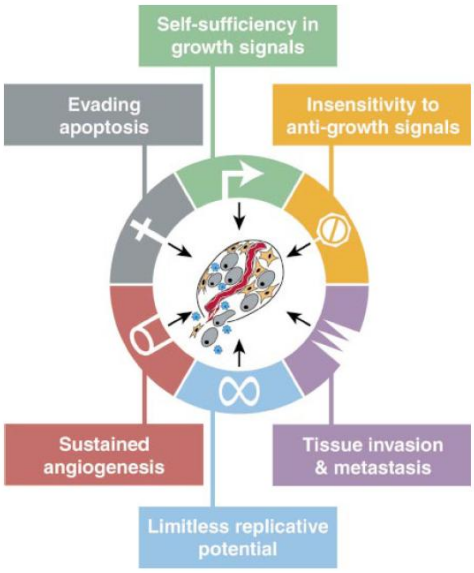

Figure 1. The Hallmarks of Cancer. This illustration was originally proposed in 2000 by Hanahan and Weinberg and encompasses the six hallmark capabilities of cancer cells (Hanahan and Weinberg, 2000).

Conceptual progress in the last decade has added two emerging hallmarks of potential generality to this list (Hanahan and Weinberg, 2011). One involves the capability to modify, or reprogram, cellular metabolism in order to most effectively support neoplastic proliferation. The second allows cancer cells to evade immunological destruction; this feature highlights the dichotomous roles of an immune system that might both antagonize and enhance tumor development and progression (Fig. 2). Additionally, two consequential characteristics of neoplasia facilitate acquisition of both core and emerging hallmarks. Genomic instability and thus mutability endows

cancer cells with genetic alterations that drive tumor progression. Inflammation by innate immune cells designed to fight infections and heal wounds can instead result in their inadvertent support of multiple hallmark capabilities, thereby manifesting the now widely appreciated tumor-promoting consequences of inflammatory responses.

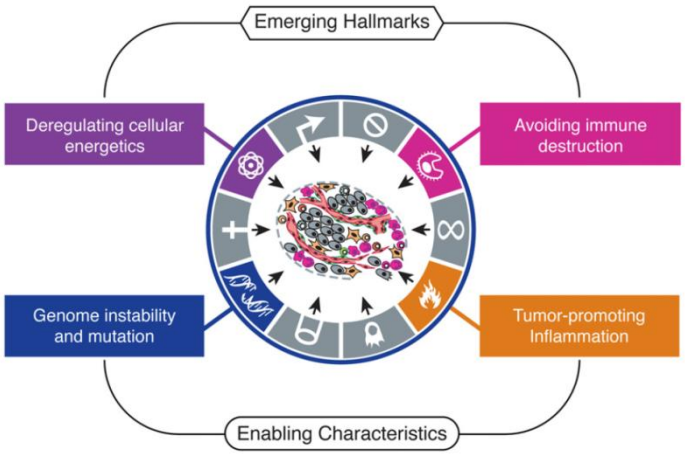

Figure 2. Emerging Hallmarks and Enabling Characteristics. Two additional hallmarks of cancer are involved in the pathogenesis of some and perhaps all cancers: reprogramming of energy metabolism and evading immune destruction. Genomic instability and tumor-promoting inflammation work as enabling characteristics for the acquisition of the hallmark properties of cancer cells (Hanahan and Weinberg, 2011).

Even though these features of cancer cells are depicted as distinct properties which can be acquired at different time points of the tumorigenic process, they are finely inter-regulated and the alteration of one of these physiological changes is able to strongly impact on the others. It follows that the boundary line between one property and the other is very labile, adding further complexity to the system.

1.2. Tumor metabolism

Tumor cells have a remarkably different metabolism from that of the tissues which they are derived from. Indeed, the metabolism of neoplastic cells must sustain higher proliferative rates and resist oxygen paucity found in the inner tumor mass; at the same time, neoplasms are continuously exposed to oxidative insults (Tennant et al., 2009).

Last century, Otto Warburg made pioneering and substantial contributions to our early understanding of cancer metabolism. He measured oxygen consumption and lactate production in tumor slices, either in the presence or absence of oxygen, finding that rapidly growing tumor cells consumed glucose at a surprisingly high rate compared to normal cells in the presence of oxygen, and most of the glucose-derived carbon was

secreted by neoplasms in the form of lactate (Warburg et al., 1927). Warburg later postulated that this phenomenon, termed '**aerobic glycolysis**', was provoked by mitochondrial impairment and was the origin of cancer cell transformation (WARBURG, 1956a; WARBURG, 1956b) promoting the erroneous idea that damaged respiration is the *sine qua non* for neoplastic transformation. Several further metabolic alterations and adaptations of cancer cells have been discovered in the following decades (Fig. 3) (Tennant et al., 2010). Nonetheless, starting from the seventies of last century, the oncogene revolution, *i.e.* the discovery of genes whose mutations could prompt tumorigenesis (Hunter, 1997; Knudson, 2002), pushed tumor metabolism to the margins of cancer research. Warburg's observations were almost forgotten for a long period, and the metabolic alterations of tumors were simply considered an epiphenomenon of changes elicited in the neoplastic cells by mutations in oncogenes and tumor suppressor genes.

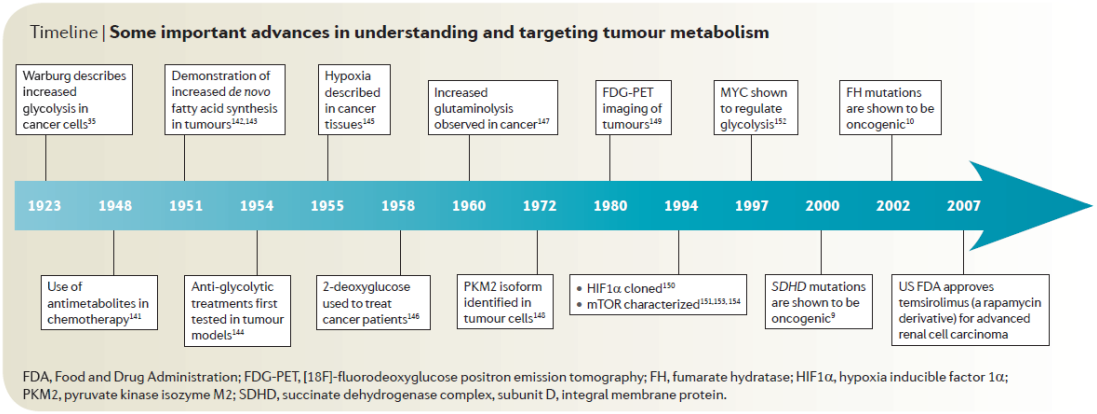

Figure 3. Timeline indicating some important advances in understanding and targeting tumor metabolism (Tennant et al., 2010).

In the same period, Crabtree observed that increased glucose availability boosts glycolysis in cancer and normal proliferating cells, while inhibiting respiration, an observation now known as the '**Crabtree effect**' (Crabtree, 1928). He further suggested that this observation is sufficient to explain the decrease in oxidative phosphorylation (OXPHOS)-derived ATP in cancer, which argues against Warburg's initial hypothesis that defects in respiration are the cause for increased glycolysis. Years later it was suggested that respiration inhibition by glycolysis was caused by glycolysis competing with OXPHOS for phosphate and ADP. However, the Crabtree effect does not provide an explanation for

the actual cause of the observed increased aerobic glycolysis in cancer (Frezza and Gottlieb, 2009).

Subsequent work showed that mitochondrial function is not impaired in most cancer cells, suggesting that the shift towards glycolysis during neoplastic transformation occurs as a consequence of regulatory mechanisms.

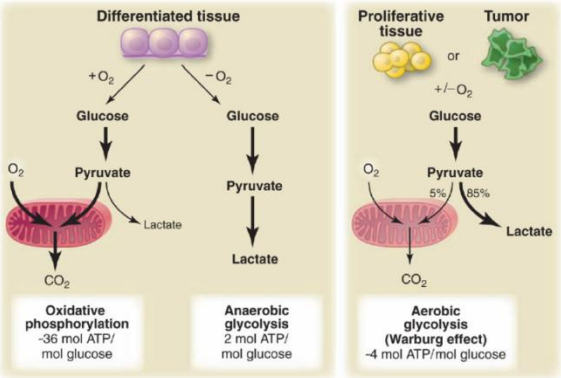

Figure 4. ATP yield of OXPHOS, anaerobic glycolysis and aerobic glycolysis (Warburg Effect) (Vander Heiden et al., 2009).

We still do not understand exactly what is the advantage obtained by tumor cells in moving their metabolic demand towards glucose usage (Fig. 4). In many cancer cells, bioenergetic reprogramming involves switching from the maximal ATP production by OXPHOS in quiescent or differentiated cells to the requirement for balancing energy needs with substrate generation for cellular biogenesis and reproduction in rapidly growing cells. The current model postulates that the preferential use of aerobic glycolysis offers the following advantages to highly proliferative cells. First, it focuses cells on the use of glucose, which is the most abundant extracellular nutrient; second, the flux of ATP derived from glycolysis can exceed the one produced during OXPHOS, despite the low efficiency of glycolysis, when glucose is provided at a sufficiently high concentration; third, glucose utilization provides essential metabolic intermediates for the biosynthesis of diverse macromolecules (lipids, proteins and nucleic acids) and for anti-oxidative defenses, with the production of NADPH (Fig. 5) (Lunt and Vander Heiden, 2011; Vander Heiden et al., 2009).

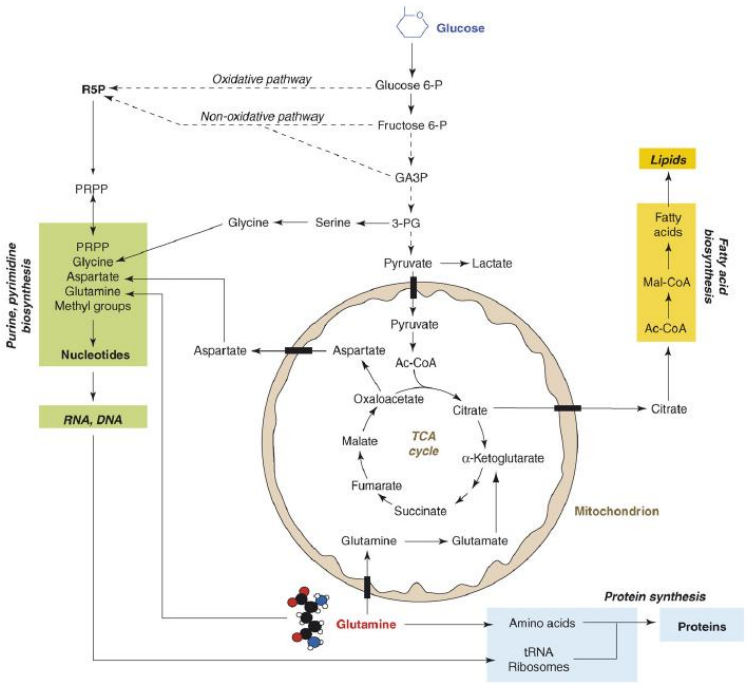

Figure 5. Tumor cells obtain biosynthetic precursors from glucose and glutamine metabolism. Glucose and glutamine, the two most abundant extracellular nutrients, contribute carbon for the synthesis of the three major classes of macromolecules (nucleic acids, lipids, and proteins) in proliferating tumor cells. Biosynthesis of purines and pyrimidines utilizes ribose 5-phosphate (R5P) produced from diversion of glycolytic intermediates into the oxidative and non-oxidative arms of the pentose phosphate pathway, and nonessential amino acids derived from glucose and glutamine. Fatty acid synthesis, used to produce cellular lipids, requires acetyl-CoA (Ac-CoA), most of which is generated from glucose and transferred from the mitochondria to the cytoplasm via citrate. Protein synthesis requires amino acids, tRNAs and ribosomes (proteins and rRNAs). Both glucose and glutamine are used to generate these molecules. In addition to its role as a carbon source, glutamine also donates nitrogen to nucleotide and amino acid synthesis. Abbreviations: P, phosphate; GA3P, glyceraldehyde 3-phosphate; 3-PG, 3-phosphoglycerate; PRPP, phosphoribosyl pyrophosphate; Mal-CoA, malonyl-CoA (Deberardinis et al., 2008).

Multiple molecular mechanisms, both intrinsic and extrinsic, converge to alter core cellular metabolism and provide support for the basic needs of dividing cells (Fig. 6). Therefore, metabolic adaptation in tumors extends beyond the Warburg effect and, besides aerobic glycolysis, there are other core fluxes, such as the pentose phosphate pathway, the *de novo* fatty acid synthesis and glutamine-dependent metabolism that cancer cells need for their high rate of replication. On the basis of these observations, the development of treatments that target tumor metabolism is receiving increasing attention, with several potential drugs targeting metabolic pathways currently in clinical trials.

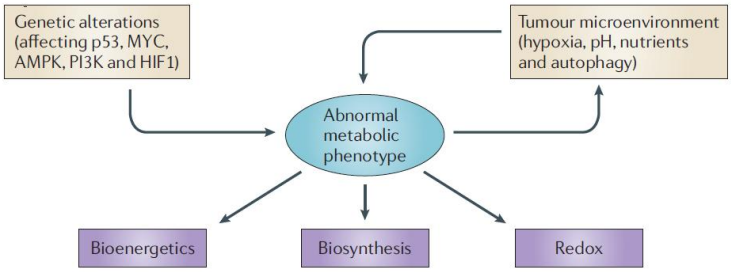

Figure 6. Determinants of the tumor metabolic phenotype. Abnormal metabolic phenotype sustains cell growth by providing rapid ATP generation to maintain energy status, increased biosynthesis of macromolecules and tightened maintenance of appropriate cellular redox status (Cairns et al., 2011).

1.2.1. Oncogene/tumor suppressor genes and cancer metabolism

Some of the mechanisms used by tumors to bring about metabolic changes include the altered expression, mutation or post-translational inactivation of an enzyme or the substitution of an enzyme isoform with a different one. Notably, most tumor suppressor genes and oncogenes play a role in this neoplastic metabolic rewiring (Fig. 7) (Ward and Thompson, 2012).

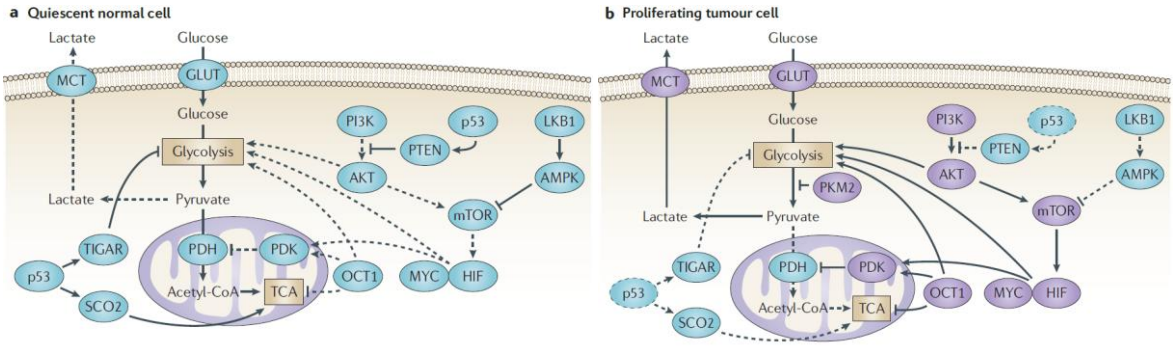

Figure 7. Molecular mechanisms driving the Warburg effect. Relative to normal cells (part a) the shift to aerobic glycolysis in tumor cells (part b) is driven by multiple oncogenic signaling pathways. PI3K activates AKT, which stimulates glycolysis by directly regulating glycolytic enzymes and by activating mTOR. The liver kinase B1 (LKB1) tumor suppressor, through AMP-activated protein kinase (AMPK) activation, opposes the glycolytic phenotype by inhibiting mTOR. mTOR alters metabolism in a variety of ways, but it has an effect on the glycolytic phenotype by enhancing hypoxia-inducible factor 1 (HIF1) activity, which engages a hypoxia-adaptive transcriptional program. HIF1 increases the expression of glucose transporters (GLUT), glycolytic enzymes and pyruvate dehydrogenase kinase, isozyme 1 (PDK1), which blocks the entry of pyruvate into the tricarboxylic acid (TCA) cycle. MYC cooperates with HIF in activating several genes that encode glycolytic proteins, but also increases mitochondrial metabolism. The tumor suppressor p53 opposes the glycolytic phenotype by suppressing glycolysis through TP53-induced glycolysis and apoptosis regulator (TIGAR), increasing mitochondrial metabolism via SCO2 and supporting expression of PTEN. OCT1 (also known as POU2F1) acts in an opposing manner to activate the transcription of genes that drive glycolysis and suppress OXPHOS. The switch to the pyruvate kinase M2 (PKM2) isoform affects glycolysis by slowing the pyruvate kinase reaction and diverting substrates into alternative biosynthetic and reduced nicotinamide adenine dinucleotide phosphate (NADPH)-generating pathways. MCT, monocarboxylate transporter; PDH, pyruvate dehydrogenase. The dashed lines indicate loss of p53 function (Cairns et al., 2011).

1.2.1.1. HIF and MYC

The **HIF1** and **HIF2** complexes are the major transcription factors that are responsible for gene expression changes during the cellular response to low oxygen conditions (Bertout et al., 2008). They are heterodimers that are composed by the constitutively expressed HIF1β (also known as ARNT) subunit, and either the HIF1α or the HIF2α (also known as EPAS1) subunits. Under normoxic conditions, the HIFα subunits undergo oxygen-dependent hydroxylation by prolyl hydroxylase enzymes, which results in their recognition by von Hippel-Lindau tumor suppressor (VHL), an E3 ubiquitin ligase, and subsequent degradation. HIFα subunits are rapidly stabilized either upon exposure to hypoxia, e.g. in the interior of the tumor mass, or under normoxic conditions by oncogenic signaling pathways, including PI3K, and by mutations in tumor suppressor proteins such as VHL, succinate dehydrogenase (SDH) and fumarate hydratase (FH) (Semenza, 2010).

Once activated, HIF1 enhances the transcription of genes encoding glucose transporters and most glycolytic enzymes, increasing the capacity of the cell to carry out glycolysis. In addition, HIF1 activates the pyruvate dehydrogenase kinases (PDKs), which inactivate the mitochondrial pyruvate dehydrogenase complex and thereby reduce the flow of glucose-derived pyruvate into the tricarboxylic acid (TCA) cycle. This reduction in pyruvate flux into the TCA cycle decreases the rate of OXPHOS and oxygen consumption, reinforcing the glycolytic phenotype and sparing oxygen under hypoxic conditions (Kim et al., 2006; Papandreou et al., 2006). Inhibitors of HIF1 or of the PDKs could potentially reverse some of the metabolic effects of HIF1 signaling and several such candidates, including the PDK inhibitor dichloroacetic acid (DCA), are currently under evaluation as anti-neoplastic agents (Onnis et al., 2009).

The first documented direct mechanistic link between an activated oncogene and altered glucose metabolism was the observation that lactate dehydrogenase isoform A (LDHA) is induced by the transcription factor **MYC**, whose deregulated activation is mandatory for the progression of a variety of malignancies (Dang et al., 2009). MYC and HIF1 share many target glycolytic enzyme genes, and MYC can activate most glycolytic enzyme genes as well as glucose transporters. Pyruvate kinase M2 (PKM2), which converts

phosphoenolpyruvate to pyruvate, replaces by alternative splicing PKM1 during cellular transformation and favors aerobic glycolysis (Christofk et al., 2008). MYC is able to induce the splicing factors that produce PKM2, further underscoring its role in cell metabolism. MYC also increases glutamine uptake by directly inducing the expression of the glutamine transporters SLC5A1 and SLC7A1 (also known as CAT1). Furthermore, MYC indirectly increases the level of glutaminase 1 (GLS1), the first enzyme of glutaminolysis, by repressing the expression of microRNA-23A and microRNA-23B, which inhibit GLS1. MYC may support antioxidant capacity by driving pentose phosphate pathway (PPP) based NADPH production through promoting the expression of the PKM2 isoform, thus diverting glucose usage from the Krebs cycle to the PPP (see Fig. 5), and also by increasing the synthesis of GSH through glutaminolysis. Moreover, once glutamine is converted into glutamate and then into α-ketoglutarate it can enter the TCA cycle. This process of anaplerosis supplies the carbon atoms required for the biosynthesis of both amino acids and fatty acids (DeBerardinis et al., 2007).

1.2.1.2. p53 and OCT1

Although the **p53** tumor suppressor has been mainly regarded as the 'guardian of the genome', its function extends to regulation of cell metabolism by stimulating mitochondrial respiration and suppressing glycolysis through transcriptional regulation (Vousden and Ryan, 2009). p53 activates the expression of HK II, which converts glucose to glucose-6-phosphate (G6P). G6P then enters either glycolysis to produce ATP, or the PPP, which supports macromolecular biosynthesis by producing reducing potential in the form of NADPH and/or ribose, the building blocks for nucleotide synthesis. At the same time, p53 suppression of phosphoglycerate mutase 2 (PGAM2) and activation of tumor protein 53-induced glycolysis and apoptosis regulator (TIGAR), which has 2,6-fructose-bisphosphatase activity and depletes PFK1 of a potent positive allosteric ligand, suppresses glycolysis and favors increased NADPH production by the PPP. Moreover, activation of SCO2 (which regulates the cytochrome *c* oxidase complex) by p53 increases the efficiency of mitochondrial respiration. Hence, loss of p53 function might be a major force behind the acquisition of the glycolytic phenotype (Jones and Thompson, 2009).

OCT1 (also known as POU2F1) is a transcription factor, the expression of which is increased in several human cancers, and it may cooperate with p53 in regulating the balance between oxidative and glycolytic metabolism. Data from studies of knockout mice and human cancer cell lines show that the transcriptional program that is orchestrated by OCT1 cooperates with the loss of p53, as it supports resistance to oxidative stress, increases glucose metabolism and inhibits mitochondrial respiration (Shakya et al., 2009). One of the OCT1 targets is an isoform of PDK (PDK4) that has the same function as the PDK enzymes that are activated by HIF1. Although the mechanisms by which OCT1 is up-regulated in tumor cells are poorly understood, its downstream effectors may be potential targets for therapeutic intervention.

1.2.1.3. The PI3K pathway

The **PI3K** pathway is one of the most commonly activated signaling pathways in human cancers by mutations in tumor suppressor genes, such as PTEN, in the components of the PI3K complex itself or by aberrant upstream signaling from receptor tyrosine kinases (Wong et al., 2010). Once activated, the PI3K pathway not only provides strong growth and survival signals to tumor cells but also has profound effects on their metabolism. The best-studied effector downstream of PI3K is **AKT1** (also known as PKB). The increased and prolonged AKT1 signaling that is associated with transformation is an important driver of the tumor glycolytic phenotype through activation of hexokinase 2 (HK II) and phosphofructokinase 1 (PFK1; also known as PFKM) and PFK2 (also known as PFKFB3), recruitment of glucose transporters to the cell surface, and inhibition of forkhead box subfamily O (FOXO) transcription factors. AKT1 also activates ectonucleoside triphosphate diphosphohydrolase 5 (ENTPD5), an enzyme that supports increased protein glycosylation in the endoplasmic reticulum and indirectly increases glycolysis by creating an ATP hydrolysis cycle. Finally, AKT1 strongly stimulates signaling by the kinase mTOR by phosphorylating and inhibiting its negative regulator tuberous sclerosis 2 (TSC2; also known as tuberin) (Robey and Hay, 2009). mTOR functions as a key metabolic integration point, coupling growth signals to nutrient availability. Activated mTOR stimulates protein and lipid biosynthesis and cell growth in response to sufficient nutrient and energy conditions and is often constitutively activated during tumorigenesis (Guertin and Sabatini, 2007). At the molecular level, mTOR directly stimulates mRNA translation and

ribosome biogenesis, and indirectly causes other metabolic changes by activating transcription factors such as hypoxia-inducible factor 1 (HIF1) even under normoxic conditions. The subsequent HIF1-dependent metabolic changes further amplify the glycolytic phenotype elicited by PI3K, AKT1 and mTOR (see Fig. 5).

1.2.1.4. AMP-activated protein kinase

AMP-activated protein kinase (**AMPK**) is a crucial sensor of energy status and has an important pleiotropic role in cellular responses to metabolic stress (Shackelford and Shaw, 2009). The AMPK pathway couples energy status to growth signals; biochemically, AMPK opposes the effects of AKT1 and acts as a potent inhibitor of mTOR. The AMPK complex thus functions as a metabolic checkpoint, regulating the cellular response to energy availability. During periods of energetic stress, AMPK becomes activated in response to an increased AMP/ATP ratio, and is responsible for shifting cells to an oxidative metabolic phenotype and inhibiting cell proliferation. Tumor cells must overcome this checkpoint in order to proliferate in response to activated growth signaling pathways, even in a less than ideal microenvironment. Several oncogenic mutations and signaling pathways can suppress AMPK signaling, which uncouples fuel signals from growth signals, allowing tumor cells to divide under abnormal nutrient conditions (Wang and Guan, 2009). Given the role of AMPK, it is not surprising that STK11, which encodes liver kinase B1 (**LKB1**) — the upstream kinase necessary for AMPK activation — has been identified as a tumor suppressor gene and is mutated in Peutz–Jeghers syndrome, which is characterized by the development of benign gastrointestinal and oral lesions and an increased risk of developing a broad range of malignancies. LKB1 is also frequently mutated in sporadic cases of non-small-cell lung cancer and cervical carcinoma. Recent evidence suggests that LKB1 mutations are tumorigenic owing to the resulting decrease in AMPK signaling and loss of mTOR inhibition (Shackelford and Shaw, 2009). Clinically, there is currently considerable interest in evaluating whether AMPK agonists can be used to re-couple fuel and growth signals in tumor cells and to shut down cell growth. Two such agonists are the commonly used anti-diabetic drugs metformin and phenformin (Kim and He, 2013). It remains to be seen whether these agents represent a useful class of metabolic modifiers with antitumor activity.

1.2.1.5. Ras signaling pathway

Ras proteins are signal switch molecules that regulate cell fate by coupling receptor activation to downstream effector pathways that control diverse cellular responses including proliferation, differentiation and survival. Ras proteins are small GTPases that cycle between inactive guanosine diphosphate (GDP)-bound and active guanosine triphosphate (GTP)-bound conformations (Ras-GDP and Ras-GTP, respectively). Growth factor binding to cell-surface receptors creates intracellular docking sites for adaptor molecules and signal-relay proteins that recruit and activate guanine nucleotide-exchange factors (GEFs), such as members of the SOS family. GEFs displace guanine nucleotides from Ras and permit passive binding to GTP, which is abundant in the cytosol, leading to Ras activation. Conversely, Ras proteins are negatively regulated by GTPase activating proteins (GAPs), which markedly stimulate intrinsic GTPase activity by stabilizing a high-energy transition state that occurs during the Ras-GTP hydrolysis reaction (Malumbres and Barbacid, 2003; Schubbert et al., 2007).

Ras-GTP regulates a complex signaling network that modulates cell behavior by binding to and activating distinct classes of effector molecules. The Raf-MEK-ERK cascade is the best characterized Ras effector pathway (McCubrey et al., 2007). ERK kinases can phosphorylate both cytosolic and nuclear substrates, which include transcription factors such as JUN and ELK1 that regulate FOS expression. Activation of these transcriptional regulators can lead to the expression of proteins that control cell-cycle progression, such as cyclin D. Ras-GTP also binds the catalytic subunit of type I PI3Ks leading to the translocation of PI3K to the plasma membrane and subsequent activation of downstream kinases such as AKT. PI3K also activates Rac, a Rho family GTPase, which has been shown to be important for transformation by oncogenic Ras in some cellular contexts. Ras can also activate a family of exchange factors for the Ral small GTPases (RalGEFs), which activate Ral leading therefore to stimulation of phospholipase D (PLD) (Fig. 8).

Many other effector pathways are directly coupled to Ras-GTP, several of which have known roles in regulating cellular responses. Ras-GTP directly binds to the Rac exchange factor tumor invasion and metastasis inducing protein 1 (TIAM1), leading to increased levels of Rac and subsequent actin reorganization. Phospholipase Cε also binds directly to

Ras-GTP, and the consequent hydrolysis of PIP2 to diacylglycerol (DAG) and inositol-1,4,5-triphosphate ($Ins(1,4,5)P_3$) serves to release Ca^{2+} and activate protein kinase C (PKC) (Karnoub and Weinberg, 2008).

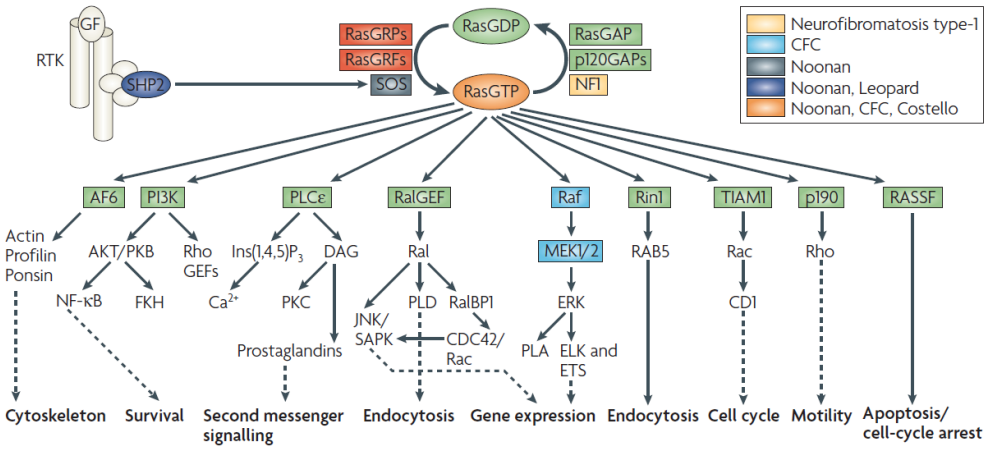

Figure 8. Ras signaling network. Ras proteins function as nucleotide-driven switches that relay extracellular cues to cytoplasmic signaling cascades. The binding of GTP to Ras proteins locks them in their active state, which enables high affinity interactions with downstream effectors. GTPase-activating proteins (GAPs), such as p120GAP or neurofibromin (NF1), enhance the intrinsic GTPase activity and hence negatively regulate Ras protein function. Conversely, guanine-nucleotide exchange factors (GEFs), such as RasGRF and son of sevenless (SOS), catalyse nucleotide ejection and therefore facilitate GTP binding and protein activation. The classical view of Ras signaling depicts Ras activation and recruitment to the plasma membrane following receptor Tyr kinase (RTK) stimulation by growth factors (GF). Activated Ras engages effector molecules — belonging to multiple effector families — that initiate several signal-transduction cascades. Activating mutations in the different components of the Ras signaling pathway are associated with different developmental disorders, such as Neurofibromatosys type-1, cardio-facio-cutaneous (CFC), Noonan, Leopard and Costello syndromes (Karnoub and Weinberg, 2008).

Mammalian genomes encode three RAS genes that give rise to four gene products: N-Ras, H-Ras, K-Ras4A, and K-Ras4B. K-Ras4A and K-Ras4B isoforms result from alternative splicing of the KRAS gene. Human cancers frequently express mutant Ras proteins, termed '**oncogenic Ras**'. Specific Ras genes are mutated in different malignancies: KRAS mutations are prevalent in pancreatic, colorectal, endometrial, biliary tract, lung and cervical cancers; KRAS and NRAS mutations are found in myeloid malignancies; and NRAS and HRAS mutations predominate in melanoma and bladder cancer, respectively. In most cases, the somatic missense Ras mutations found in cancer cells introduce amino acid substitutions at positions 12, 13 and 61. These changes impair the intrinsic GTPase activity and confer resistance to GAPs, thereby causing cancer-associated mutant Ras proteins to accumulate in the active, GTP-bound conformation (Schubbert et al., 2007). RAS can also be activated in tumors by loss of GAPs. The most significant known example is the loss of neurofibromin, which is encoded by the NF1 gene and has all the

characteristics of a tumor suppressor. Moreover, RAS signaling pathways are also commonly activated in tumors in which growth-factor-receptor tyrosine kinases have been hyper-activated. The most common examples are EGFR and ERBB2 (also known as HER2/neu), which are frequently activated by overexpression in many types of cancer, including breast, ovarian and stomach carcinomas (Downward, 2003).

Hyper-activation of RAS signaling has a key role in the establishment of many abnormal functional properties of cancer cells, such as deregulated cell growth, survival and differentiation. Moreover, in the very last years, an increasing number of observations has highlighted the effect of oncogenic RAS signaling on tumor metabolism. An inducible KrasG12V system revealed that Ras-induced mitochondrial dysfunction precedes the activation of glycolysis, suggesting that mitochondrial dysfunction is causally associated to the metabolic switch observed in cancer (Hu et al., 2012). Moreover, integrated genomic, biochemical and metabolomic analyses following KrasG12D withdrawal in a pancreatic ductal adenocarcinoma model revealed a prominent perturbation of multiple metabolic pathways. In particular, KrasG12D exerts potent control of glycolysis through regulation of glucose transporter and several rate-limiting enzymes at the transcriptional level, which collectively serve to shunt glucose metabolism toward anabolic pathways, such as the hexosamine biosynthesis pathway (HBP) for protein glycosylation and the PPP for ribose production (Fig. 9) (Ying et al., 2012).

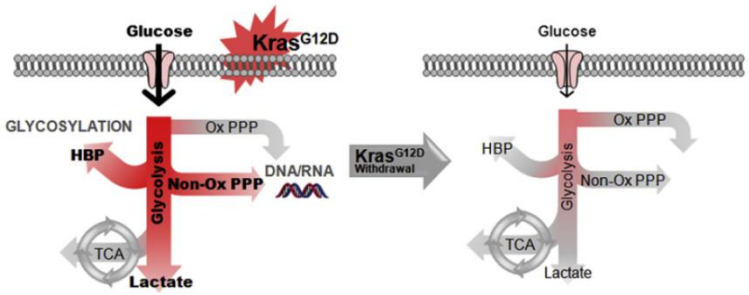

Figure 9. Schematic representation of the shift in glucose metabolism upon KrasG12D withdrawal. Activation of oncogenic Kras enables pancreatic ductal adenocarcinoma (PDAC) tumor maintenance through the increased uptake of glucose and subsequent shunting into glycolysis, the HBP pathway (to enable enhanced glycosylation) and the non-oxidative arm of the PPP (to facilitate ribose biosynthesis for DNA/RNA). Glucose flux into the oxidative arm of the PPP and the TCA cycle does not change when KrasG12D is inactivated (Ying et al., 2012).

Furthermore, Ras was shown to transcriptionally regulate several components of the autophagy machinery (Elgendy et al., 2011). Interestingly, inhibition of autophagy in Ras-transformed cells causes a striking accumulation of dysfunctional mitochondria,

suggesting that Ras might be responsible for early mitochondria dysfunction and that maintaining oxidative metabolism by increasing the clearance of dysfunctional mitochondria is critical (Guo et al., 2011).

The impact of RAS signaling on tumor metabolism is a relatively new field and more studies have to be carried out in order to elucidate which are the downstream pathways responsible for metabolism rewiring upon Ras activation. The PI3K/AKT pathway is a good candidate as its impact on cellular metabolism has already been established; however, additional signaling pathways could take part to the metabolic shift observed in tumor cells following Ras activation. An interesting work showed that the activation of the MEK-ERK pathway following growth factor stimulation can trigger the Warburg effect through modulation of the phosphorylation status of PKM2 (Yang et al., 2012). Indeed, phosphorylated PKM2 migrates to the nucleus where it leads to β-catenin transactivation and induction of c-Myc expression, which in turn up-regulates the expression of glycolytic enzymes (Fig.10).

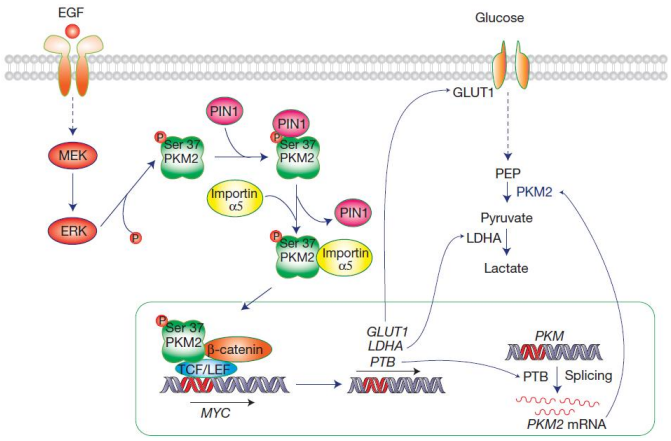

Figure 10. ERK1/2-dependent phosphorylation and nuclear translocation of PKM2 promotes the Warburg effect. EGFR activation in human cancer cells induces PKM2 nuclear translocation, which is mediated by PKM2 phosphorylation by ERK, followed by PIN1-regulated cis-trans isomerization of PKM2 and subsequent binding to importin 5. Nuclear PKM2 is required for EGF-induced-catenin transactivation and induction of c-Myc expression, which in turn and thereby up-regulates the expression of glycolytic enzymes such as GLUT1, LDHA and also the PTB-dependent expression of PKM2 (Yang et al., 2012).

1.2.2. Metabolic adaptation and microenvironment

In addition to genetic changes, the abnormal tumor microenvironment has a major role in determining the metabolic phenotype of tumor cells. Tumor vasculature is structurally and functionally abnormal, and combined with intrinsically altered tumor cell

metabolism, creates spatial and temporal heterogeneity in oxygenation, pH, and the concentration of glucose and many other metabolites. These extreme conditions induce a collection of cellular stress responses that further contribute to the distorted metabolic phenotype of tumor cells and influence tumor progression. The response to hypoxia is the best studied of tumor cell stress responses owing to the well-known effects of hypoxia on tumor radio-resistance and metastasis. Other metabolic stress conditions such as low pH and low glucose are also prevalent in solid tumors and are likely to be major determinants of the metabolic phenotype. It should be noted that the relationship between the tumor microenvironment and cancer cell metabolism is not one of simple cause and effect, in which biochemical conditions in the tumor influence cellular metabolism. Because metabolite concentrations are governed by both supply by the vasculature and demand by the tissue, changes in metabolism of both the tumor and normal stromal cells also have a profound effect on microenvironmental conditions (Cairns et al., 2011).

1.3. Mitochondria and cancer

Many vital cellular parameters are controlled by mitochondria. These include regulation of energy production, modulation of oxidation-reduction (redox) status, generation of reactive oxygen species (ROS), control of cytosolic Ca^{2+} levels, contribution to cytosolic biosynthetic precursors such as acetyl-CoA and pyrimidines, and initiation of apoptosis and necrosis through the activation of the mitochondrial permeability transition pore (mtPTP) and the release of apoptogenic proteins (Tait and Green, 2010). Changes in these parameters can impinge on biosynthetic pathways, cellular signal transduction pathways, transcription factors and chromatin structure to shift the cell from a quiescent, differentiated state to an actively proliferating one (Wallace, 2012).

Although mutations in the mitochondrial DNA (mtDNA) of cancer cells have been recognized for more than two decades (Horton et al., 1996), the role of mitochondrial alterations in cancer came to general attention only in 2000, with the discovery that mutations in the TCA cycle genes succinate dehydrogenase (SDH) (Baysal et al., 2000) and fumarate hydratase (FH) (Tomlinson et al., 2002) are causative of specific tumor subsets. More recently it was found that also mutations in isocitrate dehydrogenase 1 (IDH1) and IDH2 are tumorigenic (Fig. 11) (Ward et al., 2010).

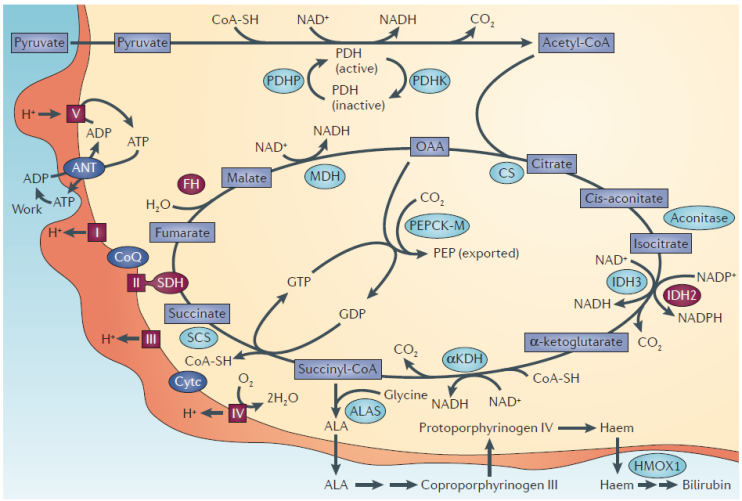

Figure 11. Mitochondrial bioenergetics and cancer cell mutations. Pyruvate dehydrogenase (PDH) can be inactivated through phosphorylation by PDH kinase (PDHK) and reactivated through dephosphorylation by PDH phosphatase (PDHP). Cancer mutations have been identified in IDH2, SDH, and FH (shown as red ovals). FH defects are associated with induction of the haemoxygenase 1 (HMOX1), which degrades haem. Cancer cell mitochondrial DNA (mtDNA) mutations have been reported in genes for complexes I, III, IV and V (shown as red squares). Hence, many of the mitochondrial gene mutations in cancer are intimately associated with OXPHOS and the redox regulation of reactive oxygen species (ROS) (Wallace, 2012).

1.3.1. Mutations that affect mtDNA

Contrary to conventional wisdom, functional mitochondria are essential for the cancer cell. Although mutations in mitochondrial genes are common in cancer cells, they do not inactivate mitochondrial energy metabolism but rather alter the mitochondrial bioenergetic and biosynthetic state.

1.3.1.1. ρ^0 cells and tumorigenesis

The requirement of cancer cells for functional mitochondria has been confirmed by the elimination of mtDNA from various cancer cells through growth in ethidium bromide (ρ^0 cells) (King and Attardi, 1996). The resulting ρ^0 cancer cells have reduced growth rates, decreased colony formation in soft agar and markedly reduced tumor formation in nude mice (Wallace, 2012). However, this model of mitochondrial dysfunction has been widely controversial given the extreme mitochondrial damage: ρ^0 cells do not show any mitochondrial respiration and fully depend on glycolysis for energy demands. Thus, these cells have been used as a model both for mitochondrial dysfunction pathologies and tumors, as they implement bioenergetic adjustments which are often shared by the two groups of diseases.

1.3.1.2. mtDNA mutations and cancer

Since mtDNA is in the proximity of ROS generation sites (the byproduct of OXPHOS) and mitochondria have relatively less sophisticated DNA protection or repair systems, mtDNA is vulnerable to high mutation rates. As a result, the mtDNA within a cell could be a blend of both wild-type and mutant species, a condition called 'heteroplasmy'. The normal situation, in which all mtDNAs are identical, is referred to as 'homoplasmy'. The neutral polymorphisms are most likely homoplasmic, whereas the pathogenic mutations are usually heteroplasmic in nature. It is expected that, due to the multiplicity of mitochondrial genomes in each cell, a threshold of mutant mtDNA must be reached before it can induce a cellular dysfunction, and a further threshold of dysfunctional cells within a tissue must be reached before such a defect becomes apparent.

Somatic and germline mtDNA mutations have been reported for a wide variety of cancers. These include renal adenocarcinoma, colon cancer cells, head and neck tumors, astrocytic tumors, thyroid tumors, breast tumors, ovarian tumors, prostate and bladder cancer, neuroblastomas and oncocytomas. Ancient mtDNA population variants have also been correlated with cancer risk. For example, the macrohaplogroup N variant in the complex I, subunit ND3 gene (ND3; also known as MTND3) at nucleotide G10398A (resulting in a T114A amino acid change) has been associated with breast cancer risk in African American women, and the 16519 T to C mtDNA control region variant is associated with endometrial cancer (Wallace, 2012).

A meta-analysis of many cancer-associated mtDNA mutations revealed that many cancer cell mtDNA mutations clearly inhibit OXPHOS. However, a significant proportion of the reported variants are the same nucleotide changes that have previously been reported as ancient adaptive mtDNA variants in human populations. Although some of these cancer 'associations' are clear misinterpretations of ancient polymorphisms, others may be valid cancer cell mutations. However, it must be highlighted that in principle two classes of mutations may affect mtDNA of cancer cells: mutations that stimulate neoplastic transformation, e.g. by facilitating cancer cell adaption to a changing bioenergetic environment through OXPHOS impairment, and those that are a by-product of primary

tumorigenic alterations, such as dysregulation of redox equilibrium, and that could further enhance cell malignancy (Brandon et al., 2006).

Intriguingly, the extent of mtDNA heteroplasmy versus homoplasmy appears to affect oxyradical formation and tumorigenicity. At heteroplasmic levels, a mutation in MT‑ND5 is associated with increased generation of oxyradicals and tumorigenicity, whereas homoplasmic MT‑ND5 mutations appear to exhibit decreased oxyradical formation and tumorigenicity. Thus, a dosage effect of mtDNA mutations may determine the extent of redox stress and tumorigenicity (Koppenol et al., 2011).

1.3.2. Defects of mitochondrial enzymes in cancer

Over the past two decades, the discovery of oncogenes and tumor suppressor genes has created a paradigm by which cell-autonomous genetic alterations were considered the main driving force for neoplastic transformation through dysregulation of a small set of crucial biological processes (Hanahan and Weinberg, 2000), whereas alterations of cell metabolism were considered as epiphenomena of the tumorigenic process. However, with the discoveries of oncogenic mutations affecting mitochondrial metabolic enzymes, it is now untenable to deny the role of metabolism in tumorigenesis. Indeed, signaling mediated by metabolites, e.g. succinate and fumarate, or other mitochondria-derived molecules has been suggested to trigger oncogenic transformation, thus establishing a new paradigm in oncogenesis: a mutation can drive neoplastic transformation by inducing the accumulation of a molecule called '**oncometabolite**'.

1.3.2.1. Succinate dehydrogenase mutations

SDH is a tetrameric enzyme placed at the crossroad between the TCA cycle and the electron transport chain (ETC), of which it is an integral part (respiratory chain complex II). Germline mutations in all the genes encoding the subunits of SDH predispose individuals to hereditary paraganglioma and phaeochromocytoma, inherited tumor susceptibility syndromes (Bardella et al., 2011; Baysal et al., 2000). It was then demonstrated that impaired HIFα degradation due to the inhibition of its hydroxylation by PHDs is at the heart of the pathology of these tumors (Briere et al., 2005; Pollard et al., 2005; Selak et al., 2005). Two models that explain anomalous HIFα stabilization under

normoxia due to SDH mutations have been proposed (Fig. 12). The first suggested that ROS, generated from an impaired complex II, oxidate iron and ascorbate, that are cofactors of PHDs, preventing HIFα hydroxylation by inhibiting PHDs. However, there are conflicting data as to ROS production in SDH deficient cells (Ishii et al., 2005; Selak et al., 2005). This controversy may be attributed to the mechanism used for SDH inactivation (mutations versus siRNAs) or to the methods used for ROS analysis. The second model demonstrated that succinate, which builds up in SDH-deficient mitochondria, can serve as a mitochondria-to-cytosol messenger that inhibits PHD activity (Selak et al., 2005). The stabilized HIF1α is then translocated into the nucleus and causes a shift from oxidative to glycolytic energy metabolism.

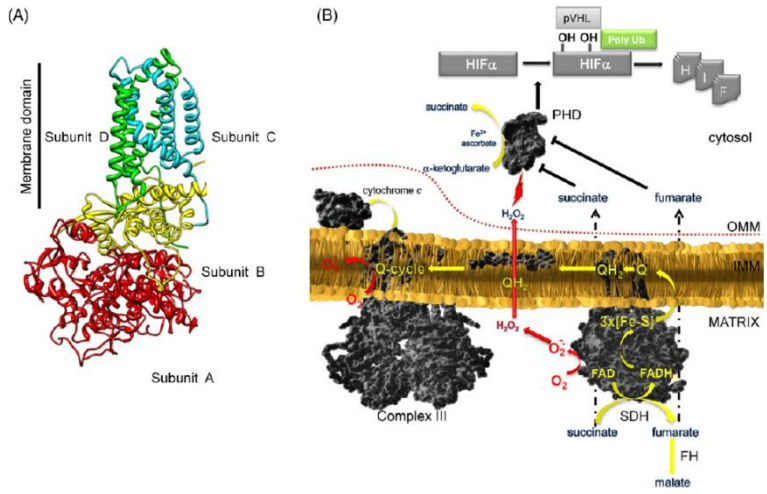

Figure 12. The physiological roles of SDH in the TCA cycle and the ETC and its potential roles in cancer. (A) Ribbon diagram of SDH structure. The catalytic subunits, *i.e.* the flavoprotein (SDHA) and the iron-sulphur protein (SDHB) are depicted in red and yellow, respectively, and the membrane anchor and ubiquinone binding proteins SDHC and SDHD are depicted in cyan and green, respectively. (B) Other than being a TCA enzyme, SDH is an additional entry point to the ETC. The electron flow in and out of complex II and III is depicted by the yellow arrows. Complex III is the best characterized site of ROS production in the ETC, where a single electron reduction of oxygen to superoxide can occur (red arrow). It was proposed that obstructing electron flow within complex II might support a single electron reduction of oxygen at the FAD site (red arrow). Superoxide is dismutated to hydrogen peroxide which can then leave the mitochondria and inhibit PHD in the cytosol, leading to HIFα stabilization. Succinate or fumarate, which accumulates in SDH- or FH-deficient tumors, can also leave the mitochondria and inhibit PHD activity in the cytosol. The red dotted line represents the outer mitochondrial membrane (OMM) (Frezza and Gottlieb, 2009).

1.3.2.2. Fumarate hydratase mutations

Homozygous null mutations in the FH gene are associated with multiple cutaneous and uterine leiomyomatas and aggressive forms of renal cell cancer (Tomlinson et al., 2002). FH converts fumarate to malate, and cells harboring FH mutations produce up to 100-fold more fumarate, sevenfold more succinate, and have a marked decrease in malate

and citrate levels. Fumarate has also been hypothesized to inhibit PHDs and stabilize HIF1α, even though this observation is still a matter of debate (Adam et al., 2011).

Increased fumarate levels have been found to activate the stress response pathway that is regulated by NFE2-related factor 2 (NRF2; also known as NFE2L2). NRF2 is normally kept at low levels through degradation by the kelch-like ECH-associated protein 1 (KEAP1) and the ubiquitin E3 ligase cullin 3 complex. However, excess fumarate can inactivate KEAP1 through succination of cysteines 151 and 288, thereby stabilizing NRF2. NRF2 binds to the antioxidant response elements (AREs) and turns on DNA stress-response genes, one of which is haem oxygenase 1 (HMOX1). The induction of HMOX1 is important to tumorigenesis because silencing or inhibiting HMOX1 in FH knock out cells reduces colony-forming capacity (Frezza et al., 2011). Inactivation of FH would not only increase fumarate and succinate levels but would also increase succinyl-CoA levels. The induction of HMOX1 could reduce the levels of these metabolites as haem biosynthesis involves combining succinyl-CoA with glycine to generate δ-aminolevulinic acid (ALA) by ALA synthetase (ALAS) to initiate porphyrin synthesis. Porphyrins are converted to haem, which is degraded by HMOX1 to result in the production and excretion of bilirubin (Fig. 11). This raises the question of why might it be beneficial for the malignant cell to reduce succinyl-CoA levels. One possibility could be that when succinyl-CoA is converted to succinate by succinyl-CoA synthetase, GTP is generated. GTP hydrolysis is in turn coupled to the conversion of oxaloacetate (OAA) to phosphoenolpyruvate (PEP) by mitochondrial PEP carboxykinase (PEPCK-M), and mitochondrial PEP is exported to the cytosol where it can be converted to pyruvate and ATP. If succinyl-CoA were in excess, this reaction could deplete the mitochondrion of OAA that is required for citrate synthesis and lipid biogenesis. Moreover, excess GTP might adversely affect the homeostasis of the mitochondrial nucleotide pool and compromise mtDNA transcription and replication (Wallace, 2012).

1.3.2.3. Isocitrate dehydrogenases

Heterozygous missense mutations in the two NADP+-dependent IDH enzymes, cytosolic IDH1 and mitochondrial IDH2, have been observed in low-grade gliomas and secondary glioblastomas, astrocytomas, chondromas and acute myeloid leukaemia (AML) (Schaap et

al., 2013). A third IDH, NAD+-dependent IDH3, is the primary TCA cycle enzyme for decarboxylating isocitrate to α-ketoglutarate (Fig. 11), yet this enzyme has not been found to be mutated in cancer. Like IDH3, IDH1 and IDH2 can oxidatively decarboxylate isocitrate to α-ketoglutarate. However, IDH1 and IDH2 reduce $NADP^+$ instead of NAD^+, and the $NADP^+$-dependent reaction is reversible because NADPH can provide sufficient energy to drive the reductive carboxylation of α-ketoglutarate to isocitrate.

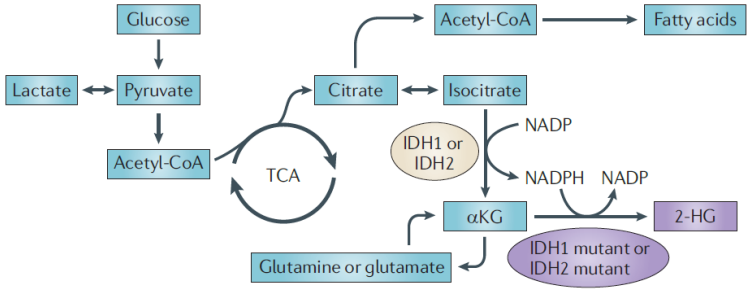

Figure 13. IDH1 and IDH2 mutations cause an oncometabolic gain of function. Instead of isocitrate being converted to α-ketoglutarate (αKG) with the production of reduced nicotinamide adenine dinucleotide phosphate (NADPH), αKG is converted to 2-hydroxyglutarate (2-HG) with the consumption of NADPH (Cairns et al., 2011).

The IDH1 and IDH2 mutations associated with the development of glioma and AML are restricted to crucial arginine residues required for isocitrate binding in the active site of the protein: R132 in IDH1, and R172 and R140 in IDH2 (Ward et al., 2010). Affected patients are heterozygous for these mutations, suggesting that these alterations may cause an oncogenic gain-of-function. It was initially proposed that these mutations might act through dominant-negative inhibition of IDH1 and IDH2 activity, which could lead to a reduction in cytoplasmic αKG concentration, inhibition of prolyl hydroxylase activity and stabilization of HIF1. However, it has recently been shown that these mutations cause IDH1 and IDH2 to acquire a novel enzymatic activity that converts αKG to 2-hydroxyglutarate (**2-HG**) in a NADPH-dependent manner (Dang et al., 2009). In fact, this change causes the mutated IDH1 and IDH2 enzymes to switch from NADPH production to NADPH consumption, with potentially important consequences for the cellular redox balance (Fig. 13). Indeed, the resulting decrease in NADPH levels would inhibit glutathione peroxidase, thus increasing H_2O_2 levels with heightened signaling effects. Moreover, decreased NADPH production would also inhibit the thioredoxins and the bifunctional apurinic/apyrimidinic endonuclease 1 (APE1; also known as redox factor 1

(REF1)), thus perturbing the redox status of crucial transcription factors and favoring proliferation and tumorigenesis (Wallace, 2012).

The product of the novel reaction, 2-HG, is a poorly understood metabolite and it remains to be determined whether the high concentrations of 2-HG are mechanistically responsible for the ability of IDH1 and IDH2 mutations to drive tumorigenesis. 2-HG is associated with alterations in cellular genomic methylation and transcription patterns and is a potent inhibitor of the αKG-dependent dioxygenases, particularly of the Jumonji C domain–containing histone lysine demethylases (KDMs) and the ten eleven translocation (TET) family of 5-methylcytosine (5mC) hydroxylases, which results in epigenetic alterations that affect the expression of genes involved in cell differentiation and the acquisition of malignant features. Furthermore, 2-HG inhibits collagen prolyl and lysyl hydroxylases (C-P4Hs and PLODs, respectively), leading to impaired collagen maturation and disrupted basement membrane formation, and stimulates PHDs activity, leading to enhanced HIF degradation and a diminished HIF response (Yang et al., 2013). Together these processes exert pleiotrophic effects on cell signaling and gene expression that probably contribute to the malignancy of IDH1/2-mutant cells.

Importantly, levels of αKG, isocitrate and several other TCA metabolites are not altered in cell lines or tissues expressing IDH1 mutations, suggesting that other metabolic pathways can adjust and maintain normal levels of these essential metabolites. Curiously, although IDH1 and IDH2 mutations are clearly powerful drivers of glioma and AML, they seem to be rare or absent in other tumor types. This observation highlights the importance of the specific cellular context in understanding metabolic perturbations in cancer cells.

1.3.3. OXPHOS assembly and regulation

Respiration can also be down-modulated through inhibition of the functional assembly of respiratory chain complexes. A recent model proposes that respiratory complexes are organized in functional super-complexes, for example aggregates of Complex I-III-IV in different stoichiometries, which form the so-called '**respirasome**' (Acin-Perez et al., 2008). The correct supra-complex assembly would be a crucial regulatory event in obtaining a fully functional respiratory chain. Recent reports have shown that OXPHOS impairment in cancer cells can be due to a dysregulation in the assembly of these super-

complexes, whose disassembly could favor the switch towards glucose metabolism (Baracca et al., 2010). It has been proposed that a combination of genetic (low transcription of some genes) and biochemical events (assembly factors deficiency, disorganization of structured super-complexes, and ROS-induced structural damage) might cause OXPHOS defects. For instance, a reduction of Complex I activity relative to other respiratory chain complexes is recurrent in a number of cancer cells of different origin. Significantly, all these tumor cells are characterized by an overproduction of ROS which is consistent with the hypothesis that Complex I-III super-complex formation allows electrons channeling, therefore preventing ROS production. If an altered Complex I cannot associate with Complex III in super-complexes, electrons are not correctly funneled from NADH through coenzyme Q to Complex III redox centers, determining ROS overproduction. This, in turn, enhances respiratory chain complex alteration resulting in further ROS production, thus establishing a vicious cycle of oxidative stress and energy depletion. These alterations could further damage cell structures and dysregulated key transduction pathways, with consequent tumor progression and metastasis (Solaini et al., 2011).

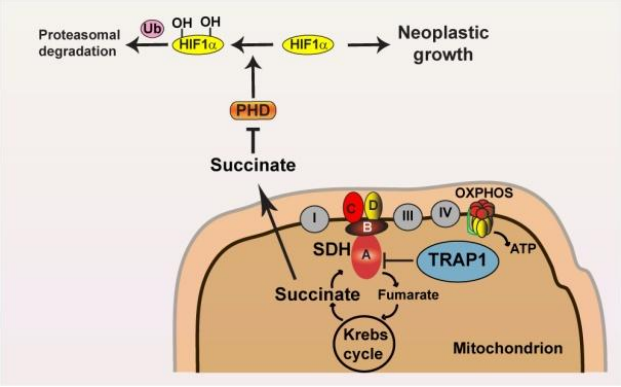

Figure 14. The mitochondrial chaperone TRAP1 promotes neoplastic growth by inhibiting succinate dehydrogenase. TRAP1 binds to and inhibits the enzymatic activity of CII leading to an increase in succinate level; this is responsible for PHD inhibition which results in HIF1α stabilization and neoplastic growth (Sciacovelli et al., 2013).

Given the importance of succinate levels in HIF1α stabilization, it is useful to highlight that Complex II (CII) is also a target of important regulation in tumors. A recent work from our laboratory showed that CII is bound and inhibited by a mitochondrial chaperone, called TRAP1, which is often up-regulated in cancer (Sciacovelli et al., 2013). TRAP1-expressing cells display a decrease in mitochondrial respiration and reorient their metabolism toward glycolysis to meet their energy demand. Despite normoxic conditions, HIF1α is

exclusively induced in TRAP1-expressing cells through the increase in succinate levels (Fig. 14); in turn, HIF1α is required for TRAP1-induced oncogenic transformation. These findings potentially have a very high impact, as targeting this oncogenic metabolic activity of TRAP1 may be an effective anti-neoplastic strategy.

1.3.4. Mitochondrial retrograde signaling

The discovery of oncometabolites points out the ability of mitochondria to communicate with the other components of the cell in order to coordinate a variety of cellular functions in an integrated way. The role of the nucleus in regulating mitochondrial function has been examined extensively but the importance of mitochondrial events in signaling to the nucleus, the so called mitochondrial '**retrograde signaling**', and to other cell growth mechanisms, has been relatively under-studied.

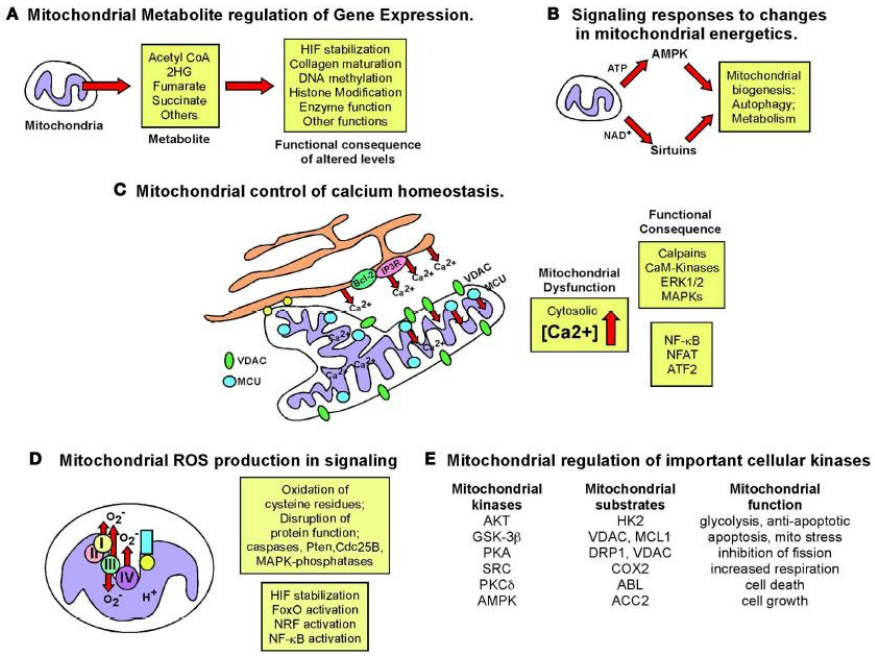

Figure 15. Retrograde signaling from mitochondria to nucleus and cytoplasm. (A) Mitochondrial control of nuclear gene expression through effects of altered production of certain metabolites, such as α-ketoglutarate and succinate, on epigenetic modification of histones, stabilization of key transcription factors, such as HIF, in addition to effects on other enzymes and proteins. (B) Altered production of NAD^+, ATP, and other changes in mitochondrial metabolism can modulate key signaling molecules in the cell, such as AMPK and the Sirtuins. (C) Mitochondria play a key role in buffering against Ca^{2+} flux into the cytosol from the extra-cellular environment or following release from the ER. Altered Ca^{2+} signaling in the cell has a strong impact on the activation of different cellular signaling cascades. (D) Mitochondrial ROS production has been one of the most extensively studied mediators of mitochondrial dysfunction and activity that elicits its effects on transcription factor activity as well as activity of key enzymes in the cell, such as caspases and phosphatases. (E) Important cellular kinases are known to localize to the mitochondria and altered mitochondrial dynamics and function may modulate the activity of these kinases not just at the mitochondria but at other sub-cellular locations if released from the mitochondria (Boland et al., 2013).

Key aspects of cellular function are influenced by signaling molecules produced and released by mitochondria as part of their normal metabolism (Fig. 15). As a consequence, altered mitochondrial physiology of cancer cells significantly reprograms the nucleus and impacts on cytoplasmic signaling pathways in ways that are important for neoplastic transformation.

It has been proposed that mitochondria and the nucleus cooperate to shape the oncogenic signaling cascade, leading to the reconciliation between the classic "gene-centric" view of cancer and the Warburg hypothesis (Frezza, 2014). Several components of the oncogenic signaling cascade affect mitochondrial function by keeping in check apoptosis and controlling mitochondrial metabolism. Although these functions are critical for shaping the cellular response to an oncogenic signal, mitochondria further integrate the signaling cascade by communicating back to the nucleus that undergoes further genetic reprogramming (Fig. 16). Events that alter any of these steps in intracellular communication contribute to the cell fate decision.

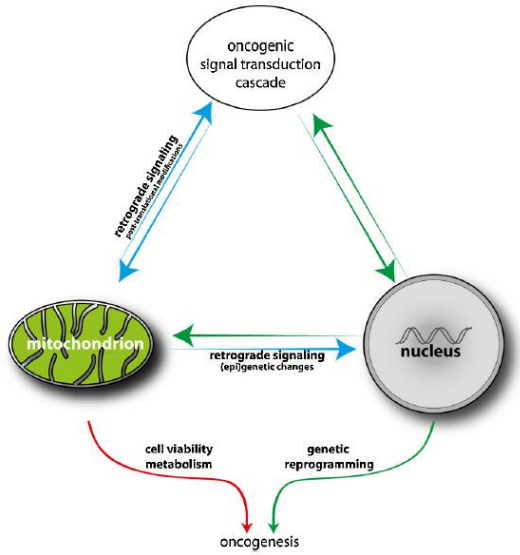

Figure 16. Mitochondria and the nucleus cooperate to shape the oncogenic signaling cascade. The classic 'gene-centric' view of cancer (green arrows) and the Warburg hypothesis (red arrows) are represented. The activation of an oncogenic signaling cascade results in the genetic reprogramming of the cells. At the same time, components of the activated signaling cascade alter mitochondrial function which, in turn, triggers a retrograde signaling response (blue arrows) that shape nuclear gene expression and the signaling cascade itself. Importantly, in some circumstances, mitochondrial dysfunction is sufficient to initiate tumorigenesis, suggesting that alterations to any of the indicated components (signal transduction, mitochondria and nucleus) are sufficient to predispose to tumorigenesis (Frezza, 2014).

1.3.5. Mitochondria as cell death modulators

The cell death machinery can be broadly divided into three classes of components — sensors, integrators (e.g. Bcl-2 family proteins) and effectors. The sensors are responsible for monitoring the extracellular and intracellular environment for conditions that influence whether a cell should live or die. These signals regulate the second class of components, which function as effectors of cell death. The sentinels include cell surface receptors that bind survival or death factors. Intracellular sensors monitor the cell's well-being and activate the death pathway in response to a variety of stress stimuli, including DNA damage, signaling imbalance provoked by oncogene action, survival factor insufficiency, or hypoxia. Further, the life of most cells is in part maintained by cell-matrix and cell-cell survival signals, whose abrogation elicits apoptosis (Hanahan and Weinberg, 2000).

Mitochondria are the cells' powerhouse, but also their suicidal powder keg. Dozens of lethal signal transduction pathways converge on mitochondria to cause the permeabilization of the mitochondrial outer membrane, leading to the cytosolic release of pro-apoptotic proteins and to the impairment of the bioenergetic functions of mitochondria (Fig. 17).

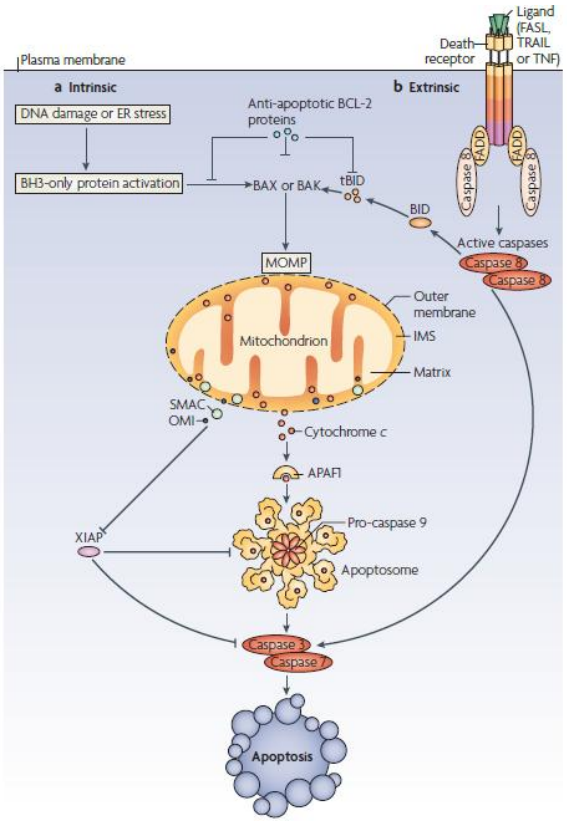

Figure 17. Intrinsic and extrinsic pathways of apoptosis. a) Intrinsic apoptotic stimuli, such as DNA damage or endoplasmic reticulum (ER) stress, activate BH3-only proteins leading to BAX and BAK activation and mitochondrial outer membrane permeabilization (MOMP). Anti-apoptotic BCL-2 proteins prevent MOMP by binding BH3-only proteins and activated BAX or BAK. Following MOMP, release of various proteins from the mitochondrial intermembrane space (IMS) promotes caspase activation and apoptosis. Cytochrome *c* binds apoptotic protease-activating factor 1 (APAF1), inducing its oligomerization and thereby forming a structure termed the 'apoptosome' that recruits and activates an initiator caspase, caspase-9. Caspase-9 cleaves and activates executioner caspases, caspase-3 and caspase-7, leading to apoptosis. Mitochondrial release of second mitochondria-derived activator of caspase (SMAC; also known as DIABLO) and OMI (also known as HTRA2) neutralizes the caspase inhibitory function of X-linked inhibitor of apoptosis protein (XIAP). b) The extrinsic apoptotic pathway is initiated by the binding of death receptors by their cognate ligands, leading to the recruitment of adaptor molecules such as FAS-associated death domain protein (FADD) and then caspase-8. This results in the dimerization and activation of caspase-8, which can then directly cleave and activate caspase-3 and caspase-7, leading to apoptosis. Crosstalk between the extrinsic and intrinsic pathways occurs through caspase-8 cleavage and activation of the BH3-only protein BID, the product of which (truncated BID; tBID) is required in some cell types for death receptor-induced apoptosis. FASL, FAS ligand; TNF, tumor necrosis factor; TRAIL, TNF-related apoptosis-inducing ligand (Tait and Green, 2010).

Moreover, opening of high conductance channels in mitochondria initiates the mitochondrial permeability transition (MPT). MPT is a universal feature of cell death and is often considered as the 'point of no return' in the cascade of events leading to cell death. The mechanisms underlying MPT are complex and reflect the key role played by mitochondria in integrating numerous endogenous and exogenous signals (e.g., cytosolic and organellar concentrations of protons, Ca^{2+}, Mg^{2+}, K^{+}, and Na^{+}, metabolites such as ATP, ADP, NAD(P), glutathione, lipid second messengers, and multiple proteins including kinases and phosphatases) (Ulivieri, 2010).

1.3.5.1. The permeability transition pore (PTP)

The mitochondrial permeability transition is an increase of mitochondrial inner membrane permeability to solutes with molecular masses up to 1500 Da. Under the conditions used in most *in vitro* studies, MPT is accompanied by depolarization, Ca^{2+} release into the cytosol, matrix swelling with inner membrane remodeling, depletion of matrix pyridine nucleotides, cessation of OXPHOS, outer membrane rupture and release of intermembrane apoptogenic proteins, including cytochrome *c*. The occurrence of swelling in isolated mitochondria, its stimulation by Ca^{2+}, phosphate (Pi) and fatty acids, its inhibition by Mg^{2+}, adenine nucleotides and acidic pH, and its detrimental effects on energy conservation, have been clearly recognized since the early studies on isolated mitochondria were carried out (Bernardi et al., 2006).

The MPT is caused by the opening of a large Ca^{2+}- and oxidative stress-activated pore, named Permeability Transition Pore (PTP), whose molecular nature is being finally delineated: the dimeric form of ATP synthase and CyP-D as regulator are currently proposed as components (Fig. 18) (Giorgio et al., 2013). Therefore, the key enzyme of life appears to be also the molecular switch that signals the presence of fully depolarized, dysfunctional mitochondria to promote cell death (Bernardi, 2013).

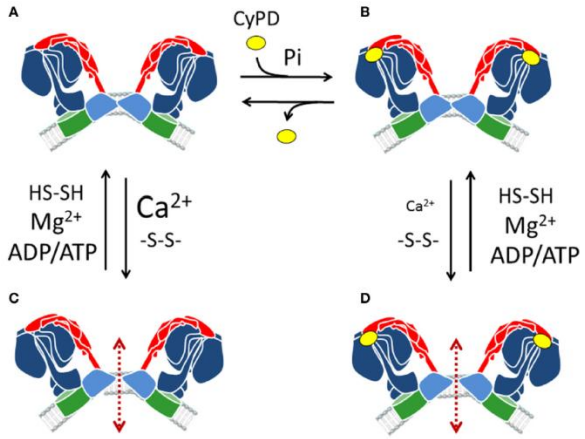

Figure 18. Hypothetical transition of F_OF_1 ATP synthase dimers to form the PTP. ATP synthase dimers (A) can undergo PTP formation when Ca^{2+} rather than Mg^{2+} is bound, possibly at the catalytic sites, in a reversible process favored by thiol oxidation (C). Binding of CyPD, which is favored by Pi (B) would increase the accessibility of the metal binding sites, allowing PTP formation at lower Ca^{2+} concentrations (as depicted here by a smaller face type) (D). Adenine nucleotides counteract PTP formation in synergy with Mg^{2+}. Red arrows denote the hypothetical pathway for solute diffusion between two F_O subunits (Bernardi, 2013).

Enhanced or inhibited MPT has been described as a feature of many human diseases such as ischemia/reperfusion, intoxication with xenobiotics, viral infections,

neurodegeneration, muscular dystrophy caused by collagen VI deficiency, cancer and many others. These diseases are favored by altered exogenous conditions (e.g., lack of oxygen, xenobiotic accumulation, pathogen infection, oxidative stress) or by mutations affecting endogenous effectors (e.g., huntingtin in Huntington disease) (Rasola and Bernardi, 2007).

1.3.5.2. Death resistance of cancer cells

Tumor cells evolve a variety of strategies to limit or circumvent apoptosis. Most common is the loss of TP53 tumor suppressor function, which eliminates this critical damage sensor from the apoptosis-inducing circuitry. Alternatively, tumors may achieve similar ends by increasing expression or function of anti-apoptotic regulators (Bcl-2, Bcl-XL) or of survival signals (growth factors, receptor tyrosine kinases), by down-regulating pro-apoptotic factors (Bax, Bim, Puma), or by short-circuiting the extrinsic ligand-induced death pathway. The multiplicity of apoptosis-avoiding mechanisms presumably reflects the diversity of apoptosis-inducing signals that cancer cell populations encounter during their evolution to the malignant state.

Apart from dysregulation in the pathways that sense apoptotic or survival stimuli, tumor cells can also modify key steps of the death execution process. Given that one of the decisive events toward cell demise is the increase of mitochondrial inner membrane permeability, cancer cells often manifest resistance against mitochondrial membrane permeabilization (Rasola and Bernardi, 2007).

Several independent mechanisms may inhibit mitochondrial permeabilization, and MPT is a key target for these regulatory devices. On theoretical grounds, these include the following: 1) alterations (e.g., up-regulation, repression) of gene expression level, resulting from genetic (e.g., amplification) or epigenetic (e.g., aberrant methylation) events; 2) loss-of-function mutations; or 3) defects in the post-translational regulation, resulting in changes of protein activity or intracellular localization/trafficking (e.g., inhibition of Bax translocation to mitochondria). All these aberrations may concern structural PTP proteins as well as MPT regulators. Altered signal transduction pathways leading to the inhibition of MPT will be discussed in the next section.

1.4. Signaling toward mitochondria

All eukaryotic cells coordinate their growth with the availability of nutrients in their environment. Signal transduction is the process by which environmental stimuli are conveyed inside a cell to induce a biological response: a ligand activates a cognate receptor that in turn prompts a chain of alterations in intracellular proteins to create a response. Signaling cascades directly regulate protein synthesis, cell growth and proliferation, metabolism, apoptosis and motility, and orchestrate post-translational modifications of proteins, mainly reversible phosphorylations, which lead to changes in interactions or subcellular localization of proteins, or to modulation of transcription. Therefore, deregulation of signal transduction pathways in tumors alters fundamental biological processes, disturbing tissue homeostasis and causing a concomitant net increase in cell number. Constitutive dysregulation of diverse transduction pathways may confer treatment resistance, since the response of cancer cells towards most cytotoxic therapies including chemo-, radio- or immunotherapy critically depends on intact signaling cascades that eventually lead to cell death. Hence, a better understanding of the molecular mechanisms that regulate cell death and survival programs in cancer cells is expected to provide the basis for the development of new and selective therapeutic strategies.

Three decades of molecular oncology have revealed that virtually every type of cancer cell displays mutations in components of the molecular pathways that transduce growth factor-derived signals. The main classes of signaling molecules that are disrupted in cancer are:

- Growth Factor receptors;
- GTPases;
- Cytosolic Serine/Threonine or Tyrosine Kinases;
- Phosphatases;
- Adaptor, chaperone and scaffold proteins.

Notably, these proteins form biochemical axes that intersect in complex networks; as a consequence, each mutation has multiple effects that impact on cell growth, proliferation, motility and survival, rendering each of these processes unrestricted by

environmental cues (Shaw and Cantley, 2006). Moreover, even if components of these signaling cascades are attractive targets for selective therapeutic interventions (Knight et al., 2010; Zhang et al., 2009), the presence of redundant circuitries can create problems of efficacy, as tumor cells can bypass the signaling cascade blocked by a specific drug; and the physiological functions of these same proteins in non-malignant cells raises important selectivity issues.

Several signaling pathways have been shown to also possess a mitochondrial branch, and both kinases and phosphatases have been found inside mitochondria. This research field is relatively new and displays numerous difficulties, first of all the absence of recognized mitochondrial import sequences in many of the cytosolic or nuclear proteins that have also been detected in mitochondria. Nonetheless, it is emerging that some crucial biological processes that occur into mitochondria can be modulated by reversible phosphorylation, under the tight control of transduction axes that originate outside the organelle. The section below illustrates how a network of phosphorylation events might control PTP by modulating the activity and localization of mitochondrial kinases and chaperones. These observations suggest that the mitochondrial pore could constitute an important downstream effector of kinase signaling pathways; in tumor cells, dysregulation of these pathways would inhibit PTP opening, contributing to the phenotype of cell death inhibition that characterizes neoplasms. Thus, components of mitochondrial signaling are attractive targets for anti-neoplastic strategies.

1.4.1. Hexokinase II (HK II)

An example of the interplay between mitochondria and cytosolic signal transduction is hexokinase (HK), an enzyme that initiates all major pathways of intracellular glucose utilization; interestingly, type II HK (HK II) couples glycolysis to OXPHOS by interacting with mitochondria, thus acting as a metabolic sensor. In highly glycolytic and extremely aggressive tumors, mitochondrial HK II activity is increased and fosters cell growth in hypoxic conditions by enhancing glycolysis, which becomes independent of oxygen availability. Furthermore, mitochondrial HK II plays an important role in maintaining the integrity of the outer mitochondrial membrane (OMM); indeed, HK II interacts with the voltage-dependent anion channel (VDAC), a protein that allows for the movement of

small metabolites across the OMM. This interaction not only facilitates glucose phosphorylation but also keeps VDAC in the open state, which counteracts OMM permeabilization. Furthermore, HK II occupies binding sites for pro-apoptotic proteins on the OMM thus preventing the release of key apoptogenic molecules from the intermembrane space (Mathupala et al., 2006).

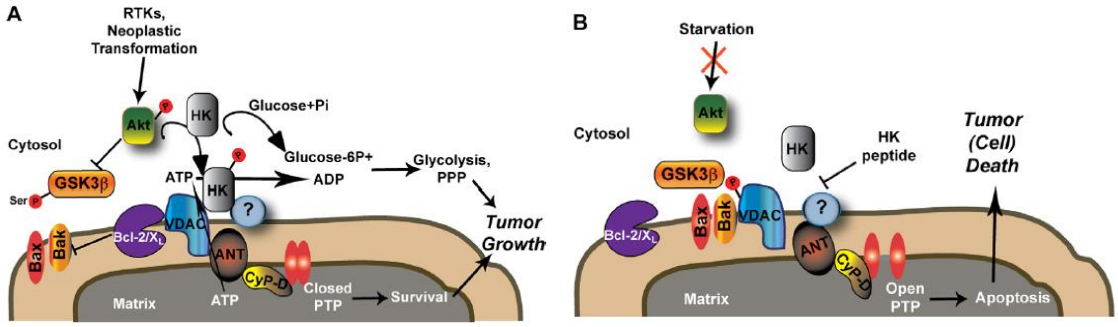

Figure 19. PTP regulation by mitochondrial hexokinase (HK). (A) Akt activation by receptor tyrosine kinases (RTKs) or during neoplastic transformation keeps HK bound to the mitochondrial surface, both through a direct HK phosphorylation and through an inactivating serine phosphorylation of GSK3β. Inactive GSK3β cannot phosphorylate VDAC, favoring its binding to HK and to anti-apoptotic Bcl-2 family proteins, and displacing the binding of pro-apoptotic Bax/Bak. However, VDAC is dispensable for HK interaction with mitochondria, suggesting that (an) unknown partner(s) is/are involved in this process. HK utilizes the ATP synthesized by mitochondria to start glucose metabolism, and stabilizes the PTP in a closed state. (B) Either Akt inactivation or treatment with a HK peptide induces HK detachment from the outer mitochondrial membrane, possibly leading to conformational changes of ANT and CyP-D and eventually to PTP opening and cell death. GSK3β is activated by Akt inhibition. The ensuing VDAC phosphorylation leads to Bcl-2/XL displacement and favors Bax/Bak activation, but PTP opening induced by HK detachment from mitochondria does not require VDAC (Rasola et al., 2010).

Notably, signal transduction pathways converge on mitochondrial HK II (Fig. 19). This is of pivotal importance in cancer, because tumor cells are endowed with hyper-activation of these same anabolic transduction pathways. The survival kinase Akt, which is activated by growth factors and is hyper-active in many tumor types, promotes HK II binding to mitochondria by phosphorylating both HK II itself and glycogen synthase kinase 3β (GSK3β), a kinase which is inhibited by this phosphorylation. Akt-dependent phosphorylation of mitochondrial HK II inhibits Ca^{2+}-induced cytochrome *c* release, and association of HK II to the OMM is favored when GSK3β is inactivated by Akt phosphorylation (Rasola et al., 2010).

Accordingly, activation of GSK3β was shown to induce release of HK II, enhancing susceptibility to cell death. This was proposed to require GSK3β phosphorylation of putative HK docking site on VDAC, which would displace Bcl-2 from its interaction with VDAC, favoring the binding between VDAC and the pro-apoptotic Bax/Bak proteins in

conditions of growth factor deprivation, resulting in increased sensitivity of mitochondria to PTP induction. However, the physiological role of GSK3-mediated phosphorylation of VDAC is unknown, as mitochondrial displacement of HK II elicits cell death also in conditions of GSK3 inhibition, in cells lacking any detectable binding between HK II and VDAC (Chiara et al., 2008), and in the absence of Bax and Bak (Majewski et al., 2004).

1.4.2. Glycogen synthase kinase 3 (GSK3)

GSK3 is a Ser/Thr protein kinase ubiquitously expressed which, at variance from the majority of kinases, is constitutively active; more than 50 substrates of GSK3 have been identified. Dysregulation of GSK3 is linked to a large number of prevalent diseases including psychiatric disorders, neurodegenerative diseases, ischemia/reperfusion injury, diabetes, and cancer. In tumors, multiple transduction pathways that are constitutively activated converge on GSK3 to induce phosphorylation at Ser 9/21 residues, leading to inhibition of GSK3 enzymatic activity. GSK3 activity is inhibited both by growth factor signaling through the PI3K pathway or the MAPK cascade, and in response to agonists that activate protein kinase A (PKA) or protein kinase C (PKC). All these signals contribute to the oncogenic process by removing the tonic inhibitory effect exerted by GSK3 on a plethora of biochemical cascades (Jope and Johnson, 2004).

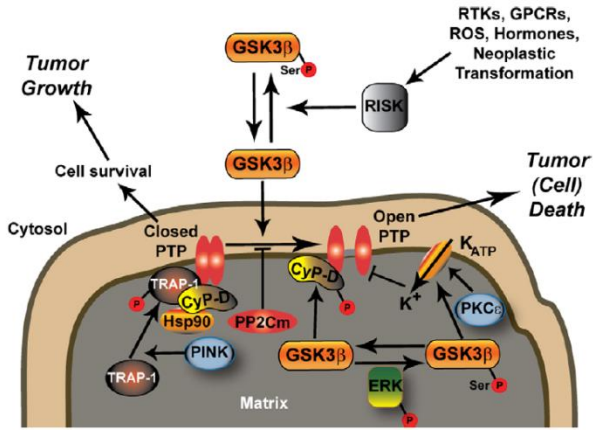

Figure 20. Several kinase pathways converge on PTP regulation. A common target is GSK3β, which is inactivated by a group of survival kinases termed RISK (reperfusion injury salvage kinases) which includes the survival kinases Akt and Erk1/2, protein kinase Cε (PKCε), protein kinase G (PKG) and p70s6K. A small pool of GSK3β is in the mitochondrial matrix, where it favors PTP opening, possibly through CyP-D phosphorylation. In tumors, mitochondrial GSK3β is inactivated by ERK-dependent phosphorylation, raising the threshold for pore opening and therefore enhancing cell survival. GSK3β inactivation, and PKCε activity, could also contribute in keeping closed the PTP by opening mitochondrial K_{ATP} channels. CyP-D regulation of the pore is also influenced by the chaperones Hsp90 and TRAP1; TRAP1 is activated by the Ser/Thr kinase PINK1. Finally, PTP opening is inhibited by the phosphatase PP2Cm through unknown mechanisms. RTKs: receptor tyrosine kinases; GPCRs: G protein coupled receptors (Rasola et al., 2010).

As is the case for HK II localization on the OMM, in mitochondria GSK3 controls the localization and the activation status of a number of proteins of the cell death machinery. Beside this, it has been established that a fraction of GSK3 resides in mitochondria where it contributes to the regulation of energy metabolism and PTP opening (Chiara and Rasola, 2013). Indeed, it has been observed that cyclophilin D (CyP-D), a mitochondrial chaperone that regulates the PTP, is directly phosphorylated by GSK3 on Ser/Thr residues therefore sensitizing PTP to opening (Fig. 20). The mitochondrial fraction of GSK3 is in turn regulated by a portion of the kinase ERK, which also locates in the mitochondrial matrix in diverse neoplastic cell types. Mitochondrial ERK inhibits GSK3 by Ser phosphorylation, thus conferring resistance to death stimuli acting as PTP inducers. In accordance to this, ERK inhibition increases GSK3-dependent phosphorylation of CyP-D and sensitization of PTP to opening, thus significantly abolishing tumor cell protection from apoptosis, whereas pharmacological inhibition of GSK3 protects from PTP opening (Rasola et al., 2010).

1.4.3. Extracellular signal regulated kinase (ERK)

As we have illustrated above, a small portion of both ERK and GSK3 is located in the mitochondrial matrix in several neoplastic cell models, and both kinases directly interact with CyP-D. Mitochondrial ERK is constitutively active after v-Ki-Ras dependent transformation or in diverse tumor models, conferring resistance to death stimuli acting as PTP inducers (Rasola et al., 2010). This protection can be ablated by inhibiting ERK with the drug PD98059 or with a selective ERK activation inhibitor peptide. Notably, these treatments enhance GSK3-dependent phosphorylation of CyP-D and PTP opening, and the effect on the pore is increased after CyP-D overexpression and absent in CyP-D knock-out cells. Conversely, ERK activation prompts the inhibitory phosphorylation of GSK3 and abolishes CyP-D phosphorylation, therefore protecting from PTP opening.

Thus, in diverse tumor cell models cell death susceptibility is modulated by the activity of mitochondrial ERK, which could directly impinge upon pore opening through the negative regulation of CyP-D phosphorylation by inhibiting the mitochondrial pool of GSK3. Mitochondria-specific ERK activation might provide a key advantage during neoplastic transformation, by placing the death/survival mitochondrial rheostat in an anti-apoptotic

mode, and it is highly probable that further mitochondrial targets of ERK could contribute to this process. To make this picture more complex, it must be highlighted that ERK is a GSK3 priming kinase, requiring the activity of a second kinase for complete GSK3 inhibition, and that GSK3 itself needs a priming kinase to phosphorylate its targets. Moreover, these reactions must be finely tuned by the action of phosphatases (Rasola et al., 2010).

1.4.4. Mitochondrial chaperones: CyP-D and TRAP1

Molecular chaperones are involved in the correct folding of nascent polypeptides and in the productive assembly of multimeric protein complexes, while minimizing the danger of aggregation in the protein-rich intracellular environment. These proteins are also involved in the conformational changes associated to molecular dynamics, as in the case of propagation of signals through reversible phosphorylations, and in the regulation of protein degradation and turn-over (Akerfelt et al., 2010). Given the importance of these processes in protecting cells against harsh conditions (e.g., heat shock or oxidative stress) deregulation of chaperone activity could play a central role in different types of disease, among which cancer. Moreover, the localization of some chaperones is restricted to mitochondria suggesting the presence of mechanisms of control of protein activity which are organelle-specific.

Cyclophilin D is a chaperone located in the mitochondrial matrix, endowed with a peptidyl-prolyl *cis-trans* isomerase activity. CyP-D is one of the best studied regulators of the PTP, and it sensitizes it to opening. However, the pore is still present in mitochondria and cells obtained from mice where the gene encoding CyP-D was knocked-out. CyP-D ablation increases the Ca^{2+} load required to open the PTP, unmasking inhibition by Pi, and abolishes sensitivity to the CyP-D ligand CsA, conclusively demonstrating that CyP-D is an important regulator of the PTP, but not a component of the channel (Baines et al., 2005; Basso et al., 2005). However, in some models CyP-D overexpression reportedly desensitizes cells from apoptosis (Schubert and Grimm, 2004) suggesting that CyP-D regulation of the PTP is not dictated only by the protein level but also by possible post-translational modifications. We have previously described how its action can be

modulated by phosphorylations events (Fig. 20); moreover, it has been recently reported that CyP-D is also target of Sirtuin-3 deacetylation (Shulga et al., 2010).

A chaperone homologous to heat shock protein 90 (Hsp90), termed tumor necrosis factor receptor-associated protein-1 (TRAP1), is highly expressed in mitochondria of tumor cells and of nervous tissue, whereas it is absent or expressed to a lower level in most normal tissues. Both TRAP1 and the mitochondrial fraction of Hsp90 interact with CyP-D and antagonize its function of PTP sensitization (Kang et al., 2007). TRAP1 knockdown enhances cell death, whereas TRAP1 overexpression confers resistance to pro-apoptotic drugs, suggesting that TRAP1 is a novel mitochondrial survival factor that acts as PTP inhibitor, and constitute a possible target of mitochondria-directed chemotherapeutics (Kang and Altieri, 2009). Importantly, TRAP1 was shown to be substrate of the Ser/Thr kinase PTEN induced kinase 1 (PINK1), and this phosphorylation was required to prevent oxidative-stress-induced apoptosis (Pridgeon et al., 2007).

Altogether, these results further indicate that phosphorylation events can be crucial in the regulation of the PTP, and molecular chaperones as TRAP1 and CyP-D might be a link between kinase pathways and the pore. Furthermore, this could have important pathogenic implications, especially in tumors, where TRAP1 overexpression could substantially contribute to PTP desensitization to several insults.

1.4.5. Neurofibromatosis type 1

A group of tumors characterized by dysregulated signaling pathways which can also converge toward mitochondria are typical of a genetic disorder called Neurofibromatosis type 1 (NF1). NF1, also referred to as peripheral neurofibromatosis or Von Recklinghausen's disease, is one of the most common human genetic diseases. It has an incidence of one in 3000-4000 individuals and equally affects males and females, as it is inherited as an autosomal-dominant trait. Spontaneous mutations occur in 50% of cases; therefore, the *NF1* locus may represent a mutational hotspot in the human genome. All affected individuals are heterozygous for loss-of-function mutations in *NF1* gene; because homozygosity in murine models has been shown to be lethal to embryos (Jacks et al., 1994), it is believed that one functional *NF1* allele is necessary for survival. Some individuals demonstrate NF1 features in a localized pattern; this syndrome is termed

segmental neurofibromatosis, and this phenotype is likely owing to a postzygotic, somatic mutation of the *NF1* gene in an early stage of fetal development (somatic mosaicism).

Diagnostic criteria for neurofibromatosis 1 (NFI)[a]

Two or more of the following features must be present for an individual to be diagnosed with NF1:

- Six or more café-au-lait spots with diameters greater than 0.5 mm before puberty or 1.5 cm after puberty
- Two or more neurofibromas or a single plexiform neurofibroma
- Freckling in the axillary and inguinal regions (Crowe's sign)
- Optic pathway tumor
- Lisch nodules (hamartomas of the iris)
- A distinctive bony lesion: dysplasia of the sphenoid bone or dysplasia/thinning of long bone cortex
- A first-degree relative diagnosed with NF1.

a Gutmann, D.H. *et al.* (1997). The diagnostic evaluation and multidisciplinary management of neurofibromatosis 1 and neurofibromatosis 2. *J. Am. Med. Assoc.* 278, 51–57

Table 1. Diagnostic criteria for neurofibromatosis type 1 (Gutmann et al., 1997).

NF1 displays a 100% penetrance, but expressivity is extremely variable. Patients affected by this disease show defects in tissues derived from the neural crest, which lead to a wide spectrum of phenotypic manifestations, including developmental, pigment and neoplastic aberrations (Cichowski and Jacks, 2001). Some diagnostic criteria have been established (Gutmann et al., 1997) (Table 1) and they include aberrant pigmentation of the skin (café au lait macules), freckling in non-sun-exposed regions, benign pigmented hamartomas of the iris (Lisch nodules), and malformations of the skeletal and cardiovascular systems.

Key clinical features of Neurofibromatosis type I

Skin	*Neurologic*
Café au lait macules	UBO on MRI
Axillary and inguinal freckling	Learning disabilities
Dermal neurofibroma	Seizure
Plexiform neurofibroma	Mental retardation
Juvenile xanthogranuloma	Aqueduct sternosis
Neoplasia	*Skeletal*
Optic glioma	Macrocephaly
MPNST	Sphenoid wing dysplasia
Pheochromocytoma	Scoliosis
Juvenile chronic myelogenous leukemia	Spinal bifida
Other CNS tumors (astrocytoma)	Pseudoarthrosis
Rhabdomyosarcoma	Thinning of long bone cortex
Duodenal carcinoid	Absence of patella
Somatostatinoma	Vertebral disc dysplasia
Parathyroid adenoma	Short stature
Cardiovascular	*Eyes*
Hypertension	Lisch nodules
Pulmonic sternosis	Hyperterrorism
Renal artery sternosis	Glaucoma
Gastrointestinal	*Psychiatric*
Constipation	Heavy psychosocial burden

Abbreviations: CNS, central nervous system; MPNST; malignant peripheral nerve sheath tumor; UBO: unidentified bright object.

Table 2. Key clinical features of Neurofibromatosis type 1 (Le and Parada, 2007).

NF1 patients are also at a higher risk of developing certain tumors, most notably optic pathway gliomas and neurofibromas, and exhibit a less penetrant variety of additional pathologies of the skin, nervous system, bones, endocrine organs, blood vessels and the eyes (Le and Parada, 2007) (Table 2). Furthermore, learning disabilities are one of the most common features in children with NF1, seen in 40% to 60% of patients; this is often accompanied by attention deficit disorder (Gutmann et al., 1997).

1.4.6. Neurofibromin structure and function

Neurofibromin is the protein product of *NF1* gene which is located on human chromosome 17q11.2 and was identified by positional cloning in 1990 (Ballester et al., 1990; Xu et al., 1990). It spans over 350kb of genomic DNA and has 60 exons. The *NF1* gene produces an 11- to 13-kb messenger ribonucleic acid (mRNA) that is expressed in almost all tissues (Wallace et al., 1990). There are alternatively spliced NF1 mRNA isoforms, and, depending on the tissue, they are differentially expressed (Daston et al., 1992). Neurofibromin is a large peptide (about 250 kDa) composed by 2818 amino acids in humans and 2820 amino acids in mice (Gutmann et al., 1991). It is ubiquitously expressed during embryonic development and it is also present in a variety of cell types in adults (Gutmann et al., 1995), but it is most abundant in the nervous system, where it is found in neurons, oligodendrocytes, and Schwann cells (Daston et al., 1992).

Sequence analysis of neurofibromin reveals a region of homology with the catalytic domain of the mammalian p120-Ras-GAP, a GTPase-activating protein (GAP) for the Ras family of proto-oncogenes (Xu et al., 1990). Moreover, neurofibromin shows an extended similarity with the *Saccharomyces cerevisiae* Ras-GAP proteins IRA1 and IRA2 (Ballester et al., 1990). Exons 20-27a of neurofibromin encode this “GAP related domain” (GRD), which induces the conversion of Ras from its active GTP-bound conformation to its inactive GDP-bound form (Fig. 21).

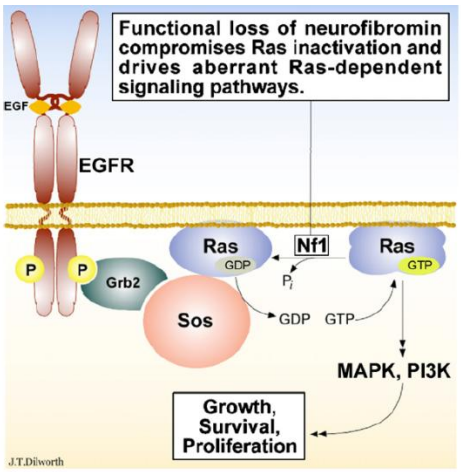

Figure 21. Loss of neurofibromin deregulates Ras signaling. In response to growth factors, receptor tyrosine kinases (in the example EGFR) recruit a guanine nucleotide exchange factor Sos, which activates Ras. In its active, GTP-bound, form, Ras initiates several signaling cascades, including the MAPK and PI3K pathways, in order to regulate cell growth, survival, and proliferation. Functional loss of neurofibromin compromises Ras inactivation and drives aberrant Ras-dependent signaling, which contributes to tumor formation and progression (Dilworth et al., 2006).

Ras is activated at the plasma membrane upon binding of growth factor receptors to specific ligands, triggering the recruitment of a complex containing the adapter protein growth factor receptor bound protein 2 (Grb2) and the Ras guanine nucleotide exchange factor Sos, which catalyzes Ras switch to its GTP-bound state. This active form of Ras then binds and activates the kinase Raf and phosphatidylinositol 3-kinase (PI3K), which are the apical inducers of two kinase signaling cascades (Fig. 22) (Le and Parada, 2007). Neurofibromin, via its GRD, exerts a reverse effect on Ras by increasing its GTP hydrolysis rate; as an unrestrained Ras activity is a major oncogenic determinant (see section 1.2.1.5) neurofibromin acts as a tumor suppressor protein. Many *NF1*-deficient tumors exhibit elevated levels of Ras-GTP, supporting the observation that neurofibromin is a key regulator of Ras signaling. Moreover, direct inhibition of Ras (with farnesyltransferase inhibitors) or of Ras pathway molecules (with MEK and AKT inhibitors) as well as replacement of the *NF1*-GRD reverses the proliferative phenotype of *NF1* deficient cells (Hiatt et al., 2001; Kim et al., 1997). These results strongly suggest that the tumorigenic potential conferred by loss of neurofibromin at least partially results from the growth advantage provided by dysregulated Ras activity.

Moreover, dysregulation in the Ras signaling pathway has been shown to play a key role in another clinical manifestation of NF1 patients: learning and memory disabilities. Indeed, $Nf1^{+/-}$ mice present learning deficits (Costa et al., 2002; Li et al., 2005), with increased GABA (γ-amino butyric acid)-mediated inhibition and specific deficits in long-

term potentiation, which can be reversed by decreasing Ras function by genetic and pharmacological manipulations. These results indicate that increased Ras activity, as a consequence of *NF1* mutations, is at least partially responsible for the learning and memory disabilities seen in *Nf1* mutant mice and, by analogy, suggest a link to the intellectual deficits described in patients.

The connection between *NF1* loss and the presence of learning deficits has also been related to the ability of neurofibromin to associate with **microtubules**, which are expressed at high level in axonal and dendritic processes of neurons. Interestingly, it has been shown that the region of the protein that is critical for this interaction resides within the GRD (Xu and Gutmann, 1997). Although microtubules may be important for neuronal connection and neurite outgrowth, the exact function of neurofibromin relative to microtubules is still under investigation. In regard to this, a recent work has demonstrated that neurofibromin interacts with the cytoplasmic Dynein Heavy Chain1 (DHC) and is involved in the correct localization of melanosomes along microtubules in melanocytes (Arun et al., 2013). This finding indicates a functional role of neurofibromin in melanosome localization which sheds insight into a possible molecular mechanism underlying Café au lait macules formation in NF1 affected individuals.

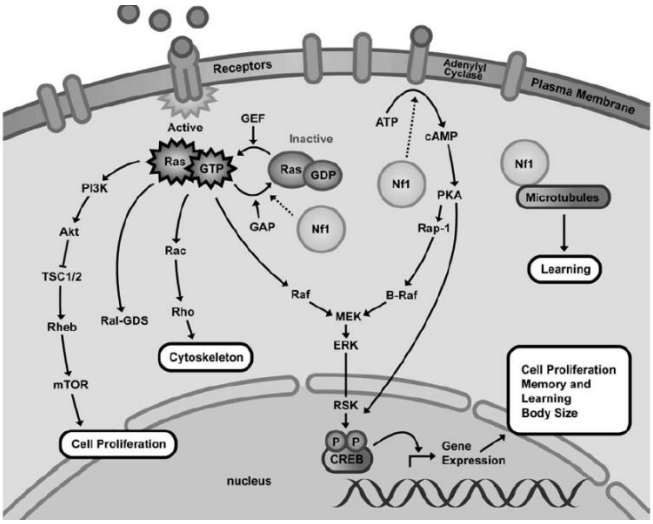

Figure 22. Interactions of neurofibromin with different cell signaling pathways. Neurofibromin accelerates inactivation of active GTP-bound Ras; therefore, Nf1 loss results in increased Ras activity and dysregulated cell growth. Neurofibromin may also be required for cAMP- and PKA-mediated gene transcription. In addition, it also associates with microtubules (Trovo-Marqui and Tajara, 2006).

The Ras-GAP domain of neurofibromin comprises only 10% of the entire polypeptide, which has raised the possibility that other regions of the molecule are important for

modulating cell growth or other processes related to NF1 disease. Initial studies in *Drosophila melanogaster* have shown that neurofibromin regulates G-protein-stimulated **adenylate cyclase (AC)** activity. The *Drosophila* NF1 protein is highly conserved, showing 60% identity of its 2803 amino acids with human NF1. Unlike *Nf1*-deficient mice, *Nf1* null mutant flies are viable and fertile; however, they are smaller in body size and this phenotype can be rescued, not by attenuating Ras activity but by increasing cAMP production through an increased expression of activated protein kinase A (PKA) (The et al., 1997). Thus, NF1 and PKA appear to interact in a pathway that controls the overall growth of *Drosophila*. Moreover, at the neuromuscular junction of *Drosophila*, neurofibromin is essential for the activation of the AC/cAMP pathway following neuropeptide stimulation which acts on G-protein-coupled receptors (Guo et al., 1997). Beside this, the cAMP concentration was significantly lower in extracts of mouse *Nf1*$^{-/-}$ neurons stimulated with GTPγS, a non-hydrolyzable or slowly-hydrolyzable G-protein-activating analog of guanosine triphosphate, providing the first evidence that neurofibromin has additional functions beside Ras regulation also in mammalian cells (Tong et al., 2002). Because *Drosophila* mutants in adenylyl cyclase activity showed learning and short-term memory defects, NF1 was hypothesized to affect learning through its control of the AC/cAMP pathway. Indeed, it has been shown that NF1-dependent activation of the adenylyl cyclase pathway is essential for mediating *Drosophila* learning and short-term memory, and that NF1 affects these processes independently of its developmental effects observed in mutant flies (Guo et al., 2000). These results suggest that some of the NF1 clinical abnormalities, such as short stature and learning disabilities, may also result from non-Ras neurofibromin functions in specific cell types whereas other features, like tumor formation, involve hyper-activation of Ras. Collectively these findings argue that defects in neurofibromin function may affect different intracellular signaling pathways which depend on the cell type.

To date, neurofibromin is known to have an additional functional domain, the **Sec14p-like domain** (Aravind et al., 1999) which is located between amino acids 1545-1816 (Fig. 23) and is homologous to the yeast Sec14p, a protein involved in the regulation of intracellular proteins and lipid trafficking. This domain belongs to a bipartite structural module that includes also a **pleckstrin homology (PH)-like domain** which is considered

responsible for the regulation of the neighboring NF1-Sec domain. Even though the biological role of Sec14p domain in NF1 is currently unknown, prediction of a Sec14p-like lipid binding domain in neurofibromin opens new lines of investigation of its Ras-GAP function in terms of regulation by lipids, and suggests that neurofibromin can be involved in other transduction pathways.

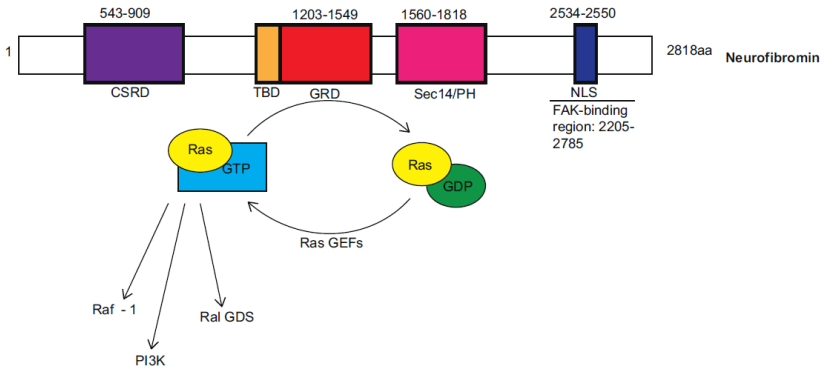

Figure 23. Diagram illustrating known functional domains within neurofibromin. Domains are indicated as follows: CSRD, cysteine/serine-rich domain; TBD, tubulin-binding domain; GRD, GAP-related domain; Sec14/PH, Sec14-homologous domain and pleckstrin homology domain; NLS, nuclear localization sequence. Numbers above each subdomain indicate the positions of the corresponding amino acids within the 2818 amino acid length of the human neurofibromin protein (Brossier and Carroll, 2012).

1.4.7. Neurofibromin localization

Even though the Ras-GAP activity currently appears to represent the only clearly defined biochemical function of this giant protein, a number of interaction partners of neurofibromin have been reported: PKA, protein kinase C (PKC), caveolin-1, focal adhesion kinase, tubulin, amyloid precursor protein, syndecan, kinesin-1, nuclear PML-bodies, the UBX-UBD protein ETEA and p97/VCP. Neurofibromin could interact with different partners also depending on its dynamic intracellular movement which regulates not only protein localization, but also protein function. Neurofibromin appears to be predominantly cytoplasmic, with different cell types displaying a variable subcellular localization. Some studies have also observed neurofibromin in the nucleus as it contains a nuclear localization sequence (NLS) at the C-terminus (Vandenbroucke et al., 2004). The possible function of neurofibromin within the nucleus remains unknown. Translocation to the nuclear compartment could be a mechanism to regulate the GAP function of neurofibromin by sequestration in the nucleus, as Ras is located at the plasma membrane.

It is possible that during development, the subcellular targeting of neurofibromin depends on posttranslational modifications, such as phosphorylation, to regulate the targeting of proteins. Indeed, neurofibromin contains multiple PKA and PKC serine or threonine phosphorylation consensus sites which are located within the N-terminus of neurofibromin and, in particular, in the cysteine-rich domain (CSRD). EGF stimulation was shown to increase the association of neurofibromin with actin through a PKC-dependent phosphorylation of neurofibromin. Moreover, this modification increases the Ras-GAP activity of neurofibromin (Mangoura et al., 2006).

1.4.8. Neurofibromin degradation

Neurofibromin is dynamically regulated by the proteasome, and its degradation and re-expression are essential for maintaining appropriate levels of Ras-GTP (Cichowski et al., 2003). Degradation is rapidly triggered in response to a variety of growth factor and requires sequences adjacent to the catalytic GAP-related domain of neurofibromin. However, whereas degradation is rapid, neurofibromin levels are re-elevated shortly after growth factor stimulation. Accordingly, Nf1-deficient mouse fibroblasts exhibit an enhanced activation of Ras, prolonged Ras and ERK activities, and proliferate in response to sub-threshold levels of growth factors. Thus, the dynamic proteasomal regulation of neurofibromin represents an important mechanism of controlling both the amplitude and the duration of Ras-mediated signaling. Like p53, neurofibromin can be inactivated in cancer by both mutations and excessive proteasomal destruction; however, little is known about the mechanisms that underlie this latter process. Only recently it has been shown that the E3 ligase Cullin 3 and the BTB adaptor protein KBTBD7 control the regulated proteasomal degradation of neurofibromin and are responsible for the pathogenic destabilization of neurofibromin in some glioblastoma cell lines (Hollstein and Cichowski, 2013).

1.4.9. NF1 as a tumor predisposition syndrome

NF1 is a genetic condition that increases the predisposition to tumor development. The most common tumor seen in individuals with NF1 is the neurofibroma, followed by optic pathway glioma which is seen in 15-20% of children with NF1. Moreover, NF1 patients can develop malignancies among which pheochromocytomas, juvenile chronic

myelogenous leukemia, malignant astrocytoma, rhadomyosarcoma of the genito-urinary tract, duodenal carcinoid, somatostatinoma and parathyroid adenoma (Le and Parada, 2007). The fact that not all NF1 patients succumb to malignancy implies that other genetic and non-genetic factors greatly influence NF1-associated tumor susceptibility.

Given the role of neurofibromin in regulating Ras activity, *NF1* gene is considered a tumor suppressor, even if a rigorous testing of this is still lacking. *Nf1*$^{+/-}$ mice are tumor prone and develop two of the malignancies associated with NF1: pheochromocytoma and myeloid leukemia (Jacks et al., 1994). In both tumor types, loss of the wild-type allele has been observed at high frequency. Moreover, both copies of the *NF1* gene are mutated in most of NF1 tumors and studies have correlated inactivation of both *NF1* alleles with deletions of the somatic *NF1* gene for benign cutaneous neurofibromas, plexiform neurofibromas, malignant peripheral nerve sheath tumors, pheochromocytomas, and juvenile myelomonocytic leukemias from NF1 patients (Gottfried et al., 2006).

Spectrum of *NF1* gene mutations[a]

Type of mutations	No. of reported independent occurrences
Chromosome rearrangements	9
Deletions of the entire gene	38
Single- and multi-exon deletion	42
Small intragenic deletions	63
Large insertions	3
Small insertions	29
Direct stop mutation (nonsense)	51
Amino acid substitution (missense)	31
Mutation in introns	26
Alteration of the 3′ untranslated region	4
Nonpolymorphic silent base exchanges	4
Total	300

[a] Originally from the National Neurofibromatosis Foundation International NF1 Genetic Analysis Consortium Database (188, 194).

Table 3. Inactivation of *NF1* gene (Gottfried et al., 2006).

Second hit inactivation of the remaining allele may occur through several different mechanisms: chromosome rearrangements, deletion of the entire gene, intragenic deletions, insertions and mutations. Furthermore, mutations may occur in noncoding regions, and methylation or transcription repression could silence *NF1* gene expression without a mutation. Point mutations affecting the correct splicing of the *NF1* gene are a common cause of NF1 (Ars et al., 2000), and they are responsible for both somatic and germline mutations. Most mutations in NF1 patients are thought to result in truncation of the protein product, which would result in an inactive protein and decreased amounts of

active neurofibromin. Small intragenic deletions and insertions account for a third of all mutations (Table 3).

Particular mutations are not typically associated with distinct phenotypic expressions of NF1, and several studies have been unable to find any genotype-phenotype correlation. The marked clinical variability between multiple affected relatives with the same germline mutation may be owing to the nature, timing, and location of the second hit mutation at the NF1 locus. Variants of other unknown genes may also modify the expression of the disease and result in distinct phenotypes. Moreover, somatic mosaicism is another potential cause of inter-individual phenotypic variation.

1.4.10. Neurofibromas

The hallmark feature of the disease is the formation of multiple peripheral nerve sheath tumors, neurofibromas, which can arise as dermal lesions or grow internally along the plexus of major peripheral nerves. While these lesions are benign, they can be debilitating and deforming. In addition, a subset of these tumors can progress to malignant neurofibrosarcomas. Neurofibromas are rarely present in childhood, but develop during puberty and pregnancy, suggesting a hormonal influence on tumor growth.

- Dermal Neurofibromas

The most common type of neurofibroma can arise from small nerve radicals or larger nerve branches and grow as discrete lesions in the dermis or epidermis ranging from 0.1 to several centimeters in diameter. They are collectively called dermal neurofibromas and patients can develop thousands of them which, depending on location, can be painful and disfiguring. One of the key features of neurofibromas is their heterogeneity as they are composed of all cell types normally found in the peripheral nerve (Fig. 24). However, the structure of the nerve fascicle seems to be highly disorganized, with increased number of Schwann cells and fibroblasts, increased collagen deposition, extensive mast cell infiltration and disruption of the perineurium. Moreover, unlike in the normal nerve, the majority of Schwann cells in neurofibromas are found dissociated from axons and axonal degeneration is present.

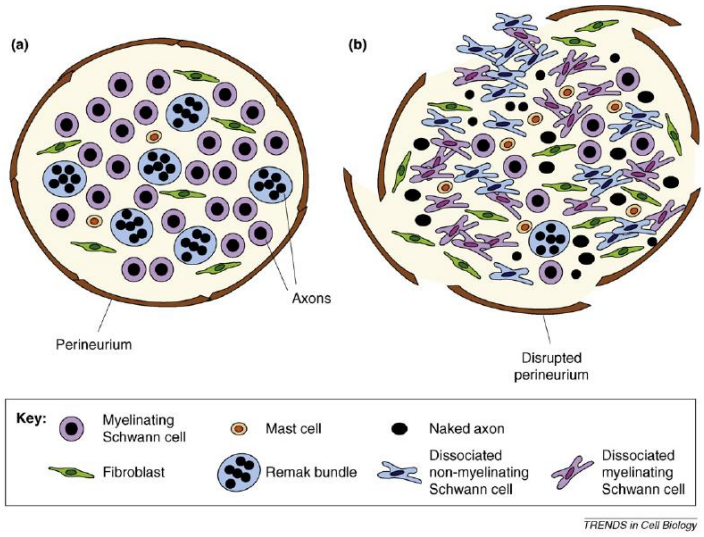

Figure 24. Structure of normal nerves and neurofibromas. Diagram showing a cross-section of (a) a normal nerve fascicle and (b) the aberrant structure of nerve fascicles in neurofibromas (Parrinello and Lloyd, 2009).

- Plexiform neurofibromas

In contrast to dermal neurofibromas, which are typically small, plexiform neurofibromas can develop internally along the plexus of major peripheral nerves and become quite large, involving an entire limb or body region. They occur in about 30% of NF1 individuals and are considered as congenital lesions. While these are benign tumors, they can be debilitating and can progress to malignancy. Indeed, plexiform neurofibromas harbor a 5% lifetime risk of transformation into malignant peripheral nerve sheath tumors (MPNSTs). These are highly malignant and metastatic cancers with a high mortality and a poor response to chemotherapy and radiation. The difference in the mechanism of tumorigenesis between cutaneous neurofibromas and plexiform is unclear; however, the timing of their development as well as their growth properties may indicate differences in the mechanism of tumor initiation.

1.4.10.1. Origin of neurofibromas

The molecular mechanisms underlying tumor development in NF1 have been obscure. Although second hit mutations affecting the inherited wild-type NF1 allele have been clearly identified in the myeloid leukemias and pheochromocytomas in NF1 patients, such mutations have been reported for only a small number of neurofibromas. The difficulty in detecting mutations may be due in part to the complex nature of these lesions, which are composed of multiple cell types, not all of which are expected to develop a second

mutation. Moreover, it has also been suggested that NF1 heterozygosity may be sufficient for development of benign neurofibromas (haplo-insufficiency), with full loss of NF1 function being restricted to the progression to MPNSTs.

Research over the past decade using mouse models has greatly enhanced our knowledge of neurofibroma development and malignant progression in NF1. The mouse and human *NF1* genes are highly related, the amino acid sequence of neurofibromin is 98% identical, and there is also significant similarity between the non-coding regions of the mRNA. Mice homozygous for null *Nf1* mutation in exon 31, a region that is often mutated in human NF1 patients, are embryonic lethal at E13.5 secondary to defective heart and malformation of the major cardiac outflow tracts. Defects in renal, hepatic and skeletal muscle development were also observed; however, nervous system pathology was limited to enlargement of sympathetic ganglia secondary to neuronal hyperplasia (Brannan et al., 1994; Gottfried et al., 2006; Jacks et al., 1994). Heterozygous *Nf1* mutant mice are viable and only have increased incidence of pheochromocytomas and myeloid leukemias beyond 10- to 12-month old; however, they do not develop peripheral nerve sheath tumors or other characteristic symptoms of human NF1. One possible explanation for this observation is that LOH necessary for neurofibroma development is impaired in mice. Perhaps, given the shorter time of gestation and lifespan compared with humans, the $Nf1^{+/-}$ mice do not have the necessary window of opportunity to undergo effective LOH in target cells to initiate neurofibroma formation. Cichowski et al. (1999) addressed this issue elegantly when they created chimeric mice by injecting $Nf1^{-/-}$ ES cells into wild-type blastocysts. These mice developed microscopic plexiform neurofibromas derived from the injected ES cells, demonstrating the requirement of *Nf1* homozygosity for tumor formation. However, the degree of chimerism in these mice occurs randomly and cannot be controlled genetically. As a result, it was difficult to establish the target cell or whether other cell types contribute to the tumorigenesis.

As in human neurofibromas Schwann cells were the most common cell type present in neurofibromas it was hypothesized that this cell type, or their precursors, could be the initiating cell for tumor development. Schwann cell-specific *Nf1*-deficient mice were derived by crossing $Nf1^{flox/flox}$ mice with the *Krox20-cre* transgenic mice, an embryonic Schwann cell-specific promoter (Zhu et al., 2002). Mice with a conditional knockout of *Nf1*

only in embryonic Schwann cells, but wild-type in all other cell lineages (*Nf1*$^{flox/flox}$; *Krox20-Cre*), exhibit microscopic hyperplasia in sensory ganglia but do not develop neurofibromas. However, when mice homozygous for *Nf1* mutation (*Nf1*$^{-/-}$) in Schwann cells but heterozygous for *Nf1* (*Nf1*$^{+/-}$) in all other somatic cells (*Nf1*$^{flox/-}$; *Krox20-Cre*) were generated, these mice developed multiple classic plexiform neurofibromas with a massive degranulating mast cell infiltration, modeling human neurofibroma (Table 4). These genetic studies implied the Schwann cell origin for neurofibroma. Nevertheless, in addition to nullizygosity at *Nf1* locus in Schwann cells, haploinsufficiency of Nf1 in the tumor microenvironment is also required for the tumorigenesis.

Genetically engineered mouse models of PNS neoplasia.

	Transgenic mouse model	Phenotype	Limitations
Early models	*Nf1* $^{\Delta 31/\Delta 31}$	Die by E13.5 due to cardiac failure	Early death prevents observation of tumorigenic effects of *Nf1* loss
	Nf1 $^{\Delta 31/+}$	Develop pheochromocytomas (15% incidence); show accelerated development of other non-NF1 tumors as compared to wild-type mice	No neurofibromas or MPNSTs observed
	Nf1 $^{-/-}$; *Nf1* $^{+/-}$ chimeras	Multiple plexiform neurofibromas present in animals with intermediate level of chimerism	Cannot control which cell types are *Nf1* $^{+/-}$ and which are *Nf1* $^{-/-}$
	Nf1 $^{flox/flox}$; *Krox20-Cre*	Schwann cell hyperplasia	No neurofibromas or MPNSTs observed
	Nf1 $^{flox/-}$; *Krox20-Cre*	Plexiform neurofibroma development by 1yr of age (demonstrating importance of both *Nf1* $^{+/-}$ and *Nf1* $^{-/-}$ cells in neurofibroma formation)	*Krox20* promoter is expressed in Schwann cells and boundary cap cells, making it hard to identify a clear progenitor

Table 4. Genetically engineered mouse models of neurofibroma formation (part 1). Both nullizygosity at *Nf1* locus in Schwann cells and haploinsufficiency of NF1 in the somatic tissue are required for neurofibroma (Brossier and Carroll, 2012).

1.4.10.2. Timing in *Nf1* loss

Even though it is well established that neurofibromas arise from Schwann cells that undergo loss of heterozygosity (LOH) at the NF1 locus, the specific cell type within the Schwann cell lineage in which this occurs has been the topic of much debate. The Schwann cell lineage is well characterized and specific markers for the different cell types within the lineage have been identified. Schwann cells originate from migrating **neural crest stem cells (NCSCs)** and develop through two sequential, intermediate glia-committed stem/progenitor cell types, called Schwann cell precursors and immature Schwann cells (Fig. 25) (Mirsky et al., 2008). Around birth, immature Schwann cells differentiate into the two main mature Schwann cell types of the peripheral nerve, myelinating and non-myelinating Schwann cells. The former myelinate single large-caliber axons and the latter wrap multiple small-caliber axons in structures known as Remak

bundles. Importantly, Schwann cell progenitors differentiate by late gestation and do not persist in the adult peripheral nervous system. Instead, upon nerve injury, the requirement for new cells is met by the regenerative ability of mature differentiated Schwann cells to transiently de-differentiate to a progenitor-like state (Parrinello and Lloyd, 2009).

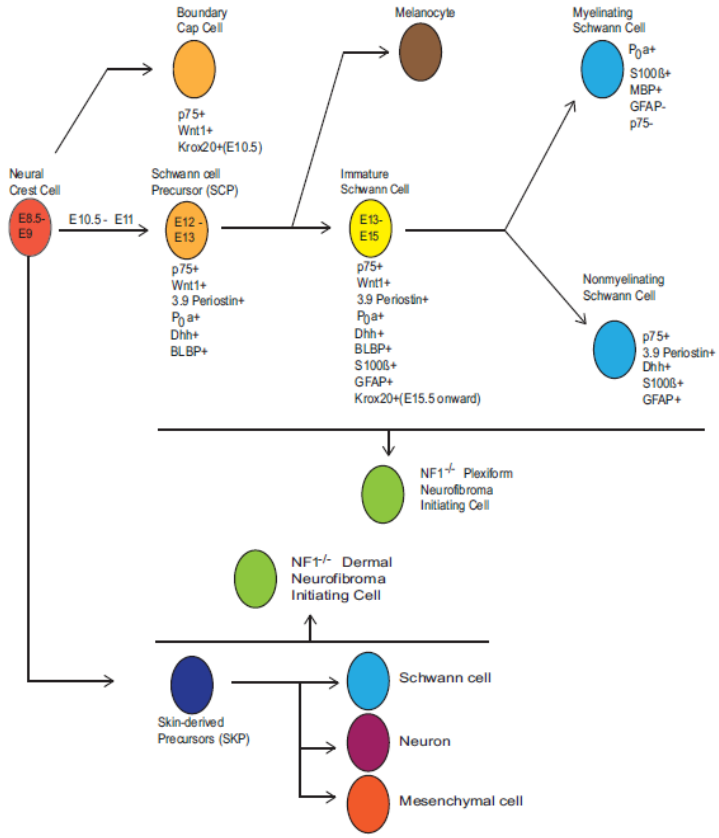

Figure 25. Schwann cell development. Neural crest cells give rise to a series of cell types in the Schwann cell lineage, one or more of which can become a neurofibroma initiating cell (NIC) following biallelic NF1 loss. Plexiform NICs are thought to be derived from Schwann cell precursors or their more differentiated progeny in deep peripheral nerves; alternative origins such as boundary cap cell or satellite cells have also been proposed. Another progenitor population arising from the neural crest has been located in the dermis, and dermal NICs may arise instead from these skin-derived precursors (SKPs) or their progeny. Times indicated are the embryonic days (E) at which specific Schwann cell precursors appear in the mouse. Listed below each cell type are useful markers of specific developmental stages and promoters which are active at these stages (Brossier and Carroll, 2012).

Three independent groups have recently tested whether neurofibromas originate from embryonic stem cells or differentiated adult cells by generating conditional mouse models in which *Nf1* LOH was induced in the Schwann cell lineage at different times during embryonic development (Table 5) (Joseph et al., 2008; Wu et al., 2008; Zheng et al., 2008). Elimination of *Nf1* expression in neural crest cells, the earliest stage in Schwannian differentiation, was achieved by mating $Nf1^{flox/-}$ mice with *Wnt1-Cre*, *Mpz-Cre*, and *Pax3-*

Cre animals. Although these mice had abnormal sympathetic ganglia and adrenal glands and died at birth, they did not develop neurofibromas. Given the early death of these animals, the observation of the tumorigenic effects of *Nf1* loss is prevented. However, the authors observed that *Nf1* loss significantly increased the frequency of stem cells at early embryonic stages but they were no more detectable by late gestation (Joseph et al., 2008) indicating that early progenitors with stem cell properties do not persist in the adult where they could give rise to neurofibroma. This observation together with the fact that *Nf1$^{flox/-}$; Krox20-Cre* mice do develop neurofibromas, and Krox20 is not expressed in neural crest cells, argues that *Nf1* loss in neural crest cells is not required for neurofibroma pathogenesis.

Genetically engineered mouse models of PNS neoplasia.

		Transgenic mouse model	Phenotype	Limitations
Tumor cell of origin models	Nf1 ablation in migrating neural crest	*Nf1$^{flox/-}$; Wnt1-Cre,*	Died at birth; no neurofibromas developed	Early death prevents observation of tumorigenic effects of *Nf1* loss
		Nf1$^{flox/-}$; Mpz-Cre		
		Nf1$^{flox/-}$; Pax3-Cre		
	Nf1 ablation in Schwann Cell precursors	*Nf1$^{flox/-}$; 3.9Periostin-Cre*	Died by 4 weeks after birth; no neurofibroma development observed	Early death prevents observation of tumorigenic effects of *Nf1* loss
		Nf1$^{flox/-}$; P_{0a}-Cre	Plexiform neurofibroma formation observed by 15–20 months	Due to broad P_0a promoter expression in the Schwann cell lineage, a definitive cell of origin still could not be identified
		Nf1^{floxflox}; Dhh-Cre	Plexiform and subcutaneous neurofibroma development (demonstrating that an *Nf1$^{+/-}$* microenvironment might not be strictly required for neurofibroma formation)	*Dhh* promoter expression in progenitor cells capable of differentiation into both Schwann cells and endoneurial fibroblasts
	Nf1 ablation in SKPs	*Nf1$^{flox/-}$; CMV-CreERT2; Rosa26*	Dermal neurofibromas generated ~6 months following topical tamoxifen administration	Likely that ablation of *Nf1* in non-SKP cells in dermis contributes to neurofibroma formation

Table 5. Genetically engineered mouse models of neurofibroma formation (part 2). The timing of neurofibromin inactivation is the key determinant of neurofibroma formation in the peripheral nerve, with Nf1 loss restricted to a narrow window of embryonic development corresponding to the late precursor-early immature Schwann cell stage (E12-13) (Brossier and Carroll, 2012).

Mouse models in which *Nf1* was ablated in Schwann cell precursors (SCPs; also known as neural crest stem cells) were obtained using *3.9Periostin-Cre* (which is active in SCPs by E11) and *P0a-Cre* (expressed in SCPs beginning at E12.5) driver lines. While the majority of *Nf1$^{flox/-}$; 3.9Periosin-Cre* animals died by the 4th postnatal week (Joseph et al., 2008), *Nf1$^{flox/-}$; P0a-Cre* animals survived and formed neurofibromas in adult limb nerve (Zheng et al., 2008). Interestingly, the proliferating cells in these neurofibromas were p75+, GFAP+ and BLBP−, suggesting that mature non-myelinating Schwann cells rather than SCPs were the cell type giving rise to neurofibromas in this model. In keeping with this idea, hyper-proliferative non-myelinating Schwann cells were found in the postnatal sciatic nerves of *Nf1$^{flox/-}$; P0a-Cre* mice prior to neurofibroma development. The time-

window of tumor development is consistent with findings from Wu and colleagues, who showed that recombination of Nf1 driven by the Desert Hedgehog (Dhh) promoter at E12.5 in Schwann cell precursors resulted in neurofibroma development in peripheral nerve roots, but not in nerve trunks (Wu et al., 2008). Unlike the tumors arising in *Nf1*$^{flox/-}$*; P0a-Cre* mice, neurofibromas developing in *Nf1*$^{flox/flox}$*; Dhh-Cre* mice contained numerous BLBP+ cells, suggesting that immature Schwann cells were the progenitors for these tumors. Interestingly, the development of neurofibromas in *Nf1*$^{flox/flox}$*; Dhh-Cre* mice occurred despite the presence of a wild-type Nf1 microenvironment; no evidence was found for Cre-mediated recombination in mast cells, endothelial cells or endoneurial fibroblasts, despite the fact that Dhh-expressing progenitors capable of differentiating into both Schwann cells and endoneurial fibroblasts have been found in peripheral nerve (Joseph et al., 2004) (Fig. 26). Therefore, neoplastic transformation of NCSCs or non-neuronal restricted nerve progenitors could potentially yield clonal tumors containing both Schwann cells and fibroblasts.

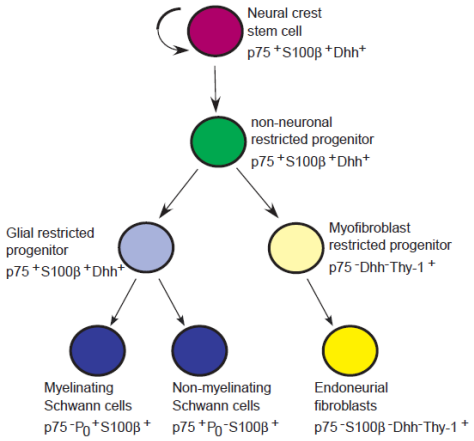

Figure 26. Model of peripheral nerve development. NCSCs self-renew in peripheral nerves to generate additional NCSCs, as well as undergoing restriction under the influence of Nrg1, Delta and Bmp4. The resulting restricted progenitors lack neuronal potential (non-neuronal) but undergo lineage commitment to form both glial and myofibroblast progenitors. Glial progenitors differentiate to form both myelinating and non-myelinating Schwann cells, and myofibroblast progenitors differentiate to form endoneurial fibroblasts (Joseph et al., 2004).

Given these contradictory results, it is not yet clear whether the neoplastic Schwann cells within plexiform neurofibromas are derived from mature non-myelinating Schwann cells, immature Schwann cells or both cell types. The possibility that these neoplastic Schwann cells arise from another source such as boundary cap cells also has not yet been ruled out. Intriguingly, these findings could have implications for our understanding of the

enormous variability in the severity of the human disease, even among members of the same family.

Given the marked differences in the clinical behavior of dermal and plexiform neurofibromas, it is possible that the neoplastic cells in these neurofibroma subtypes are derived from distinct progenitors. Neural-crest derived precursor cells capable of both Schwannian and melanocytic differentiation, termed skin-derived precursors (SKPs) (Fig. 25), are present in the dermis of adult mice. Consistent with the hypothesis that SKPs give rise to dermal neurofibromas, topical administration of tamoxifen to neonatal *Nf1*$^{flox/-}$*; CMV-CreERT2; Rosa26-LacZ(stop)* mice results in dermal neurofibroma formation at the site of tamoxifen administration (Le et al., 2009). Further, SKPs isolated from these animals and treated *ex vivo* with tamoxifen to inactivate *Nf1* were also capable of generating neurofibromas upon autologous subcutaneous transplantation into pregnant mice, indicating that these progenitors (and not other cell types residing in the dermis) were the cell of origin of the dermal neurofibromas. Interestingly, *Nf1*$^{-/-}$ SKPs were also capable of forming plexiform neurofibromas when auto-grafted into sciatic nerves. Thus, while SKPs residing in the dermis may be the cell of origin of dermal neurofibromas, these cells are apparently highly similar to the neurofibroma-initiating cells in peripheral nerve. The distinct clinical behavior of these tumors may primarily reflect differences in their microenvironment rather than their cell of origin (Brossier and Carroll, 2012).

1.4.10.3. Role of tumor microenvironment

Zhu and colleagues showed that Nf1 loss in Schwann cell progenitors alone is not sufficient for tumor environment, as a heterozygous environment is needed (Zhu et al., 2002). In neurofibromas, *Nf1*$^{+/-}$ fibroblasts demonstrate abnormal responses to cytokines, increased collagen deposition, and increased proliferation. *Nf1*$^{+/-}$ mast cells have increased infiltration to pre-neoplastic peripheral nerves in comparison with wild-type mast cells and have increased proliferation *in vitro* and *in vivo* (Gottfried et al., 2006). These cells appear to function as critical intermediaries between *Nf1*$^{-/-}$ Schwann cells and other *Nf1*$^{+/-}$ cell types in the microenvironment. *Nf1*$^{-/-}$ Schwann cells secrete elevated levels of Kit ligand, a growth factor which activates the c-Kit membrane tyrosine kinase (Fig. 27). *Nf1*$^{+/-}$ mast cells show increased c-Kit expression and an enhanced chemotactic

response to Kit ligand relative to wild-type mast cells, leading to increased recruitment of these cells into the nascent tumor (Viskochil, 2003). Kit ligand also induces enhanced activation, degranulation, and TGF-β secretion in *Nf1*$^{+/-}$ mast cells. TGF-β in turn acts upon *Nf1*$^{+/-}$ fibroblasts and promotes increased production of collagen, a molecule which is found in abundance in neurofibromas.

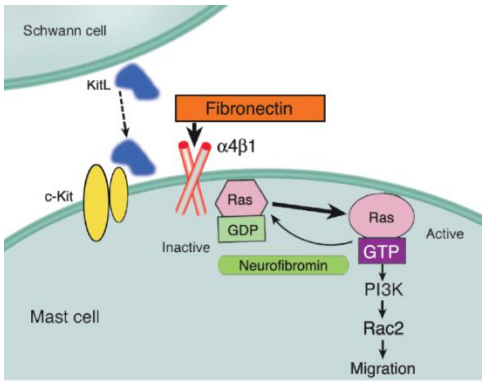

Figure 27. Molecular pathways involved in mast cell recruitment to neurofibromas. A neurofibromin-deficient Schwann cell (Nf1$^{-/-}$) secretes five times the normal Kit ligand, which serves as a chemo-attractant for mast cells expressing c-Kit. Mast cell migration is mediated by the Ras/PI3K/Rac2 signal transduction pathway, which is enhanced in Nf1$^{+/-}$ cells. Although not shown, endothelial cells also play a role in mast cell migration through the interaction of the endothelial cell VCAM-1 receptor and α4β1 integrin of the mast cell (Viskochil, 2003).

An essential role for mast cells in neurofibroma formation has been elegantly demonstrated using bone marrow transplantation in knock-out mice (Table 6). As noted above, *Nf1*$^{flox/flox}$*; Krox20-Cre* mice do not develop neurofibromas. However, when *Nf1*$^{flox/flox}$*; Krox20-Cre* mice were lethally irradiated and transplanted with *Nf1*$^{+/-}$ bone marrow, they developed multiple plexiform neurofibromas that were infiltrated by donor mast cells (Yang et al., 2008). In contrast, when donor marrow from *Nf1*$^{+/-}$ mice with hypoactive c-Kit receptors (*Nf1*$^{+/-}$*; c-KitW41/W41* mice) was used, no tumors formed, indicating that c-Kit signaling in bone marrow-derived elements was critical for neurofibroma formation. Consistent with the hypothesis that *Nf1*$^{+/-}$ mast cells are critically important for neurofibroma pathogenesis, no neurofibromas formed in lethally irradiated *Nf1*$^{flox/-}$*; Krox20-cre* mice transplanted with wild-type bone marrow, despite the presence of *Nf1* haploinsufficient fibroblasts and endothelial cells in the peripheral nerve.

Genetically engineered mouse models of PNS neoplasia.

	Transgenic mouse model	Phenotype	Limitations
Tumor microenvironment models	*Nf1*$^{flox/flox}$; *Krox20-Cre* transplanted with *Nf1*$^{+/-}$ bone marrow	Developed plexiform neurofibromas infiltrated by donor mast cells (demonstrating importance of Nf1 haploinsufficiency in hematopoeitic lineage for neurofibroma formation)	Other *Nf1*$^{+/-}$ cell types within the hematopoietic lineage may contribute to neurofibroma development
	Nf1$^{flox/flox}$; *Krox20-Cre* transplanted with *Nf1*$^{+/-}$; *c-Kit*$^{W41/W41}$ bone marrow	No neurofibromas developed (demonstrating importance of c-Kit signaling in Nf1 haploinsufficient cells in the hematopoeitic lineage)	
	Nf1$^{flox/+}$; *Krox20-Cre* transplanted with *Nf1*$^{+/+}$ bone marrow	No neurofibromas developed (demonstrating importance of Nf1 haploinsufficiency in hematopoeitic lineage for neurofibroma formation)	

Table 6. Genetically engineered mouse models of neurofibroma formation (part 3). The timing of neurofibromin inactivation is the key determinant of neurofibroma formation in the peripheral nerve, with Nf1 loss restricted to a narrow window of embryonic development corresponding to the late precursor-early immature Schwann cell stage (E12-13) (Brossier and Carroll, 2012).

Although it is clear that mast cell recruitment is essential for neurofibroma formation and that Nf1 haploinsufficiency in other cell types cannot overcome this requirement, it remains to be determined whether Nf1 haploinsufficiency in these other cell types promotes neurofibroma growth. It is also unclear what pro-tumorigenic function(s) are performed by the recruited mast cells after their arrival in the nascent neurofibroma and whether these effects are directed at the neoplastic Schwann cells or other intra-tumoral cell types (Brossier and Carroll, 2012). At present, an entire series of pro-tumorigenic interactions between the various cell types composing a neurofibroma can be envisioned (Fig. 28). However, the existence and functional significance of most of these interactions remains to be determined.

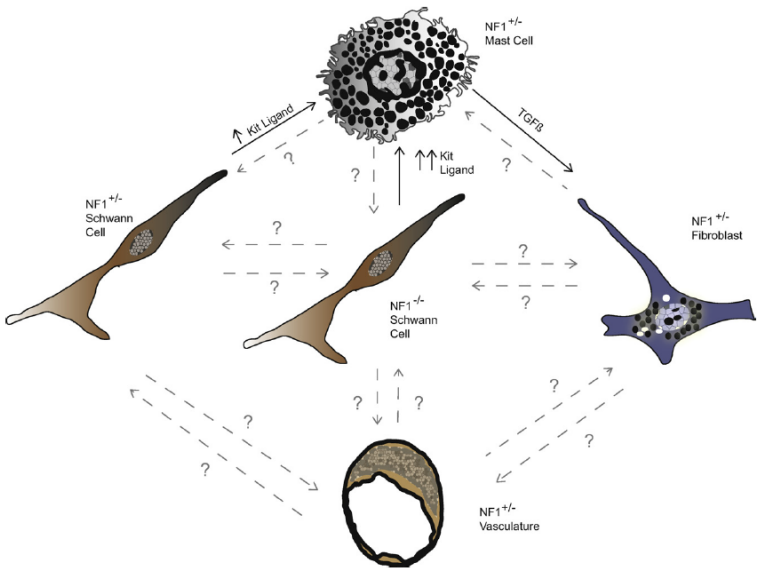

Figure 28. Established and potential interactions between *Nf1*$^{-/-}$ Schwann cells and other *Nf1* haploinsufficient cell types intrinsic to peripheral nerve. Established interactions are depicted with solid black arrows and font, while potential interactions are depicted with gray dashed arrows labeled with question marks (Brossier and Carroll, 2012).

1.5. Aim of the project

Our interest is toward the investigation of how oncogenic signaling cascades affect mitochondrial physiology. Indeed, we believe that mitochondria play a pivotal role in shaping the oncogenic signaling cascade and readjustments in mitochondrial physiology can contribute to the tumorigenic process.

In particular, we are focused on the Ras-MEK-ERK signaling pathways which display a mitochondrial branch, as a fraction of ERK is present in the mitochondrial matrix of cancer cells. We would like to investigate which is the impact of the hyper-activation of this signaling cascade on mitochondrial physiology, in terms of respiration and mechanisms of cell death resistance, in extreme models of cancer cells (ρ^0 cells) and when this pathway is deregulated by modifications of upstream regulators (neurofibromin loss). We would like to understand to which extent mitochondrial rewiring contributes to the neoplastic process and how these changes are achieved through the deregulation of oncogenic signaling cascades.

2. Materials and Methods

2.1. Chemicals and antibodies

Tetramethylrhodamine methyl ester (TMRM) and ATP determination Kit were from Molecular Probes (Eugene, OR); FITC-conjugated annexin-V was from Boehringer Mannheim (Indianapolis, IN); indirubin-3'-oxime and CsA were from Calbiochem (San Diego, CA); cyclosporin H (CsH) was a generous gift of Dr. Urs Ruegg, Geneva; all other chemicals were from Sigma (Milan, Italy).

Mouse monoclonal anti GSK-3α/β, Grim19, SDHA and UQCRC1, goat polyclonal anti calnexin, HK II and VDAC1, and rabbit polyclonal anti ERK2, PARP and TOM20 antibodies were from Santa Cruz Biotechnology (Santa Cruz, CA); rabbit polyclonal anti phospho-ERK1/2 (Thr202/Tyr204) and anti phospho GSK-3α/β (Ser21/9) and rabbit monoclonal anti caspase-3 antibodies were from Cell Signaling (Beverly, MA); mouse monoclonal anti phospho-Ser/Thr, GAPDH, CyP-D and anti prohibitin antibodies were from Qiagen, Millipore, Calbiochem and Lab Vision (Fremont, CA), respectively; mouse monoclonal anti HSP90 and TRAP1 antibodies were from BD Biosciences; rabbit polyclonal anti AIF and NF1 antibodies were from Exalpha Biologicals (Shirley, MA) and Novus Biologicals, respectively; the mouse monoclonal OXPHOS antibody cocktail recognizing CI (NDUFB8), CII (SDHB), CIII (core2), CIV (COXII) and CV (α), and the mouse monoclonal anti NDUFS3 antibody were from Mito-Sciences (Eugene, OR); rabbit monoclonal anti NDUFS1 was from Abcam. Peptides MIASHLLAYFFTELNβA-GYGRKKRRQRRRG (TAT-HK II) and GYGRKKRRQRRRG-βA-EEEAKNAAAKLAVEILNKEKK (TAT-Ctrl) were synthesized by a solid phase method using an automatized peptide synthesizer (model 431-A, Applied Biosystems, Foster City, CA).

2.2. Cell cultures and transfections

The human 143B osteosarcoma and the derived 206 ρ^0 cell lines were kindly provided by Lodovica Vergani (Deparment of Neurosciences, University of Padova, Padova, Italy). Mouse embryonic fibroblasts (MEFs) cells from C57BL/6J mice of three different genotypes (*Nf1*$^{+/+}$, *Nf1*$^{+/-}$ and *Nf1*$^{-/-}$), immortalized by transfection with SV40 whole genome DNA, were obtained from Dr R. Stein (Tel Aviv University, Ramat Aviv, Israel). 143B and MEFs cells were grown in high glucose (4500 mg/L) Dulbecco's modified Eagle's medium (DMEM) supplemented with 10% fetal bovine serum (FBS), 100 units/ml

penicillin, and 100 μg/ml streptomycin (Invitrogen) in a humidified atmosphere of 5% CO_2/95% air at 37°C. Medium of ρ^0 cells was supplemented with 50 mg/L uridine, essential amino acids and vitamins.

TRAP1 stable interference of human cells was achieved by transfecting cells with a panel of TRAP1 shRNAs from Sigma; scrambled shRNAs were always used as negative controls. Cells were transfected with Lipofectamine 2000 (Invitrogen) and stable interfered cells were selected in 2 μg/ml puromycin (Sigma).

2.3. Epifluorescence microscopy

Mitochondrial membrane potential (Δψm) was measured either by epifluorescence microscopy or by flow cytometry (see below). For epifluorescence microscopy cells were seeded onto 24 mm-diameter round glass coverslips and grown for 2 days in DMEM. Δψm was measured based on the accumulation of TMRM in the presence of CsH, which inhibits the multidrug resistance pump but not the PTP. Cells were incubated in bicarbonate- and phenol red-free DMEM supplemented with 10 mM Hepes and 1.6 μM CsH and loaded with 20 nM TMRM for 30 min at 37°C. At the end of each experiment, mitochondria were fully depolarized by the addition of 4 μM of the protonophore FCCP. Cellular fluorescence images were acquired with an Olympus IX71/IX51 inverted microscope equipped with a xenon light source for epifluorescence illumination and with a 12-bit digital cooled CCD camera (Micromax, Princeton Instruments, Trenton, NJ). For detection of fluorescence 568 ± 25 nm bandpass excitation and 585 nm longpass emission filter settings were used. Images were collected every 3 min with an exposure time of 100 msec (6% illumination intensity) using a 40X, 1.3 NA oil immersion objective (Olympus). Data were acquired and analyzed using Cell R software (Olympus). Clusters of several mitochondria (10–30) were identified as regions of interest, and fields not containing cells were taken as the background. Sequential digital images were acquired every minute, and the average fluorescence intensity of all relevant regions was recorded and stored for subsequent analysis.

2.4. Cytofluorimetric analyses

Flow cytometry recordings were performed to determine cell death, mitochondrial membrane potential and mitochondrial mass. Briefly, for cell death analysis cells were incubated at 37°C in 135 mM NaCl, 10 mM HEPES, 5 mM $CaCl_2$ (FACS mix solution) with FITC-conjugated Annexin-V (Boehringer Mannheim) and propidium iodide (PI, 1 μg/ml; Sigma), to detect phosphatidyl-serine exposure on the cell surface (increased FITC-conjugated Annexin-V staining) and loss of plasma membrane integrity (PI permeability and staining); Annexin-V and PI negative cells were considered viable. For mitochondrial membrane potential analysis cells were incubated for 15 min at 37°C in FACS mix solution with TMRM (20 nM) and CsH (1.6 μM). For mitochondrial mass analysis cells were incubated for 15 min at 37°C in FACS mix solution with 10-N-nonyl acrydine orange (NAO, 20 nM; Invitrogen), which binds to cardiolipin in mitochondrial membranes. Changes in forward and side light scatter were assessed at the same time to measure alterations in cell dimension and granularity, respectively. Samples were analyzed on a FACSCanto II flow cytometer (Becton Dickinson). Data acquisition and analysis were performed using FACSDiva software.

2.5. *In vitro* tumorigenesis assays

For the soft agar assay, cells were grown in 6 cm Petri dishes covered by a bottom layer composed of DMEM medium mixed with low melting point agarose (Promega) at a final concentration of 1.0%, and by a top layer of DMEM medium supplemented with 2% serum and mixed with low melting point agarose at a final concentration of 0.6%. Cells ($2.5x10^5$) were added during the preparation of the upper layer, where they remained embedded. Dishes were then maintained in a humidified atmosphere of 5% CO_2-95% air at 37°C for three weeks, changing the medium (DMEM 2% serum) on the top of the two layers every 3^{th} day. At the 25^{th} day, dishes were washed in PBS and colonies were stained with Crystal Violet 0.005% and analyzed with Image Analyzer custom software.

2.6. *In vivo* tumorigenesis assays

Experiments were performed in 8-week-old SCID mice (Charles River, Wilmington, MA) treated in accordance with the European Community guidelines. Six mice were injected

subcutaneously bilaterally in the flanks with 2.5 and $5x10^6$ MEFs in 200 µl of serum-free sterile PBS mixed with Matrigel. Tumor growth was evaluated on alternate days by calliper measuring. After one month, mice were sacrificed and tumors stored at -80°C.

2.7. Cell lysis and mitochondria fractionation

Total cell extracts were prepared at 4°C in a buffer composed of 150 mM NaCl, 20 mM Tris-HCl pH 7.4, 5 mM EDTA, 10% glycerol, 1% Triton X-100 (Lysis Buffer), in the presence of phosphatase and protease inhibitors (Sigma). Lysates were then cleared with a centrifugation at 18,000 x g for 30 min at 4°C, and proteins were quantified using a BCA Protein Assay Kit (Thermo Scientific-Pierce).

Mitochondria were isolated after cell disruption with a glass-Teflon or electrical potter (Sigma) in a buffer composed of 250 mM sucrose, 10 mM Tris-HCl, 0.1 mM EGTA-Tris, pH 7.4. Nuclei and plasma membrane fractions were separated by a first mild centrifugation (700 x g, 10 min); mitochondria were then spinned down at 7,000 x g, 10 min, and washed twice (7,000 x g, 10 min each). All procedures were carried out at 4°C. In order to define sub-mitochondrial protein localization, isolated mitochondria were digested with trypsin at different concentrations at 4°C for 1 hour. Trypsin was then inactivated with a protease inhibitor cocktail (Sigma), and mitochondria were lysed and spun at 18,000 x g at 4°C for 10 min.

2.8. Immunoprecipitation and western blotting

Protein immunoprecipitations were carried out on 4 mg of total cellular extracts. Lysates were pre-cleared by incubating them with protein A-Sepharose beads (Sigma) for 1 hour at 4°C; they were then incubated in agitation for 18 hours at 4°C with the antibody conjugated to fresh protein A-Sepharose beads. Where indicated, an unrelated antibody was added as a negative isotype control. Beads were then washed several times in Lysis buffer.

Proteins extracted from total or mitochondrial cell lysates or from immunoprecipitations were then boiled for 5 min in Laemmli sample buffer, separated in reducing conditions on SDS-polyacrylamide gels and transferred onto Hybond-C Extra membranes (Amersham) following standard methods. Primary antibodies were incubated for 16 hours at 4°C, and

horseradish peroxidase-conjugated secondary antibodies were added for 1 hour at room temperature. Proteins were visualized by enhanced chemiluminescence (Millipore).

2.9. Blue native polyacrylamide gel electrophoresis (BN-PAGE)

BN-PAGE experiments were performed on pellets of mitochondria isolated as described. ETC complexes were extracted from 200 µg of mitochondria by resuspending them at 10 mg/ml in a buffer composed of 1M aminocaproic acid, 50 mM Bis Tris pH 7, in the presence of 2% n-dodecyl-β-D-maltoside (DDM) at 4°C. Immediately after extraction mitochondria were spinned at 100,000 x g for 30 min and supernatants were loaded on 1D-Native-PAGE 3-12% Bis-Tris pre-cast gradient gels (Invitrogen) after addition of Coomassie Blue G250 (Invitrogen). Bands were visualized after 18 hours of Coomassie Blue G-250 staining. Bands corresponding to different ETC complexes were cut and subjected to 2D-SDS-PAGE, in order to separate single protein components which were identified by Western immunoblotting.

2.10. ETC complex I and II activity assays

To measure the enzymatic activity of respiratory chain complexes, cells were homogenized with an electric potter (Sigma) in a buffer composed of 250 mM sucrose, 10 mM Tris-HCl, 0.1 mM EGTA-Tris, pH 7.4, Percoll 10%, protease and phosphatase inhibitors and mitochondria were isolated as described above. Mitochondrial enriched fractions (20-40 µg per trace) were used for spectrophotometric recordings.

For complex I activity, the rotenone-sensitive NADH-CoQ oxidoreductase activity was detected following the decrease in absorbance due to the oxidation of NADH at 340 nm (ε=6.2 mM^{-1} cm^{-1}). Reaction was performed at 30°C in 10 mM Tris-HCl pH 8 buffer containing 5 µM alamethicin, 3 mg/ml BSA, 5 µM sodium azide, 2 µM antimycin A, 65 µM Coenzyme Q1, and 100 µM NADH. The NADH-ubiquinone oxidoreductase activity was measured for 3-5 min before the addition of rotenone (10 µM), after which the activity was measured for an additional 3-5 min.

Complex II activity was measured by following the reduction of 2-6 dichlorophenolindophenol (DCPIP) at 600 nM (ε=19.1 mM^{-1} cm^{-1}). Mitochondria were pre-incubated for 10 min at 30°C in a buffer composed of 25 mM potassium phosphate

pH 7.2, 20 mM sodium succinate, and 5 µM alamethicin. After the pre-incubation time, sodium azide (5 µM), antimycin A (2 µM), rotenone (2 µM) and DCPIP (50 µM) were added for 1 min to the medium. Reaction was performed at 30°C and started after the addition of an intermediate electron acceptor (Coenzyme Q1, 65 µM).

Each measurement of ETC complex activity was normalized for citrate synthase (CS) activity. To measure CS activity, citrate formation was determined with a spectrophotometer as an increase in absorbance at 420 nm at 37°C. Reaction buffer was composed of 100 mM Tris-HCl pH 8, 0.1% Triton X-100, 100 µM 5,5'-dithiobis-(2-nitrobenzoic acid) (DTNB), 300 µM Acetyl -CoA, and 500 µM Oxaloacetate.

2.11. Oxygen consumption rate (OCR) and extracellular acidification rate (ECAR) measurements

The rate of oxygen consumption was assessed in real-time with the XF24 Extracellular Flux Analyzer (Seahorse Biosciences), which allows to measure OCR changes after up to four sequential additions of compounds. Cells ($2x10^4$/well) were plated the day before the experiment in a DMEM/10% serum medium; experiments were carried out on confluent monolayers. Before starting measurements, cells were placed in a running DMEM medium (supplemented with 25 mM glucose, 2 mM glutamine, 1 mM sodium pyruvate, and without serum and sodium bicarbonate) and pre-incubated for 1h at 37°C in atmospheric CO_2. An accurate titration with the uncoupler FCCP was performed for each cell type, in order to utilize the FCCP concentration that maximally increases OCR. Together with OCR measurements, values of ECAR were also recorded as the absence of sodium bicarbonate allows changes in the pH of the medium.

2.12. Measurement of mitochondrial Ca^{2+} retention capacity

The Ca^{2+} retention capacity (CRC) assay was used to assess PTP opening in whole cells following trains of Ca^{2+} pulses and measured fluorimetrically at 25°C in the presence of the Ca^{2+} indicator Calcium Green-5N (1 µM; Molecular Probes). Cells were washed in an isotonic buffer (130 mM KCl, 1 mM Pi-Tris, 10 mM Tris-Mops, and 0.1 mM EGTA-Tris, pH 7.4), and then permeabilized with 150 µM digitonin (20 min, 4°C), increasing EGTA to 1 mM. Digitonin was then eliminated and permeabilized cells were placed in low (10 µM)

EGTA in the presence of 2 µM rotenone/5 mM succinate, 10 µM cytochrome *c*, and Calcium Green-5N, which does not permeate mitochondria. Cells were then exposed to Ca^{2+} spikes (5 µM), and fluorescence drops were used to assess mitochondrial Ca^{2+} uptake. PTP opening was detected as a fluorescence increase. Calcium Green-5N fluorescence was measured with a Fluoroskan Ascent FL fluorimeter (Thermo Electron Corporation).

2.13. Intracellular ATP determination

Intracellular ATP was quantified by the luciferin/luciferase method using the ATP determination kit by Invitrogen/Molecular Probes following manufacturer's instructions. Cells were kept for two hours in the different experimental conditions, washed with PBS, lysed in boiling water to avoid ATPase activity. 2.5 µg of proteins were analyzed in a 100 µl final volume 96-well plates that were read using a Fluoroskan Ascent FL microplate reader. A standard curve was generated using solutions of known ATP concentrations. ATP levels were calculated as nmoles ATP/mg of protein and normalized to levels of control cultures.

2.14. Statistics

Unless otherwise stated each experiment was repeated at least three times. Data are presented as average ± S.E. or, for clarity, as representative experiments (see figure legends for details).

3. RESULTS

3.1. Permeability transition pore of ρ^0 cells: regulatory mechanisms shared with cancer models

Cells entirely depleted of their mtDNA (ρ^0 cells) have no respiration, as mtDNA encodes 13 essential subunits of respiratory chain complexes and of ATP synthase. Therefore, these cells rely entirely on glycolysis for ATP synthesis, and can be maintained in culture as long as their medium contains, beside glucose, a pyrimidine and pyruvate. Hydrolysis of glycolytic ATP by ATP synthase acting in reverse mode is fundamental for the maintenance of the mitochondrial membrane potential of these cells (Buchet and Godinot, 1998). Investigators have used ρ^0 cells to address the question of whether mitochondrial respiratory function is required for apoptosis (Chomyn and Attardi, 2003). It has indeed been demonstrated that ρ^0 cells are able to undergo apoptosis and release cytochrome *c* from their mitochondria, and are protected from apoptosis by Bcl-2 overexpression (Jacobson et al., 1993). Concomitantly with cytochrome *c* release, ρ^0 cells undergo caspase-3 activation and mitochondrial membrane depolarization, indicating that the key apoptotic steps are conserved in cells without functional mitochondrial respiration (Jiang et al., 1999). However, occurrence of PTP in ρ^0 cells is still debated (Kwong et al., 2007) and a formal definition of the role played by OXPHOS complexes in PTP regulation is still lacking.

ρ^0 cells have also been used as an extreme model for the study of disorders caused by mtDNA mutations (mitochondrial diseases), and as a potential model for the investigation of bioenergetics of neoplasias; indeed, ρ^0 cells can be considered as possessing an extreme 'Warburg phenotype' since they completely lack respiration and their ATP production is fully uncoupled from oxygen availability. Furthermore, as we have discussed in the introduction, several mtDNA mutations and reduction in their copy number have been reported in diverse type of tumors (Brandon et al., 2006). Therefore, as a proof of principle, we investigated whether ρ^0 cells actually possess a PTP and, if so, whether they share common PTP regulatory mechanism with cancer cell models: deployment of HK II on the mitochondrial surface and presence of a mitochondrial ERK-GSK3 signaling axis that regulates the phosphorylation of CyP-D.

3.1.1. Paper

The results of this study are illustrated in the following publication (see Appendix section) whose reference is:

Masgras, I., Rasola, A., and Bernardi, P. (2012). Induction of the permeability transition pore in cells depleted of mitochondrial DNA. Biochim. Biophys. Acta 1817, 1860-1866.

3.2. On the role of neurofibromin in regulation of mitochondrial bioenergetics

We have then investigated the involvement of mitochondrial signaling pathways in cells with different neurofibromin expression levels. Our hypothesis was that neurofibromin-dependent deregulation of the mitochondrial branch of ERK signaling could impact on cell metabolism and survival, and therefore on the process of neoplastic transformation.

3.2.1. Mouse embryonic fibroblasts express neurofibromin, whose depletion induces ERK activation

Nf1$^{+/+}$, *Nf1*$^{+/-}$ and *Nf1*$^{-/-}$ mouse embryonic fibroblasts (MEFs) were analyzed for the expression level of neurofibromin, which was in accordance with the different genotypes (Fig. 3.1A).

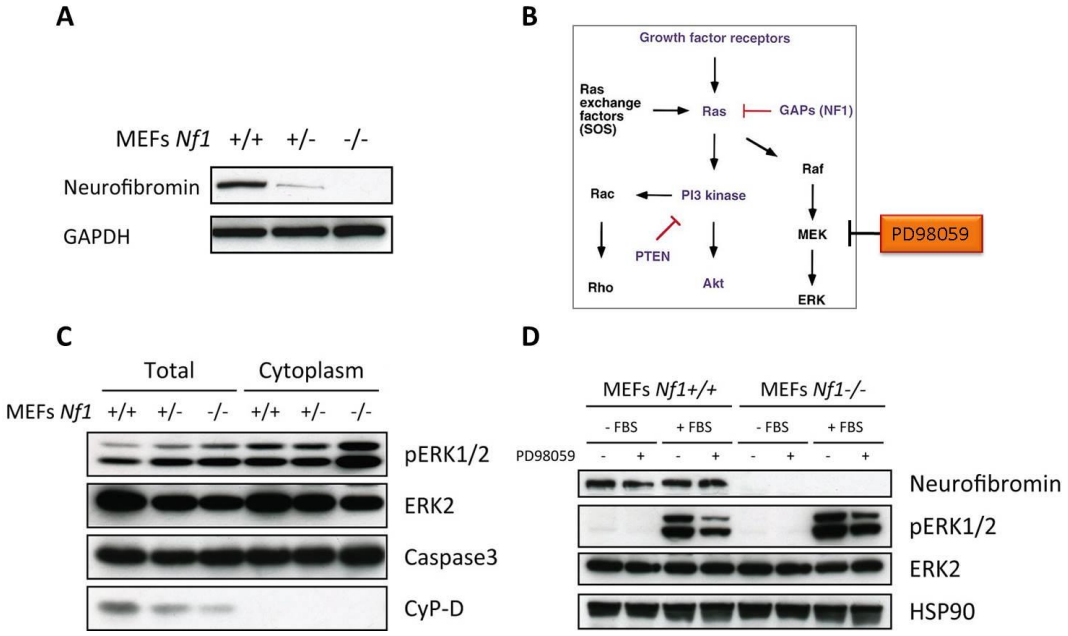

Figure 3.1. ERK is hyper-active upon neurofibromin depletion. (A) Neurofibromin level in MEFs wild-type, heterozygous and homozygous for *Nf1* deletion. (B) Simplified version of the Ras pathway (Cichowski and Jacks, 2001). Genes encoding highlighted proteins have been found to be mutated or amplified in human cancer (blue). (C) Phosphorylation status of ERK1/2 (pERK1/2) in total and cytoplasmic extracts of the indicated genotypes of MEFs. (D) Analysis of ERK1/2 activation upon 20 minutes of FBS stimulation (20%) in the presence or absence of the MEK inhibitor PD98059 (40 µM). Before growth factor stimulation, cells were starved for 1.5 hours. In the Western immunoblots of (A), (C) and (D), GAPDH, caspase-3 and HSP90 were used as loading control; in (C) CyP-D was used as a mitochondrial marker.

The absence of neurofibromin deregulates different signaling pathways (Fig. 3.1B). We investigated whether the Ras-MEK-ERK cascade was affected by *Nf1* deletion by analyzing

the expression level of the active form of ERK1/2 (the phosphorylated form, pERK1/2). We found that heterozygous and homozygous MEFs for *Nf1* deletion displayed an increase in ERK activation that was more pronounced in knock-out cells (Fig. 3.1C). These differences could be better highlighted if cells were kept in serum-free medium followed by FBS stimulation indicating that, after activation, Ras cannot be readily turned off if neurofibromin is absent; moreover, treatment with the inhibitor PD98059, which acts on the kinase upstream to ERK (MEK), was able to partially prevent ERK activation (Fig. 3.1D).

3.2.2. *Nf1* deletion induces tumorigenic properties in MEFs

It has been previously shown that mice in which the *Nf1* gene was selectively turned off in Schwann cells require a heterozygous environment for the *Nf1* locus in order to develop neurofibromas (Zhu et al., 2002); however, the role of *Nf1* knock-out fibroblasts in neurofibroma development has never been ruled out. Therefore, we decided to investigate the possible tumorigenic properties of MEFs upon *Nf1* deletion. To this aim we performed a soft agar assay, an *in vitro* tumorigenic assay in which cells are embedded in an agar matrix; only transformed cells can grow in an anchorage-independent way and form colonies, as they become capable of escaping anoikis cell death signals. As shown in Figure 3.2A, $Nf1^{-/-}$ MEFs are able to form colonies when embedded in an agar matrix; this indicates that neurofibromin loss is sufficient to induce a tumorigenic potential in these cells. Interestingly, the colony forming capability is abrogated when cells are treated with the MEK inhibitor PD98059, suggesting that the Ras-MEK-ERK pathway plays a key role in conferring tumorigenic potential to MEFs that do not have neurofibromin (Fig. 3.2B). We excluded toxic effects of the inhibitor used as it did not induce death of cells kept in the same growing conditions used for the soft agar assay (Fig. 3.2C). Moreover, the ability of $Nf1^{-/-}$ cells treated with PD98059 to form colonies was not a matter of time, since wild-type MEFs are not able to form colonies even after a longer (one month) period of incubation in soft agar (data not shown).

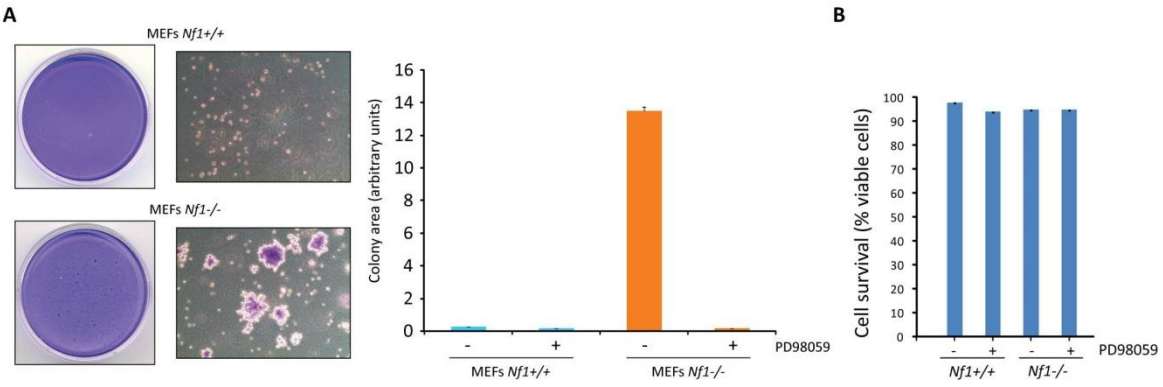

Figure 3.2. Absence of *Nf1* promotes *in vitro* tumorigenesis of MEFs. (A) Colony formation of cells embedded in soft agar matrix. Representative areas showing colony growth are reported. (B) Total colony area at the 23th experimental day with 2% serum in the presence or absence of the inhibitor PD98059 (40 µM). (C) Cell survival upon treatment for 3 weeks with PD98059 (40 µM) of cells grown at 2% FBS.

We have also tested the *in vivo* tumorigenic properties of wild-type and knock-out cells; to this purpose, MEFs of the two genotypes have been injected subcutaneously into both flanks of nude mice in the presence of Matrigel, a mixture of compounds that mimics the extracellular matrix. Growth was monitored and we observed that only cells without neurofibromin were able to form a tumor mass within a month from the injection (Fig. 3.3A and B). Interestingly, we extracted the cells from the tumors and put them back in culture, finding that the cells obtained *ex vivo* did not express neurofibromin. This indicates that the tumor mass is fully formed by injected cells (Fig.3.3C).

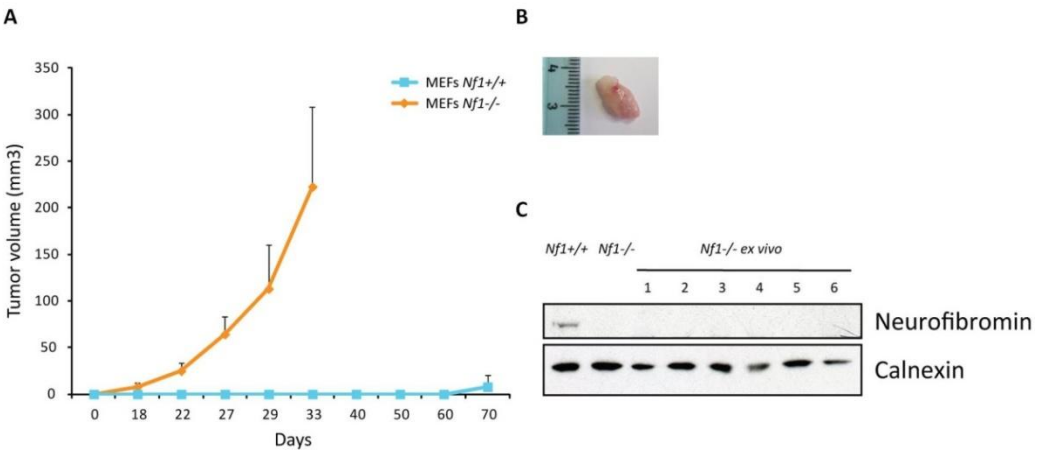

Figure 3.3. Absence of *Nf1* promotes in vivo tumorigenesis of MEFs. (A) Kinetics of tumor growth in nude mice after subcutaneous injection of MEFs with a Matrigel bolus. (B) Representative tumor grown from *Nf1*$^{-/-}$ MEFs. (C) Neurofibromin expression in wild-type and knock out MEFs and in 6 cell samples obtained *ex vivo* from tumors grown from *Nf1*$^{-/-}$ MEFs. Calnexin was used as a loading control.

We thus observed that *Nf1* loss induces tumorigenic properties in fibroblasts. Until now it was believed that only Schwann cells acquire tumorigenic properties in neurofibromas

following *Nf1* LOH, whereas fibroblasts and other cell types would only provide environmental cues for neoplastic progression. These data suggest that fibroblasts could directly take part in neurofibroma development; this observation could be extremely important for the comprehension of neurofibroma onset and growth, and needs further investigation.

3.2.3. Loss of *Nf1* strongly impacts on cell metabolism

Remodeling of energy metabolism is a recognized hallmark of cellular transformation that supports the sustained proliferation of cancer cells under conditions that restrict normal cell growth. It has been reported that oncogenic Ras is characterized by a decrease in glucose utilization through the TCA cycle and an enhanced glucose uptake (Chiaradonna et al., 2006). Therefore, we decided to investigate whether inactivation of the Ras regulator neurofibromin also affects cell metabolism.

To this purpose, we investigated mitochondrial respiration using an Extracellular Flux Analyzer (Seahorse Bioscience) that allows the measurement of the oxygen consumption rate (OCR) in adherent cells both in basal condition and upon treatment with several compounds. We found that neurofibromin loss markedly reduced basal respiration in unstimulated cells (Fig. 3.4A); furthermore, the fraction of oxygen consumption coupled to ATP synthesis, which was calculated by adding the ATP synthase blocker oligomycin, was also lower in cells without neurofibromin (Fig. 3.4A, blue and red traces for wild-type and knock-out cells, respectively). Addition of low concentrations of the uncoupler FCCP is able to stimulate maximal respiration, another important mitochondrial parameter that can be used to uncover defects or modulations of the respiratory function. Maximal respiration achieved by knock-out cells was lower compared to the wild-type counterpart, indicating that neurofibromin loss decreases the respiratory capacity of mitochondria. In order to exclude possible toxic effects of FCCP treatment in combination with ATP synthase inhibition, we added the uncoupler in the presence or absence of oligomycin (Fig. 3.4A); however, we observed that *Nf1*$^{-/-}$ cells display a very low stimulation of respiration, even in the absence of oligomycin, which could not be improved by increasing the concentration of the uncoupler. The comparison between the two cell lines is striking as, unlike wild-type cells, *Nf1*$^{-/-}$ MEFs already utilize almost their maximal respiratory

capacity under basal conditions, an arrangement implying that any additional ATP requirement must be provided by glycolysis. Additions of the ETC inhibitors rotenone and antimycin A almost fully abolished the OCR, indicating that the respiration recorded was of mitochondrial origin (Fig. 3.4B).

The differences in mitochondrial respiration that we have observed could be due to differences in cell number. To exclude this possibility, OCR data were normalized both for the cell number and the protein content. Moreover, changes in mitochondrial mass between the two cell types could affect OCR results. However, when the mitochondrial mass was evaluated by staining the cells with NAO, a fluorescent probe that binds the mitochondrial lipid cardiolipin, we detected comparable levels of mitochondrial mass in the two cell types (Fig. 3.4C).

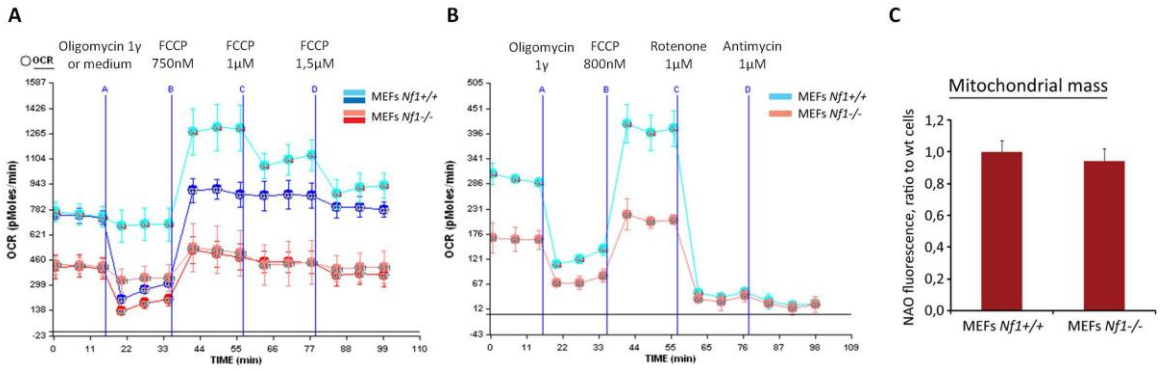

Figure 3.4. *Nf1* deletion lowers mitochondrial respiration. (A) Representative traces of oxygen consumption rate (OCR) experiments performed on monolayers of living MEFs in basal condition and upon addition of the ATP synthase inhibitor oligomycin (blue and red traces for $Nf1^{+/+}$ and $Nf1^{-/-}$, respectively) or medium (light blue and orange for $Nf1^{+/+}$ and $Nf1^{-/-}$, respectively), and of increasing concentration of the uncoupler FCCP. (B) Representative traces of OCR measurements performed on $Nf1^{+/+}$ (light blue trace) and $Nf1^{-/-}$ (orange trace) MEFs. Subsequent additions of oligomycin, FCCP, the ETC complex I inhibitor rotenone and the ETC complex III inhibitor antimycin A are reported. (C) Measurement of mitochondrial mass by mean fluorescence intensity of NAO-stained MEFs expressed as ratio to values of wild-type cells.

Even though the mitochondrial respiration was strikingly decreased in $Nf1^{-/-}$ cells, their mitochondria were polarized similarly to the wild-type counterpart, indicating that they were functional (Fig. 3.5A). Moreover, we could not identify remarkable differences in mitochondrial distribution or morphology under standard growing conditions (Fig. 3.5B).

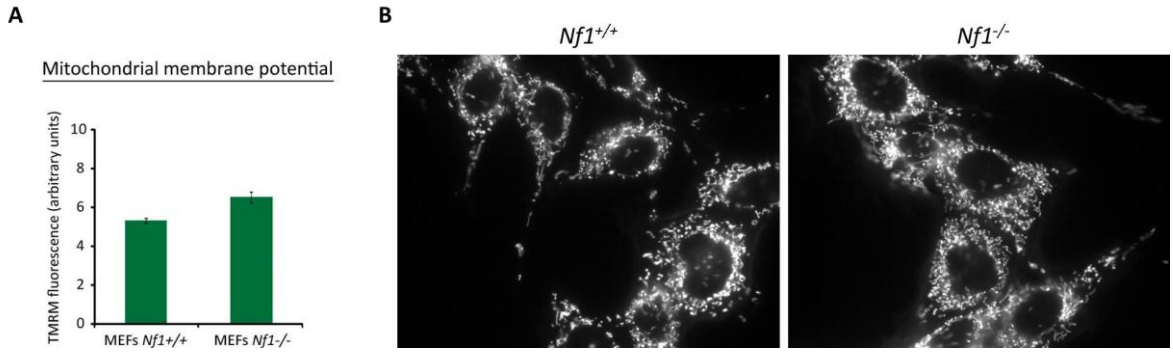

Figure 3.5. Upon *Nf1* deletion mitochondrial membrane potential and morphology do not change. (A) Measurement of mitochondrial membrane potential by mean fluorescence intensity of TMRM-stained MEFs. (B) Epifluorescence microscopy images showing mitochondrial morphology of TMRM-stained MEFs.

In addition to OCR, these experiments allowed to monitor the extracellular acidification rate (ECAR), which is mainly caused by lactate efflux from the cells and is therefore proportional to the rate of conversion of pyruvate to lactic acid. Hence, the ECAR increases when the glycolityc flux is diverted from entering the TCA cycle, which can be due to an increase in glycolytic activity, a decrease in the rate of TCA, or both. Consistently with OCR measurements, the ECAR achieved upon addition of glucose was higher in knock-out cells compared to wild-type cells (Fig. 3.6A); as the ECAR was fully inhibited by 2-Deoxy-D-glucose (2-DG), an inhibitor of hexokinase, we concluded that cells depleted of *Nf1* are more glycolytic. Furthermore, we investigated the amount of ATP that is produced by glycolysis. To this aim, we kept cells in the absence of glucose in combination with the glycolytic inhibitor 5-thio-glucose (5TG) in order to completely repress the glycolytic pathway (Fig. 3.6B). The drop in ATP levels detected upon glycolysis inhibition was higher in $Nf1^{-/-}$ cells compared to wild-type MEFs, indicating that cells depleted of *Nf1* rely on glycolysis to synthesize ATP more than their wild-type counterparts. Nevertheless, we could not appreciate significant differences in the total ATP content between the two cell lines (data not shown) indicating that knock-out cells do not suffer of energy depletion.

These observations are in line with previous reports describing a metabolic shift toward glycolysis in cells with oncogenic hyper-active Ras (Chiaradonna et al., 2006; Hu et al., 2012); in our study, the absence of neurofibromin, a Ras negative regulator, leads to a similar phenotype, suggesting that deletion of *Nf1* gene impacts on cell metabolism mainly acting through the Ras signaling pathway.

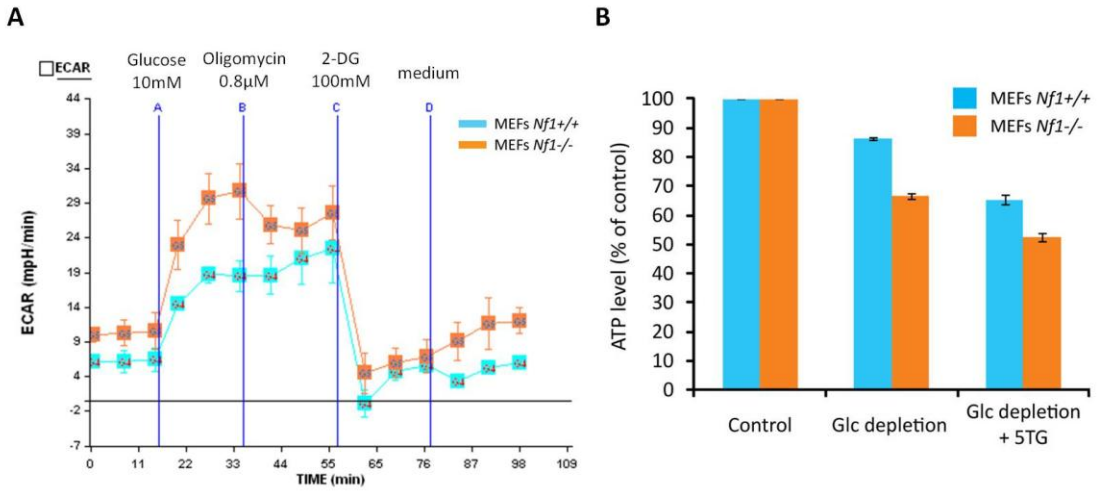

Figure 3.6. *Nf1* deletion induces glycolytic metabolism. (A) Representative traces of extracellular acidification rate (ECAR) experiments performed on monolayers of living MEFs $Nf1^{+/+}$ (light blue trace) and $Nf1^{-/-}$ (orange trace). Subsequent additions of glucose, the ATP synthase inhibitor oligomycin, the glycolysis inhibitor 2-Deoxy-D-glucose (2-DG) and medium were carried out. (B) ATP levels were measured under standard culture conditions or upon glucose depletion (2 hours) in the presence or absence of the hexokinase inhibitor 5-thio-glucose (5TG).

3.2.4. *Nf1* deletion leads to a modulation of the RC complex I (NADH dehydrogenase)

Variations in OCR could result from several mechanisms of respiratory chain regulation, among which differences in synthesis/degradation rates of RC proteins, changes in the assembly/stability of RC complexes or super-complexes and regulation by post-translational modifications. In order to investigate these possibilities, we started from the analysis of the expression level of different proteins of the respiratory chain complexes. Interestingly, complex I (NADH dehydrogenase) was affected by *Nf1* loss, as the expression of its subunits NDUFSB8 and Grim19 was lowered in $Nf1^{-/-}$ cells; instead, expression of other complexes did not change between the two cell types (Fig. 3.7A). As complex I is a huge multimer composed by several subunits, we wondered whether the decrease in the expression of the subunits that we have analyzed could impact on the overall amount of complex I assembled in mitochondria. To answer this question, we extracted single ETC complexes from isolated mitochondria and performed an electrophoresis under native conditions (blue native polyacrylamide gel electrophoresis, BN-PAGE) (Wittig and Schagger, 2008). This technique is used for the isolation of protein complexes from biological membranes in order to estimate their native protein masses; furthermore, it can be applied to identify physiological protein-protein interactions (see 3.2.6 section). Separated complexes were stained with Coomassie Blue G-250, which

revealed a decrease in the amount of the band corresponding to complex I. Native complexes were recovered from gel by cutting the corresponding bands and were subjected to a second dimension electrophoresis performed in denaturing conditions (SDS-PAGE); this allowed separation of complexes into single protein components, which were therefore identified by Western immunoblotting (Fig. 3.7B). In accord with SDS-PAGE data, we found a decrease in Complex I components, whereas the amount of other respiratory chain complexes as complex II, III and V was not affected by *Nf1* loss. In accordance to this data, the rotenone-sensitive NADH-CoQ oxidoreductase activity measured in isolated mitochondria was remarkably lower in *Nf1*$^{-/-}$ cells compared to wild-type (Fig. 3.7C).

These data indicate that *Nf1* loss leads to a modulation of mitochondrial respiration mainly due to a decrease in complex I level that thus down-regulates its activity. We could not reveal modulation of the expression level of other RC complexes but we cannot exclude alterations of their activity achieved through different mechanisms (see section 3.2.6).

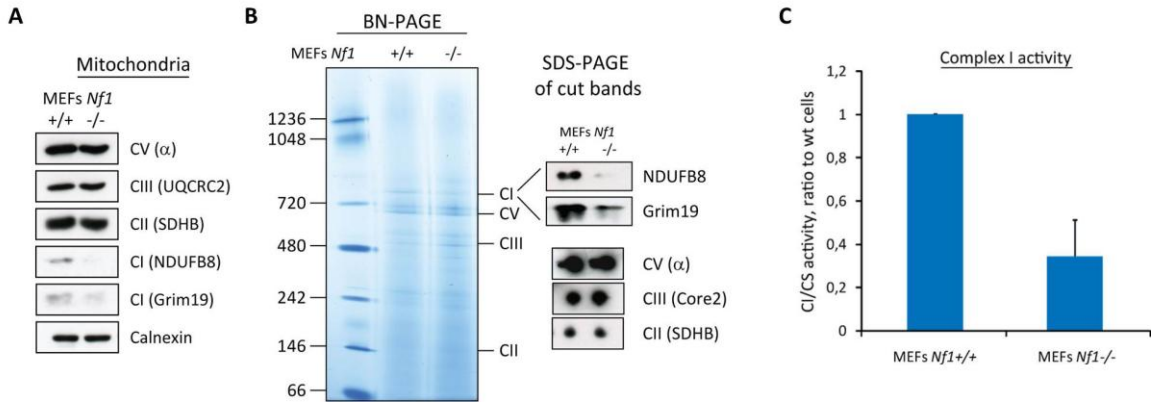

Figure 3.7. *Nf1* deletion is accompanied by a decrease in the RC complex I (NADH dehydrogenase). (A) Analysis of mitochondrial protein level of different subunits of respiratory chain complexes. Calnexin was used as a loading control. (B) Isolated mitochondria were subjected to blue native gel electrophoresis to separate ETC complexes. Bands corresponding to complex I, III and V were excised, run on a SDS-PAGE and probed with anti NDUFB8 and Grim19, anti Core2, and anti α antibodies in order to detect subunits of complex I, III and V, respectively. (C) Complex I (rotenone-sensitive NADH-CoQ oxidoreductase) activity measured in isolated mitochondria. Values were normalized for citrate synthase (CS) activity and shown as ratio to wild-type cells.

3.2.5. ERK activation is responsible for RC complex I modulation

The signaling cascades regulated by neurofibromin can affect gene transcription, by regulating key transcription factors such as Myc, Elk1, Fos, and Ets, or modulate the synthesis or post-translational modification of a wide variety of proteins.

Given the strong impact of *Nf1* loss on the expression level of complex I subunits, we wondered whether this could be due to the hyper-activation of ERK. In order to test this hypothesis, we prevented ERK activation by inhibiting MEK with PD98059 for 3 days. In accord with this hypothesis, we found that this treatment affected the expression of Grim19, a subunit of complex I, but not the expression of components of other RC complexes, such as CII and CV (Fig. 3.8A). Moreover, we confirmed complex I modulation also by analyzing the expression level of other of its subunits in isolated mitochondria (Fig. 3.9B). This effect is present in both wild-type and knock-out cell lines as under basal condition a fraction of ERK was in the phosphorylated form; however, the increase in complex I expression was stronger in *Nf1*$^{-/-}$ cells.

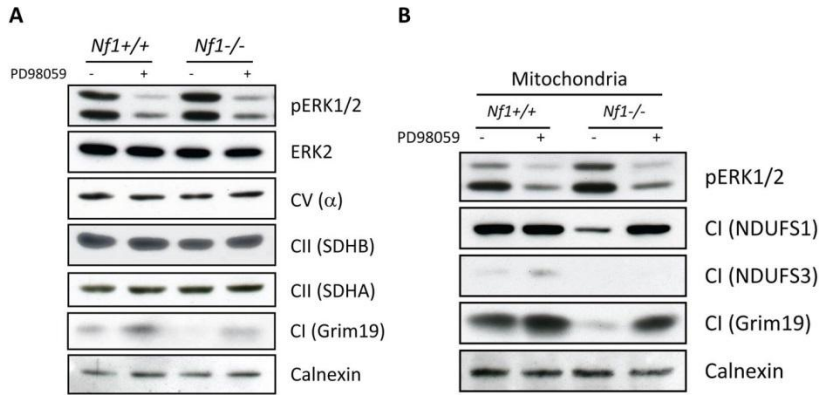

Figure 3.8. ERK inhibition specifically modulates RC complex I expression. (A) Expression level of different subunits of RC complexes upon treatment for 3 days with the MEK inhibitor PD98059 (40 μM) which prevents ERK activation (pERK1/2) in total lysates. (B) Expression level of different subunits of RC complex I in mitochondrial lysates following 3 days PD98059 (40 μM) treatment. Calnexin was used as a loading control.

Hereafter, we investigated whether the treatment with PD98059 also affected the amount of assembled complex I, in order to understand if the increase in the subunits that we have analyzed actually results in a modulation of the entire RC complex I. Performing a blue native gel electrophoresis under basal conditions or after a 3 days ERK inactivation (Fig. 3.9B), we observed that ERK inhibition increased the quantity of assembled complex I; as observed before with experiments on the single subunits, also

the assembly of other RC complexes did not vary following ERK inhibition. Moreover, ERK inactivation leaded to an increase in complex I activity, as measured by the rotenone-sensitive NADH-CoQ oxidoreductase activity in isolated mitochondria of control and treated cells (Fig. 3.9C).

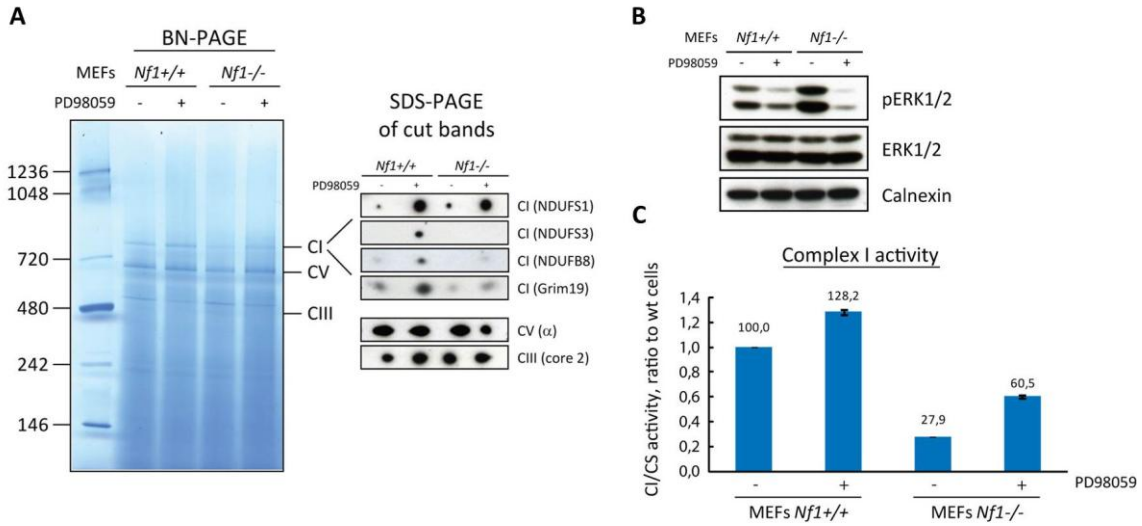

Figure 3.9. Inhibition of ERK increases the amount and activity of RC complex I. (A) Blue native gel electrophoresis of mitochondria isolated from cells treated or not for 3 days with PD98059 (40 μM). Bands corresponding to complex I, III and V were excised, run on a SDS-PAGE and probed with anti NDUFS1, NDUFS3, NDUFB8 and Grim19 antibodies to detect complex I, and anti Core2 and anti α antibodies to detect complex III and V, respectively. (B) Expression level of active and total ERK in total lysates of cells used in (A). Calnexin was used as a loading control. (C) Complex I (rotenone-sensitive NADH-CoQ oxidoreductase) activity measured in isolated mitochondria from cells treated or not for 3 days with PD98059 (40 μM). Values were normalized for citrate synthase (CS) activity and shown as ratio to wild-type untreated cells.

These results indicate that the activation level of the kinase ERK plays an important role in determining specifically the expression level of complex I subunits; preventing ERK activation was able to modulate complex I amount and activity, and the range of variation detected was dependent on the initial phosphorylation status of ERK.

3.2.6. *Nf1* loss results in modulation of RC complex II (succinate dehydrogenase) activity

We then investigated whether the inhibition of respiration of *Nf1*$^{-/-}$ cells could also depend on changes in the activity of other RC complexes, beside complex I. Previous work from our laboratory has demonstrated that inhibition of SDH activity can contribute to the tumorigenic process by modulating HIF1 transcriptional activity and the redox equilibrium of the cell (Sciacovelli et al., 2013). We therefore focused on the succinate-CoQ reductase (SQR) enzymatic activity of complex II (succinate dehydrogenase) which

was decreased in *Nf1*$^{-/-}$ cells compared to wild-type MEFs (Fig. 3.10A). As described before (see Fig. 3.7A), the expression level of complex II did not vary in the absence of neurofibromin. Therefore, we explored the possibility that SDH activity could be regulated at a post-transcriptional level by the Ras-MEK-ERK pathway. Indeed, we found that a fraction of ERK was localized inside mitochondria (Fig. 3.10B) in accord with data obtained in our laboratory on different tumor cell models (Rasola et al., 2010); interestingly, even though the amount of ERK found in mitochondria was similar in all three genotypes, *Nf1*$^{-/-}$ cells showed a remarkable increase in the activation status of mitochondrial ERK in comparison to wild-type and *Nf1*$^{+/-}$ MEFs. Notably, when we excised the BN-PAGE band corresponding to SDH complex and run it on a SDS-PAGE, we detected an unprecedented co-migration between complex II, active ERK and TRAP1 (Fig. 3.10C).

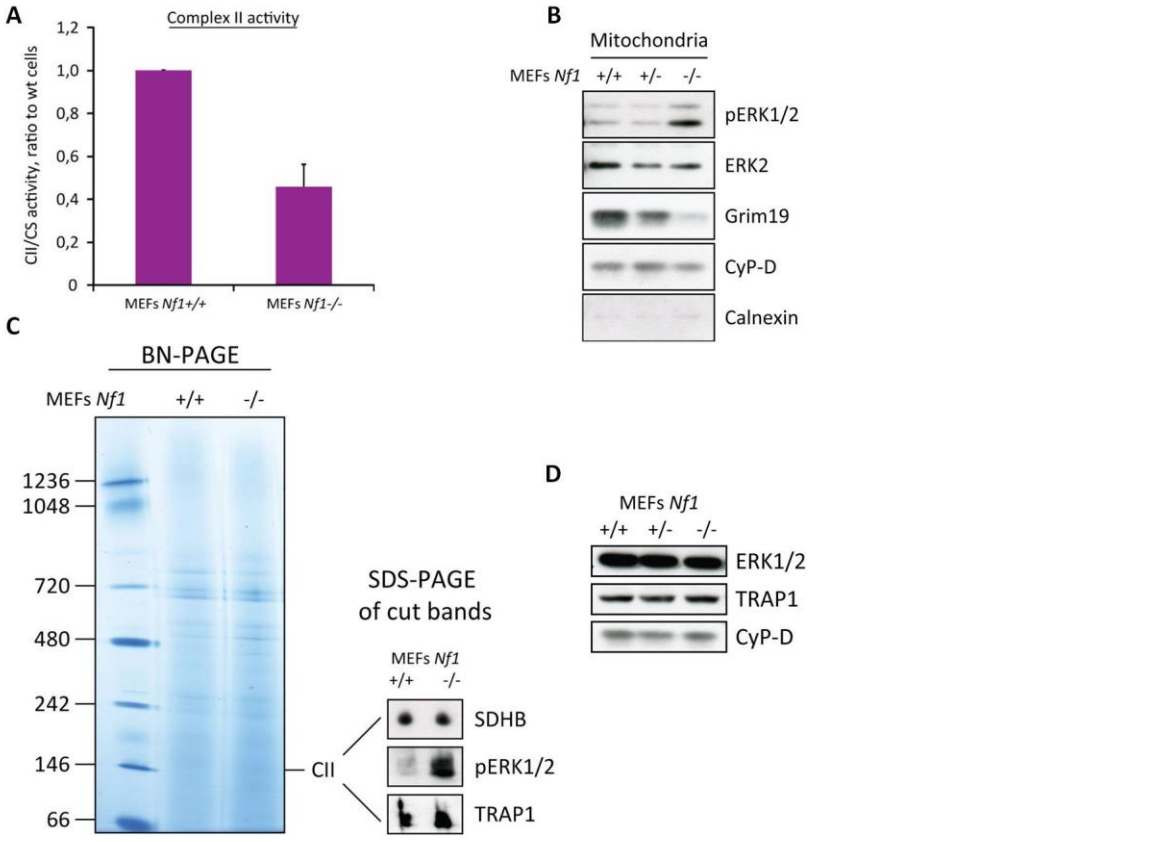

Figure 3.10. Modulation of RC complex II (succinate dehydrogenase) following *Nf1* deletion. (A) Succinate-CoQ reductase (SQR) enzymatic activity of complex II in isolated mitochondria. Values were normalized for citrate synthase (CS) activity and shown as ratio to wild-type cells. (B) Analysis of the mitochondrial fraction of active ERK. Isolated mitochondria were subjected to partial trypsinization to get rid of non-mitochondrial contaminants. CyP-D was used as loading control; Calnexin was used as extra-mitochondrial marker. (C) Isolated mitochondria were subjected to blue native gel electrophoresis to separate ETC complexes. Bands corresponding to complex II were excised, run on a SDS-PAGE and probed with anti SDHB (for complex II detection), anti pERK1/2, and anti TRAP1 antibodies. (D) Expression level of TRAP1 and ERK2 in total lysates of MEFs. CyP-D was used as a loading control.

The mitochondrial chaperone TRAP1, which is induced in most tumor types, was recently reported to be required for neoplastic growth as it confers transforming potential to non-cancerous cells (Sciacovelli et al., 2013). Indeed, as described in section 1.3.3 of Introduction, it was found that TRAP1 binds to and inhibits succinate dehydrogenase, promoting tumorigenesis by priming the succinate-dependent stabilization of the pro-neoplastic transcription factor HIF1α, independently of hypoxic conditions. We investigated the expression level of TRAP1 in the three genotypes finding that they were comparable (Fig. 3.10D). Therefore, differences in the interaction between complex II, ERK and TRAP1 between wild-type and knock-out cells could not be explained by diversity in the expression level of these proteins; and if the assembly of this multimeric complex down-regulates SDH activity in *Nf1*$^{-/-}$ cells, this could occur by post-translational modifications affecting the catalytic site of SDH.

3.2.7. TRAP1 plays a key role in the tumorigenic properties of MEFs depleted of neurofibromin

Hence, we decided to investigate whether the different co-migration between complex II and TRAP1 observed in MEFs with or without neurofibromin could explain the difference in complex II activity. We down-regulated TRAP1 levels by RNA interference (Fig. 3.11A) and analyzed the SQR enzymatic activity in isolated mitochondria of control and interfered cells; however, we could not find differences in complex II activity upon TRAP1 modulation (Fig. 3.11B). Consistently, TRAP1 down-regulation did not affect basal respiration in none of the two cell types; nevertheless, we surprisingly found that TRAP1 interference increased maximal respiration in *Nf1*$^{-/-}$ but not in wild type cells (compare the traces in Fig. 3.11C after uncoupling with FCCP). These results indicate that *Nf1*$^{-/-}$ cells display a respiratory reservoir upon TRAP1 down-regulation, suggesting that this chaperone exerts an inhibitory effect on mitochondrial respiration which can be unveiled only under certain conditions (FCCP stimulation).

In addition to this, given the important role of TRAP1 in the tumorigenic process of different cancer cell models, we examined whether it plays a similar role also in cells that are depleted of *Nf1*. To test this hypothesis, we performed an *in vitro* tumorigenic assay, finding that TRAP1 interference abrogates the ability of *Nf1*$^{-/-}$ MEFs to form colonies in

soft agar matrix. These observations point to a principal role of TRAP1 in the tumorigenic process of cells depleted of *Nf1* gene; nevertheless, it remains to be established whether it works primarily through inhibition of succinate dehydrogenase activity and/or through other mechanisms.

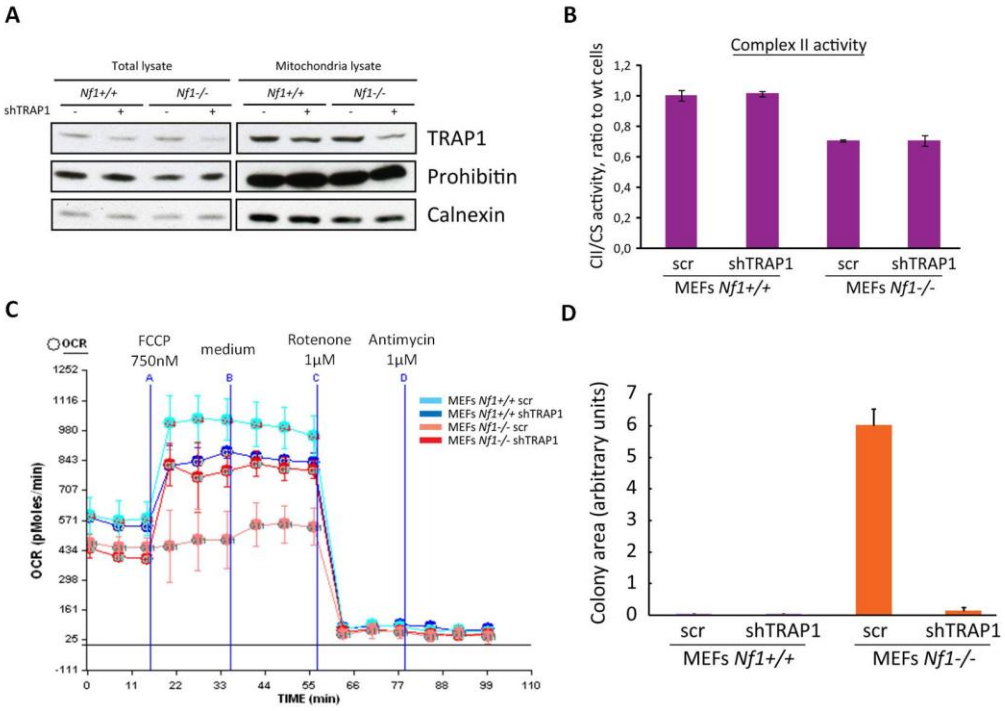

Figure 3.11. TRAP1 down-regulation modulates the tumorigenic properties of *Nf1*$^{-/-}$ MEFs. (A) Expression level of TRAP1 upon RNA interference. Prohibitin and Calnexin were used as loading controls. (B) Succinate-CoQ reductase (SQR) enzymatic activity of complex II on isolated mitochondria of *Nf1*$^{+/+}$ and *Nf1*$^{-/-}$ MEFs upon TRAP1 knock-down. Values were normalized for citrate synthase (CS) activity and shown as ratio to wild-type cells. (C) Representative traces of OCR measurements performed on monolayers of living MEFs *Nf1*$^{+/+}$ (blue trace) and *Nf1*$^{-/-}$ (trace) transfected with a shRNA against TRAP1 (light blue and red traces, respectively). Subsequent additions of the uncoupler FCCP, the ETC complex I inhibitor rotenone and the ETC complex III inhibitor antimycin A were carried out. (D) Total colony area at the 23th experimental day with 2% serum of *Nf1*$^{+/+}$ and *Nf1*$^{-/-}$ MEFs upon TRAP1 down-regulation.

3.2.8. OXPHOS modulation and cell death resistance: is there a connection in *Nf1*-deficient MEFs?

Our study has shown that deletion of *Nf1* gene in mouse embryonic fibroblasts leads to metabolic rearrangements in favor of a glycolytic metabolism; moreover, we have observed that *Nf1* loss in these cells is able to promote neoplasm growth. Still, it remains to be elucidated if metabolic reprogramming has a direct link to tumorigenesis. A possible connecting point is the modulation of the PTP opening as a major player in cell death susceptibility.

We have studied PTP opening using the Ca^{2+} retention capacity assay, which allows the measurement of the amount of Ca^{2+} threshold needed to open the channel; consequently, the number of Ca^{2+} pulses which are taken up by mitochondria is used as indication of the susceptibility of the PTP to opening. We observed that *Nf1*$^{-/-}$ MEFs take up more Ca^{2+} before pore opening, which indicates that the PTP of knock-out cells is more resistant to induction (Fig. 3.12A). The reasons for such a modulation could be of several origins; even so, we detected more HK II bound to mitochondria of cells without neurofibromin (Fig. 3.12B), therefore we would like to investigate whether they are more sensitive to HK displacing agents.

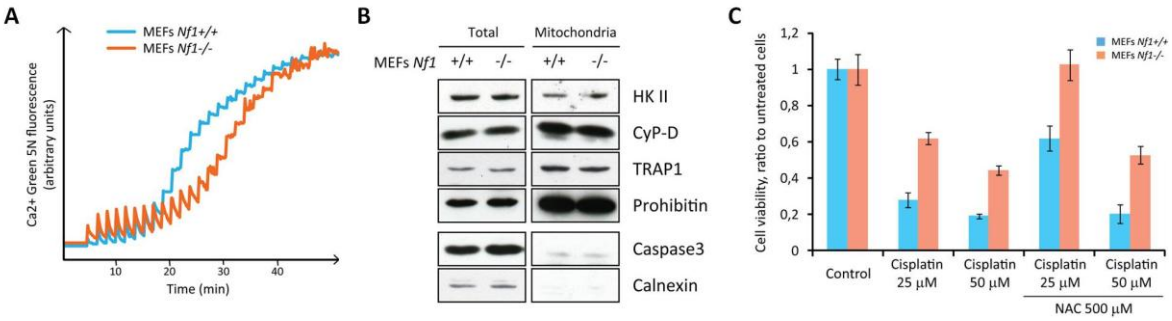

Figure 3.12. Resistance to PTP opening and cell death of *Nf1*-deficient cells. (A) PTP opening was measured with the whole-cell Ca^{2+} retention capacity assay (CRC). Ca^{2+} Green-5N fluorescence is reported as arbitrary units on the y axis. (B) Analysis of the mitochondrial fraction of active HK II. Isolated mitochondria were subjected to trypsinization at 4°C for 1 hour at a mitochondria:trypsin ratio of 35:2 (w/w). CyP-D, TRAP1 and Prohibitin were used as loading controls; Caspase-3 and Calnexin were used as extra-mitochondrial markers. (C) Cell viability of cells treated with cisplatin (25 and 50 µM) for 16 hours in the presence or absence of NAC (500 µM). Values were normalized for cell viability of untreated cells.

Neurofibromin-deficient MEFs have been reported to be more resistant than neurofibromin-expressing cells to apoptosis suggesting that neurofibromin might act as a sensitizer of apoptosis (Shapira et al., 2007). Moreover, the resistance to apoptosis caused by neurofibromin deficiency was not attributable to an inherent enhancement of the apoptotic threshold due to changes in the expression levels of key apoptotic proteins (e.g., Bcl-2 family and caspases) suggesting that a more direct pro-apoptotic action of neurofibromin could be lacking. It is known that an unbalance in reactive oxygen species (ROS) plays an important role in committing cells to death and the respiratory chain is one of the major regulators of ROS production (Lemarie and Grimm, 2011); it follows that changes in the functionality of OXPHOS activity could affect ROS generation and the ensuing PTP induction and cell death.

We measured cell survival upon treatment with the chemotherapeutic drug cisplatin finding that *Nf1*-deficient cells are more resistant to death (Fig. 3.12C). As the toxicity of this drug was prevented by N-acetyl cysteine (NAC) we could hypothesize that it exerts a pro-oxidant action which could be of different entity in the two cell lines. It has been recently shown by our group that the rapid rise in ROS levels prompted by cisplatin treatment is strictly regulated by complex I (Ciscato et al., 2013); this points our interest toward the possible connection between cell death escape of *Nf1*$^{-/-}$ cells and the modulation of OXPHOS activity. Therefore, we would like to investigate the cell death sensitivity of *Nf1* knock-out cells to treatments with ROS-inducing agents that mainly target complex I (e.g., EM20-25, AUL12) (Chiara et al., 2012).

4. DISCUSSION

In contrast to normal differentiated cells, which rely primarily on mitochondrial oxidative phosphorylation to supply the energy needed for cellular processes, most cancer cells instead rely on aerobic glycolysis, a phenomenon termed 'the Warburg effect' (Vander Heiden et al., 2009). Therefore, the attention toward tumor metabolism rewiring has risen progressively in the last years and an increasing body of research indicates that the capability to modify, or reprogram, cellular metabolism is crucial to most effectively support neoplastic proliferation (Hanahan and Weinberg, 2011). Beside this, given the principal role of mitochondria in modulating both bioenergetic processes and the cell death machinery, a possible connection between the metabolic adaptations and the capability to escape cell death that characterize tumor cells starts to stand out. Indeed, mitochondrial respiration is strongly connected to cell death induction for several reasons: first of all the respiratory chain is the major source for the production of ROS, which play an important role in determining cell fate; moreover, the functionality of OXPHOS contributes to the establishment of the threshold level for PTP opening so that, when a dysfunction in respiratory chain complexes is present, the PTP is more sensitized to inducing signals (Porcelli et al., 2009).

We have reported in this study that cells forced to glycolytic metabolism due to complete mtDNA depletion (ρ^0 cells) acquire typical feature of cancer cells. Indeed, similar to tumor cells (Chiara et al., 2008; Mathupala et al., 2006) ρ^0 cells are characterized by a relocation of the glycolytic enzyme HK II to the mitochondrial surface where it contributes to the maintenance of the PTP in the closed state, thus increasing the threshold level for cell death induction. Indeed, these cells are more sensitive to HK II detaching agents (clotrimazole and a HK II-derived peptide), supporting a model by which the protective role of mitochondrial HK II is caused by its inhibition of PTP opening. In addition to this, we have detected a constitutive activation of the ERK-GSK3 signaling pathway that converge on mitochondria of ρ^0 cells in order to maintain CyP-D in a dephosphorylated state, thus enhancing the threshold for PTP induction. Again, these data are in accord with what was reported for neoplastic cells (Rasola et al., 2010). Our study has shown that ρ^0 cells can undergo a CsA-sensitive permeability transition, thus forcing these cells to set up mechanisms of PTP resistance as a death-escaping strategy. Interestingly, regulation of PTP by mitochondrial HK II is a mechanism strictly interconnected with the

metabolic status of these cells, suggesting that the sole rewiring of cell metabolism from OXPHOS to aerobic glycolysis could be sufficient for the modulation of one of the main actors of cell death machinery: the PTP. Furthermore, this is also a target of signaling cascades that are often deregulated in cancers, and this brings to the second part of my dissertation.

Metabolic pathways active in proliferating cells are directly controlled by signaling cascades involving known oncogenes and tumor suppressor genes (Vander Heiden et al., 2009). Indeed, the majority of oncogenic mutations can affect multiple hallmark capabilities of cancer cells (e.g., proliferative signaling, energy metabolism, angiogenesis, invasion, and survival) (Hanahan and Weinberg, 2011). Recent evidences show that oncogenic signaling pathways, such as the Ras-ERK transduction axis, have mitochondrial branches. This suggests that deregulated kinase signaling in mitochondria could be directly responsible for tumor metabolic rewiring. In this conceptual framework we have investigated whether the absence of neurofibromin, which hyper-activates the Ras-ERK pathway and is linked to tumor development in individuals affected by Neurofibromatosis type 1, is able to modify mitochondrial bioenergetics, thus contributing to growth advantage and cell death escape of neoplastic cells.

We have observed that loss of neurofibromin elicits tumorigenic properties in MEFs both *in vitro* and *in vivo*; indeed, these cells acquire the capability to grow in an anchorage-independent way and form tumors when injected into nude mice. The up-regulation of the Ras-MEK-ERK pathway is of fundamental importance for the pro-tumorigenic properties gained upon *Nf1* deletion as its inactivation by the MEK inhibitor PD98059 fully prevents neoplastic growth. Our observations are important in the frame of the cellular heterogeneity of neurofibromas, the most common tumor type that affects NF1 patients. There is no doubt that neurofibromin loss in Schwann cells play a principal role in tumor formation (Zhu et al., 2002); nevertheless, fibroblasts could also participate to this process, not only as bystander cells that modulate signaling circuitries of Schwann cells, but also as transformed cells by themselves. This possibility is strengthen by the fact that neoplastic transformation (e.g., neurofibromin inactivation) of NCSCs or non-neuronal restricted nerve progenitors could potentially lead to clonal tumors containing both Schwann cells and fibroblasts (Joseph et al., 2004).

Even though the growth advantages of cells with inactivated neurofibromin have been previously described (Muir et al., 2001; Wu et al., 2005), their metabolic characterization has not been enquired so far. On the contrary, several studies have shown important metabolic alterations in cells with oncogenic Ras (see section 1.2.1.5 of Introduction). We found that *Nf1* loss in MEFs leads to a metabolic shift toward glycolysis with a strong decrease in mitochondrial respiration. This is principally achieved through a modulation of RC complex I; in detail, there is a decrease in the expression level of complex I subunits with a consequent impairment of its activity. Interestingly, we observed that these changes are dictated by the up-regulation of the kinase ERK, which is able to impact on the expression level of complex I subunits. As the transcriptional profiling of oncogenic Ras-expressing cells was found strongly altered (Gaglio et al., 2011), we presume that, in a parallel way, the metabolic alterations detected following *Nf1* deletion could also be explained by changes at the level of transcription. Indeed, beside the important function of ERK in regulating the phosphorylation status of several transcription factors, it has been very recently reported that it regulates the translocation event of PKM2 to the nucleus where it modulates gene transcription, thus contributing to the Warburg effect (Yang et al., 2012).

We also detected a decrement in RC complex II activity following *Nf1* deletion which is not paralleled by changes in protein level of its subunits; nonetheless, we found that in *Nf1*$^{-/-}$ MEFs complex II strongly interacts with the active mitochondrial fraction of ERK and the chaperone TRAP1. As TRAP1 has been shown to promote neoplastic growth through inhibition of succinate dehydrogenase (Sciacovelli et al., 2013), we silenced its expression by RNA interference, finding that the tumorigenic properties of *Nf1*$^{-/-}$ MEFs were abolished. These results suggest that inhibition of mitochondrial respiration following neurofibromin loss could prompt neoplastic transformation in a TRAP1-dependent manner, providing an unprecedented connection between metabolic changes and tumorigenesis in a NF1 model; therefore, inhibition of TRAP1 in neurofibromin-deficient cells could be a therapeutic strategy against cancer growth; however, it remains to be determined if TRAP1 triggers tumorigenesis through the already reported mechanism of HIF1α stabilization due to succinate accumulation and/or thanks to additional functions (e.g., oxidative stress resistance) (Costantino et al., 2009). In fact, TRAP1 down-regulation

does not affect complex II activity in our model; yet, it stimulates maximal respiration in cells without neurofibromin.

In conclusion, even if it is becoming increasingly clear that oncogenic deregulation of the Ras signaling pathway prompts a variety of bioenergetic changes, little is known about the role played by metabolic adaptations in NF1 tumorigenesis. We have shown that *Nf1*-deficient cells display a remarkable rewire of cellular bioenergetics which could potentially participate in a determinant manner to the tumorigenic process. We will further examine the mechanisms that are responsible for the neoplastic growth investigating the pathways that are shaped by mitochondrial function (e.g., HIF1α stabilization, PTP modulation).

APPENDIX

Biochimica et Biophysica Acta 1817 (2012) 1860–1866

Contents lists available at SciVerse ScienceDirect

Biochimica et Biophysica Acta

journal homepage: www.elsevier.com/locate/bbabio

Induction of the permeability transition pore in cells depleted of mitochondrial DNA☆

Ionica Masgras, Andrea Rasola *, Paolo Bernardi *

Consiglio Nazionale delle Ricerche Institute of Neurosciences, University of Padova, Padova, Italy
Department of Biomedical Sciences, University of Padova, Padova, Italy

ARTICLE INFO

Article history:
Received 20 January 2012
Received in revised form 16 February 2012
Accepted 21 February 2012
Available online 28 February 2012

Keywords:
Mitochondrion
ρ^0 cell
Permeability transition
Cyclophilin D
Hexokinase
GSK3β

ABSTRACT

Respiratory complexes are believed to play a role in the function of the mitochondrial permeability transition pore (PTP), whose dysregulation affects the process of cell death and is involved in a variety of diseases, including cancer and degenerative disorders. We investigated here the PTP in cells devoid of mitochondrial DNA (ρ^0 cells), which lack respiration and constitute a model for the analysis of mitochondrial involvement in several pathological conditions. We observed that mitochondria of ρ^0 cells maintain a membrane potential and that this is readily dissipated after displacement of hexokinase (HK) II from the mitochondrial surface by treatment with either the drug clotrimazole or with a cell-permeant HK II peptide, or by placing ρ^0 cells in a medium without serum and glucose. The PTP inhibitor cyclosporin A (CsA) could decrease the mitochondrial depolarization induced by either HK II displacement or by nutrient depletion. We also found that a fraction of the kinases ERK1/2 and GSK3α/β is located in the mitochondrial matrix of ρ^0 cells, and that glucose and serum deprivation caused concomitant ERK1/2 inhibition and GSK3α/β activation with the ensuing phosphorylation of cyclophilin D, the mitochondrial target of CsA. GSK3α/β inhibition with indirubin-3′-oxime decreased PTP-induced cell death in ρ^0 cells following nutrient ablation. These findings indicate that ρ^0 cells are equipped with a functioning PTP, whose regulatory mechanisms are similar to those observed in cancer cells, and suggest that escape from PTP opening is a survival factor in this model of mitochondrial diseases. This article is part of a Special Issue entitled: 17th European Bioenergetics Conference (EBEC 2012).

1. Introduction

The creation of cells depleted of mitochondrial DNA (mtDNA), termed ρ^0 cells [1,2], has been a major advance in the study and understanding of mtDNA diseases. The availability of ρ^0 cells allowed their repopulation with different mitochondrial genomes, and thus provided an essential tool to define key pathogenic parameters such as the degree of heteroplasmy and threshold levels of mutant mtDNA [3,4]. ρ^0 cells represent an extreme case of mitochondrial dysfunction that has also attracted considerable interest in the fields of bioenergetics and cell death [5–18], in particular about the intrinsic pathway to apoptosis that is triggered by release of mitochondrial apoptogenic proteins [19] and about the effector mechanisms of necrosis caused by bioenergetic failure [20].

One candidate mechanism for the irreversible commitment to cell death is the mitochondrial permeability transition pore (PTP), an inner membrane cyclosporin (Cs) A-sensitive, high-conductance channel whose opening causes mitochondrial depolarization and a variety of effects that depend on the PTP open time [21]. Whereas short open times may take part in physiological Ca^{2+} signalling by providing mitochondria with a fast Ca^{2+} release channel [22–26], longer openings lead to rearrangement of the cristae and to matrix swelling and eventually prompt outer membrane rupture followed by release of cytochrome *c* and of other proapoptotic proteins (such as AIF, Smac/DIABLO and endonuclease G) for which there is no selective release pathway in the outer membrane [27].

Despite the crucial importance of PTP in cell biology and in the pathogenesis of a number of diseases [28], its molecular composition remains an unsolved riddle. The activity of RC complexes and of ATP synthase can influence the PTP, as ROS generated as a respiratory by-product can elicit pore openings [29]. We have demonstrated that the PTP modulator cyclophilin D (CyP-D) binds and inhibits the ATP synthase [30] and that the activity of RC complex I contributes to setting the threshold voltage for PTP opening [31], providing molecular and conceptual bases for the existence of a functional interplay between

Abbreviations: Cs, cyclosporin; CyP-D, cyclophilin D; $\Delta\psi_m$, mitochondrial membrane potential difference; EGTA, ethylene glycol-bis(2-aminoethyl)-N,N,N',N'-tetraacetic acid; FCCP, carbonylcyanide-*p*-trifluoromethoxyphenyl hydrazone; HK II, Hexokinase II; PTP, permeability transition pore; TAT-HK II, KMIASHLLAYFFTELNβA-GYGRKKRRQRRRG peptide; RC, respiratory chain; TMRM, tetramethylrhodamine methyl ester

☆ This article is part of a Special Issue entitled: 17th European Bioenergetics Conference (EBEC 2012).

* Corresponding authors at: Department of Biomedical Sciences, University of Padova, Viale Giuseppe Colombo 3, I-35121 Padova, Italy. Fax: +39 0498276361.
E-mail addresses: rasola@bio.unipd.it (A. Rasola), bernardi@bio.unipd.it (P. Bernardi).

0005-2728/$ – see front matter © 2012 Elsevier B.V. All rights reserved.
doi:10.1016/j.bbabio.2012.02.022

respiration and the PTP. Moreover, we have recently shown that PTP opening plays a pathogenic role in two models of mitochondrial diseases endowed with inactivation of RC complex I, *i.e.* HL180 cybrids harboring two missense mutations causative of Leber Hereditary Optic Neuropathy in the mtDNA ND6 gene [32,33], and the cell line XTC.UC1 (derived from a thyroid oncocytoma [34]) that bears a disruptive frameshift mutation in the mtDNA ND1 gene [35]. Nonetheless, whether the PTP is involved in other mtDNA disease models is not known, and a formal definition of the role played by RC complexes in PTP regulation and molecular composition is still lacking.

Cells devoid of mtDNA also constitute a potential model for the study of the bioenergetics of neoplasias, where mitochondrial respiration is decreased and ATP is largely provided by inducing glycolysis and uncoupling it from oxygen availability, the Warburg effect [36–38]. Thus, ρ^0 cells can be considered as possessing an extreme "Warburg phenotype". Furthermore, reduction of mtDNA copy number was reported in diverse types of tumors such as stomach, colon, lung [39], hepatocellular [40], ovarian [41] and breast carcinomas [42] and astrocytomas [43]; mtDNA was also reported to affect angiogenesis, invasiveness [44,45] and resistance to death of tumor cells [15,46]. We and others have observed that mitochondria from tumor cells display an increased resistance to PTP opening as a death-escaping strategy, and this is achieved both by deploying hexokinase (HK) II on the mitochondrial surface, where it maintains the PTP in a closed state through a poorly defined signal transduction cascade directed to matrix components such as CyP-D [47]; and by constitutively inducing an ERK/GSK3 signalling pathway that maintains CyP-D in a dephosphorylated state, thus enhancing the threshold for PTP induction [48,49].

In keeping with these data, here we observe that in human osteosarcoma 206 ρ^0 cells the PTP is induced both by HK II detachment from mitochondria, and by modulation of an ERK/GSK3/CyP-D transduction axis following glucose and serum depletion.

2. Materials and methods

2.1. Materials, cell cultures and growth conditions

Tetramethylrhodamine methyl ester (TMRM) was from Molecular Probes (Eugene, OR); FITC-conjugated annexin-V was from Boehringer Mannheim (Indianapolis, IN); indirubin-3′-oxime and CsA were from Calbiochem (San Diego, CA); cyclosporin H (CsH) was a generous gift of Dr. Urs Ruegg, Geneva; all other chemicals were from Sigma (Milan, Italy). Mouse monoclonal anti GSK-3α/β, Grim19, SDHA and UQCRC1, goat polyclonal anti calnexin, HK II and VDAC1, and rabbit polyclonal anti ERK2, PARP and TOM20 antibodies were from Santa Cruz Biotechnology (Santa Cruz, CA); rabbit polyclonal anti phospho-ERK1/2 (Thr202/Tyr204) and anti phospho GSK-3α/β (Ser21/9) and rabbit monoclonal anti caspase-3 antibodies were from Cell Signaling (Beverly, MA); mouse monoclonal anti phospho-Ser/Thr, CyP-D and anti prohibitin antibodies were from Qiagen, Calbiochem, and Lab Vision (Fremont, CA), respectively; rabbit polyclonal anti AIF antibody was from Exalpha Biologicals (Shirley, MA); the mouse monoclonal OXPHOS antibody cocktail recognizing CI (NDUFB8), CII (SDHB), CIII (core2), CIV (COXII) and CV (α) was from Mito-Sciences (Eugene, OR). Peptides MIASHLLAYFFTELNβA-GYGRKKRRQRRRG (TAT-HK II) and GYGRKKRRQRRRG-βA-EEEAKNAAAKLAVEILNKEKK (TAT-Ctrl) were synthesized by a solid phase method using an automatized peptide synthesizer (model 431-A, Applied Biosystems, Foster City, CA).

The human 143B osteosarcoma and the derived 206 ρ^0 cell lines were kindly provided by Lodovica Vergani (Department of Neurosciences, University of Padova, Padova, Italy). Cells were grown in high glucose (4500 mg/l) Dulbecco's modified Eagle's medium (DMEM) containing 10% fetal bovine serum, 4 mM L-glutamine, 110 mg/l sodium pyruvate, 100 units/ml penicillin, and 100 μg/ml streptomycin in a humidified incubator at 37 °C with 5% CO_2. Medium of ρ^0 cells was supplemented with 50 mg/l uridine, essential amino acids and vitamins.

2.2. Mitochondrial membrane potential and cell death

Mitochondrial membrane potential ($\Delta\psi_m$) was measured either by epifluorescence microscopy or by flow cytometry (see below). For epifluorescence microscopy cells were seeded onto 24 mm-diameter round glass coverslips and grown for 2 days in DMEM. $\Delta\psi_m$ was measured based on the accumulation of TMRM in the presence of CsH, which inhibits the multidrug resistance pump but not the PTP [50,51]. Cells were incubated in bicarbonate- and phenol red-free DMEM supplemented with 10 mM Hepes and 1.6 μM CsH and loaded with 20 nM TMRM for 30 min at 37 °C. At the end of each experiment, mitochondria were fully depolarized by the addition of 4 μM of the protonophore FCCP. Cellular fluorescence images were acquired with an Olympus IX71/IX51 inverted microscope equipped with a xenon light source for epifluorescence illumination and with a 12-bit digital cooled CCD camera (Micromax, Princeton Instruments, Trenton, NJ). For detection of fluorescence 568 ± 25 nm bandpass excitation and 585 nm longpass emission filter settings were used. Images were collected every 3 min with an exposure time of 100 ms (6% illumination intensity) using a 40×, 1.3 NA oil immersion objective (Olympus). Data were acquired and analyzed using Cell R software (Olympus). Clusters of several mitochondria were identified as regions of interest, and fields not containing cells were taken as the background. Sequential digital images were acquired every minute, and the average fluorescence intensity of all relevant regions was recorded and stored for subsequent analysis.

For FACS analysis cells were resuspended in 135 mM NaCl, 10 mM Hepes, 5 mM $CaCl_2$ and incubated for 15 min at 37 °C with TMRM (20 nM) and CsH (1.6 μM) or with FITC-conjugated Annexin-V, to detect mitochondrial membrane depolarization (reduced TMRM staining) or phosphatidylserine exposure on the cell surface (increased FITC-conjugated Annexin-V staining) respectively. Changes in forward and side light scatter were assessed at the same time to measure alterations in cell dimension and granularity, respectively. Samples were analyzed on a FACSCanto II flow cytometer (Becton Dickinson, San Diego, CA, USA). Data acquisition and analysis were performed using FACSDiva software. Regions were designed on diagrams to evaluate the percentage of cell subpopulations as indicated in Fig. 3.

2.3. Cell lysis, fractionation, western immunoblot analysis

Total cell extracts were prepared at 4 °C in 150 mM NaCl, 20 mM Tris–HCl pH 7.4, 5 mM EDTA, 10% glycerol, 1% Triton X-100 in the presence of phosphatase and protease inhibitors (Sigma). To prepare mitochondrial extracts, cells were placed in isolation buffer (250 mM sucrose, 10 mM Tris–HCl, 0.1 mM EGTA–Tris, pH 7.4) and homogenized at 4 °C. Mitochondria were then isolated by differential centrifugation in mitochondrial isolation buffer. Unless otherwise stated, mitochondria were treated with trypsin at 4 °C for 1 h at a mitochondria:trypsin ratio of 35:1 (w/w). After trypsin inactivation with a protease inhibitor cocktail (Sigma), mitochondria were spun at 18,000 × *g* at 4 °C for 10 min. For immunoprecipitation, 4 mg of extracted proteins per reaction was incubated with antibodies conjugated to protein A-Sepharose beads (Pharmacia, Pfizer, Cambridge, MA) at 4 °C overnight. Negative controls were performed by incubating lysates on beads in the absence of primary antibodies. Samples were separated under reducing conditions on SDS-polyacrylamide gels and transferred onto Hybond-C Extra membranes (Amersham). Primary antibodies were incubated 16 h at 4 °C, and horseradish peroxidase-conjugated secondary antibodies were added for 1 h at room temperature. Proteins were visualized by enhanced chemiluminescence (Millipore). Densitometric analysis was performed with Quantity One software (Bio-Rad Laboratories).

2.4. Statistics

Unless otherwise stated each experiment was repeated at least three times. Data are presented as average ± S.E. or, for clarity, as representative experiments (see figure legends for details).

3. Results

3.1. Characterization of ρ^0 cells

In order to characterize the 206 ρ^0 human osteosarcoma cell line, we assessed the expression of a panel of respiratory chain (RC) subunits, whose assembly requires proteins encoded by mitochondrial DNA (mtDNA) genes with the exception of RC complex II. As expected, we found that 206 ρ^0 cells were totally devoid of RC complexes I and IV, whereas they displayed a level of nuclear-encoded RC proteins of RC II and III and of the ATP synthase comparable to the parental 143B ρ^+ cells (Fig. 1A).

We also monitored $\Delta\psi_m$ *in situ* by measuring cell accumulation of TMRM. Under our loading conditions mitochondrial depolarization corresponds to a decrease of mitochondrial fluorescence, since the accumulated probe is still below the quenching threshold [52]. It should be noted that cells were also treated with CsH, which does not affect the PTP but inhibits the multidrug resistance pump and therefore normalizes cytosolic loading with TMRM, which is a substrate of the pump and could therefore be extruded at rates that vary widely in different cell types [50]. Both ρ^+ and ρ^0 osteosarcoma cells displayed a punctuate pattern of TMRM labelling, which disappeared after treatment with the uncoupler FCCP (Fig. 1B), thus confirming that TMRM accumulation in ρ^0 cells is due to the existence of a $\Delta\psi_m$.

3.2. HK II detachment from mitochondria as a PTP-inducing strategy

As ρ^0 cells lack oxidative phosphorylation, they must entirely rely on glycolytic activity to generate ATP. Accordingly, we found that the expression level of the first enzyme of the glycolytic chain, hexokinase, and in particular HK isoform II, which is upregulated in tumor cells, was increased in 206 ρ^0 cells compared to parental 143B ρ^+ cells (Fig. 1C). A large fraction of HK II was located in mitochondria (Fig. 1D), as already observed in tumor cell models [47,53]. Since unbinding of HK II from the organelles prompts PTP opening [47], we induced HK II detachment in order to assess the presence of a PTP in ρ^0 cells. As a first strategy, we used the drug clotrimazole (CTM), and found that in ρ^0 cells it both caused detachment of HK II (Fig. 2A) and

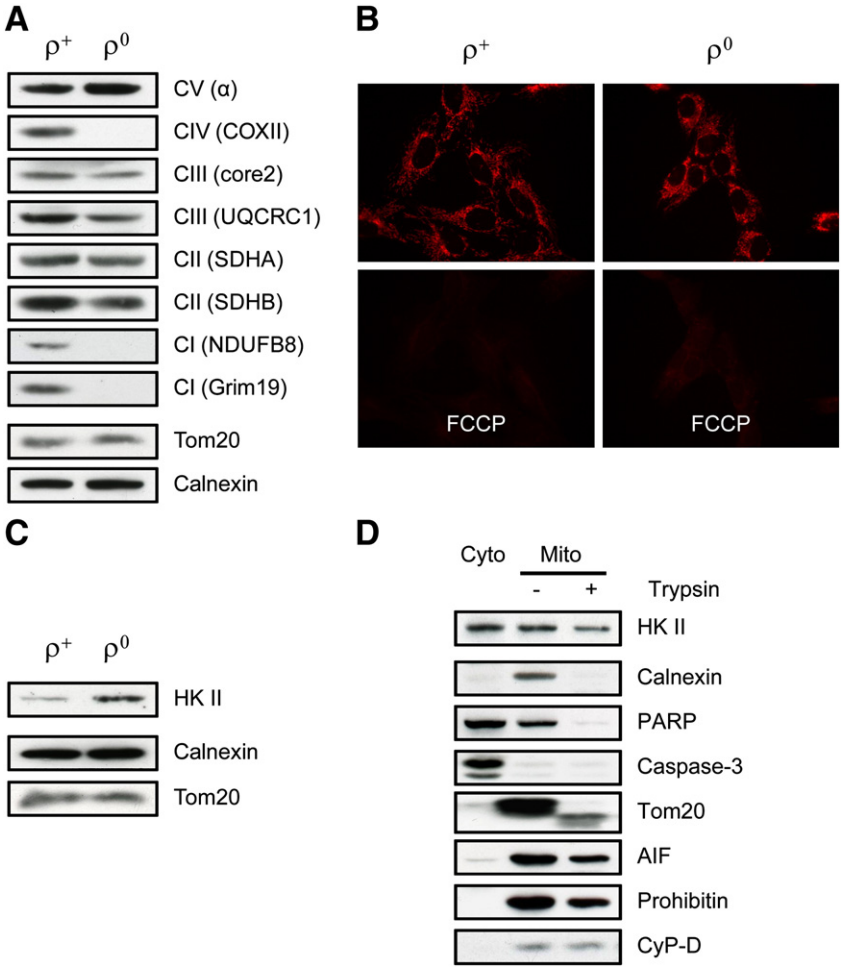

Fig. 1. ρ^0 cells display a mitochondrial membrane potential and upregulate HK II. A, immunoblot analysis of RC protein expression from complex V (CV) to complex I (CI) in 143B human osteosarcoma ρ^+ cells and in 206 ρ^0 cells. B, epifluorescence microscopy images of ρ^+ and ρ^0 cells loaded with 20 nM TMRM before (*upper panels*) and after (*lower panels*) the addition of 4 μM FCCP. C, immunoblot analysis of HK II expression in total cell extracts from ρ^+ and ρ^0 cells; D, immunoblot analysis showing a mitochondria-bound fraction of HK II in ρ^0 cells; the lanes refer to the cytosolic (Cyto) and to the mitochondrial fraction (Mito) before (−) or after (+) treatment with 2 μg trypsin every 70 μg of mitochondria. Calnexin and Tom20 are used as loading controls in A and C; calnexin, PARP and caspase-3 are endoplasmic reticulum, nucleus and cytosol markers, respectively, used to assess the purity of mitochondria in D; Tom20 and AIF are markers of the outer mitochondrial membrane and of the intermembrane space, respectively, whereas prohibitin and CyP-D are matrix proteins.

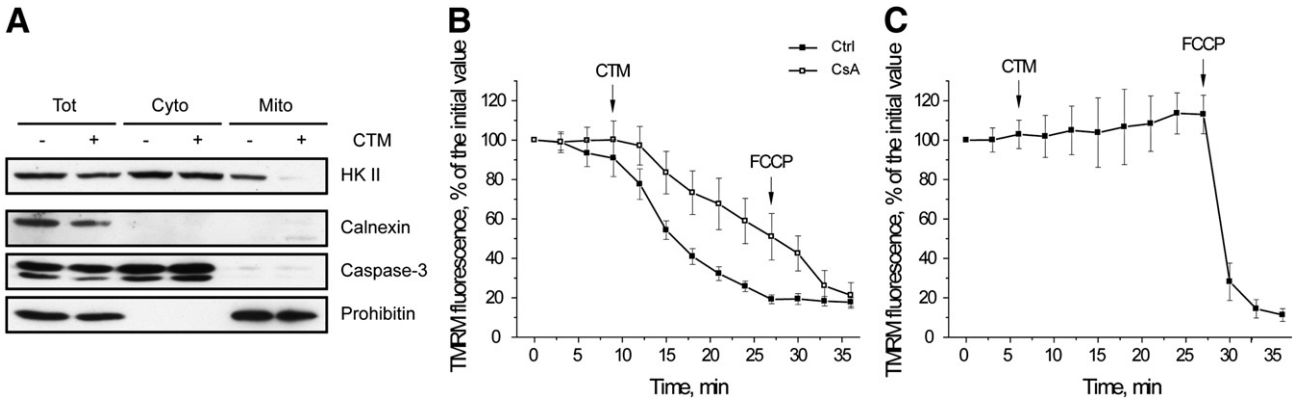

Fig. 2. Treatment with CTM induces detachment of HK II from mitochondria and mitochondrial depolarization in 206 human osteosarcoma ρ^0 cells. A, immunoblot analysis of HK II expression in total lysates (Tot), cytosolic (Cyto) or mitochondrial fractions (Mito) before (−) or after (+) treatment with 50 μM CTM for 1 h; the mitochondrial fraction was subjected to trypsinization at 4 °C for 1 h at a mitochondria:trypsin ratio of 35:1 (w/w); prohibitin is used as a mitochondrial loading control. B, C, TMRM epifluorescence intensity of 206 ρ^0 (panel B) and 143B ρ^+ (panel C) cells; where indicated 10 μM CTM and 4 μM FCCP were added in the absence (closed symbols) or presence (panel B, open symbols) of 1.6 μM CsA.

mitochondrial depolarization, as assessed by a kinetic analysis of TMRM staining performed with epifluorescence microscopy (Fig. 2B), whereas it was ineffective in ρ^+ cells (Fig. 2C). Notably, preincubation with CsA, a drug that targets the PTP regulator CyP-D, markedly delayed the mitochondrial depolarization induced by CTM (Fig. 2B). In parallel, we used a HK II-derived peptide (TAT-HK II) made cell permeant through linking with a hydrophobic stretch of the HIV-1 TAT protein, which displaces HK II from mitochondria with very high selectivity [47]. After having confirmed the effect of the peptide on HK II binding to mitochondria of ρ^0 cells (Fig. 3A), in keeping with the CTM data, we found that TAT-HK II was unable to affect $\Delta\psi_m$ of 143B ρ^+ cells (Fig. 3B), but it triggered a rapid mitochondrial depolarization in 206 ρ^0 cells (Fig. 3C–E). Again, cell pretreatment with CsA markedly inhibited the effect of TAT-HK II (Fig. 3D–E). Taken together, these data indicate that 206 ρ^0 cells are

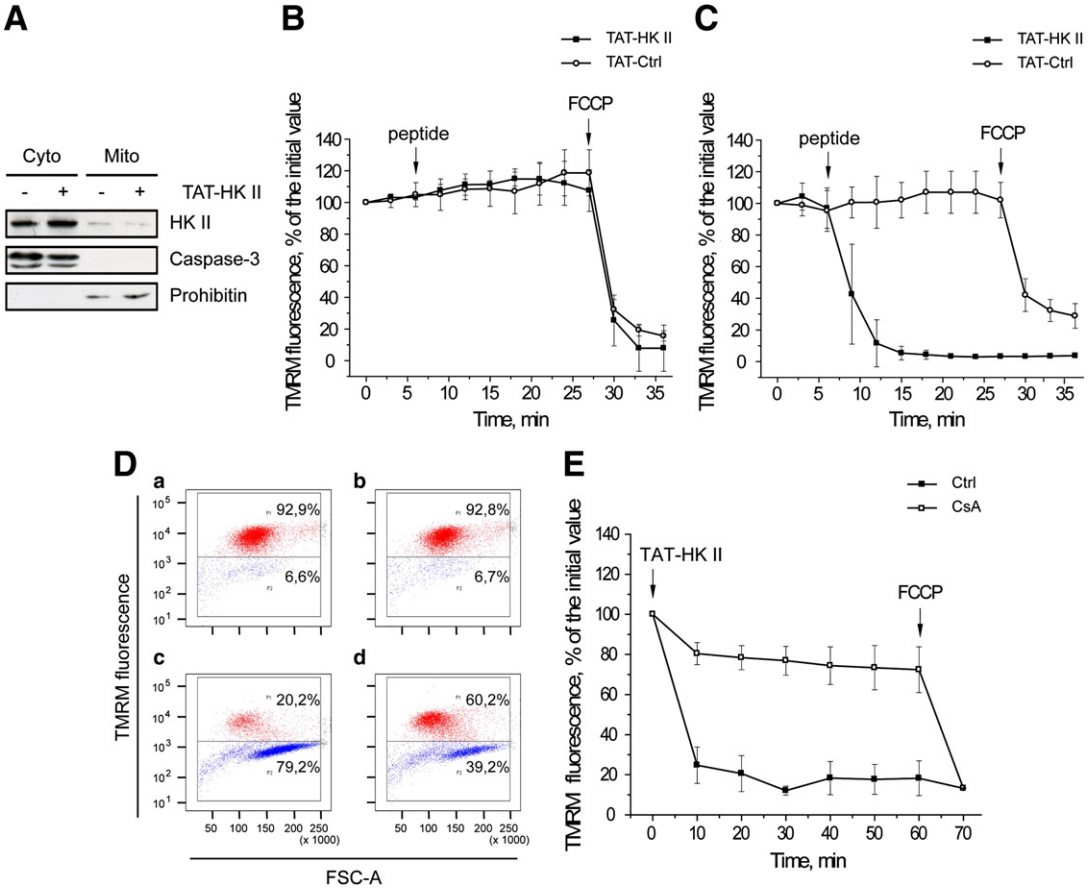

Fig. 3. The TAT-HK II peptide induces HK II detachment from mitochondria and the ensuing mitochondrial depolarization and PTP opening in 206 human osteosarcoma ρ^0 cells. A, immunoblot analysis of HKII expression in cytosolic (Cyto) and mitochondrial (Mito) fractions treated with TAT-Ctrl peptide (−) or TAT-HK II peptide (+) for 1 h; mitochondrial fraction was subjected to trypsinization at 4 °C for 1 h at a mitochondria:trypsin ratio of 35:1 (w/w); prohibitin is used as a mitochondrial loading control. B,C, TMRM epifluorescence intensity of 143B ρ^+ (panel B) and 206 ρ^0 cells (panel C) cells; where indicated 5 μM TAT-HK II peptide (closed symbols) or 5 μM TAT-Ctrl peptide (open symbols) were added. D, output of multiparametric FACS analysis showing the TMRM fluorescence intensity and forward light scattering (FSC-A) of ρ^0 cells in the absence of additions (panel a) and after treatment with 1.6 μM CsA (panel b), 2.5 μM TAT-HK II peptide (panel c) or 2.5 μM TAT-HK II peptide in cells pretreated with 1.6 μM CsA (panel d). E, kinetic FACS analysis of TMRM fluorescence intensity of ρ^0 cells; where indicated, 2.5 μM TAT-HK II peptide was added to naive cells (closed symbols) or to cells that had been treated with 1.6 μM CsA (open symbols).

endowed with a mitochondrial PTP, whose opening can be triggered by mitochondrial detachment of the HK II enzyme.

3.3. Nutrient starvation is another way to induce PTP opening in 206 ρ^0 cells

We and others have recently shown that PTP opening is regulated in tumor cell models by an ERK/GSK3/CyP-D transduction axis; in mitochondria, GSK3 favors PTP opening by phosphorylating CyP-D, but a constitutively active ERK opposes this signalling by phosphorylating and inhibiting GSK3 [48,49]. Therefore, we tried to elicit PTP opening by exposing 206 ρ^0 cells to starvation through serum and glucose depletion, thus blocking ERK and triggering this transduction pathway. As expected, in these conditions we observed both ERK inhibition and GSK3 activation (Fig. 4A; active ERK1/2 is Ser/Thr phosphorylated, whereas active GSK3α/β is Ser/Thr dephosphorylated). Moreover, 206 ρ^0 cells underwent a rapid mitochondrial depolarization that was sensitive to CsA (Fig. 4B); remarkably, in 143B ρ^+ cells a 4 hour serum and glucose depletion was unable to induce major changes in the ERK/GSK3 signaling axis (Fig. 4A), and these cells did not undergo any mitochondrial depolarization (Fig. 4B). To better assess the role played by ERK and GSK3 in PTP opening of 206 ρ^0 cells, we explored the presence of a mitochondrial fraction of these enzymes. As reported in Fig. 4C, we could find both ERK1/2 and GSK3α/β in 206 ρ^0 mitochondria, and modulation of their activity in mitochondria following serum and glucose depletion paralleled that observed in the whole cells; in addition, a partial tryptic digestion of the mitochondrial fraction revealed that both kinases are located in the matrix, as they display a pattern of trypsin resistance similar to that of matrix prohibitin (Fig. 4D). In accord with an enhancing role played on PTP opening by GSK3-dependent phosphorylation of CyP-D, we observed that CyP-D is Ser/Thr phosphorylated in 206 ρ^0 cells after serum and glucose starvation (Fig. 4E), and that the GSK3 inhibitor indirubin-3′-oxime inhibited cell death in these conditions (Fig. 4F).

Notably, when 206 ρ^0 cells were depleted of serum and glucose we could observe HK II detachment from mitochondria (Fig. 4C), suggesting that these conditions might converge on a PTP-opening signal that involves HK II partition between mitochondria and cytosol.

4. Discussion

In the present manuscript we have shown (i) that ρ^0 cells can undergo a CsA-sensitive permeability transition; (ii) that opening of the PTP plays a role in cell death caused by HK II detachment from mitochondria and by glucose and serum deprivation; and (iii) that ρ^0 cells undergo adaptive changes that are remarkably similar to those of highly glycolytic tumor cells such as increased expression of HK II on the mitochondrial outer membrane and regulation of PTP opening through GSK3-dependent Ser/Thr phosphorylation of CyP-D.

The occurrence of PTP opening in ρ^0 cells is debated: two studies could not find protective effects of CsA on either cell death induced by staurosporine [13] or on caspase-3 activation induced by thapsigargin [18]. Yet, a negative result cannot rule out with certainty a role of the PTP. Indeed, CsA desensitizes but does not block the pore [54], which may be very prone to opening in ρ^0 cells given (i) their lower $\Delta\psi_m$ [9,11] and (ii) the voltage-dependence of the PTP [55], which in ρ^0 cells may be poised very close to the resting potential. Here we demonstrate that CsA can inhibit mitochondrial depolarization induced in ρ^0 cells both by HK II detachment and by serum and glucose depletion. These results strongly argue in favor of the existence of a PTP in cells

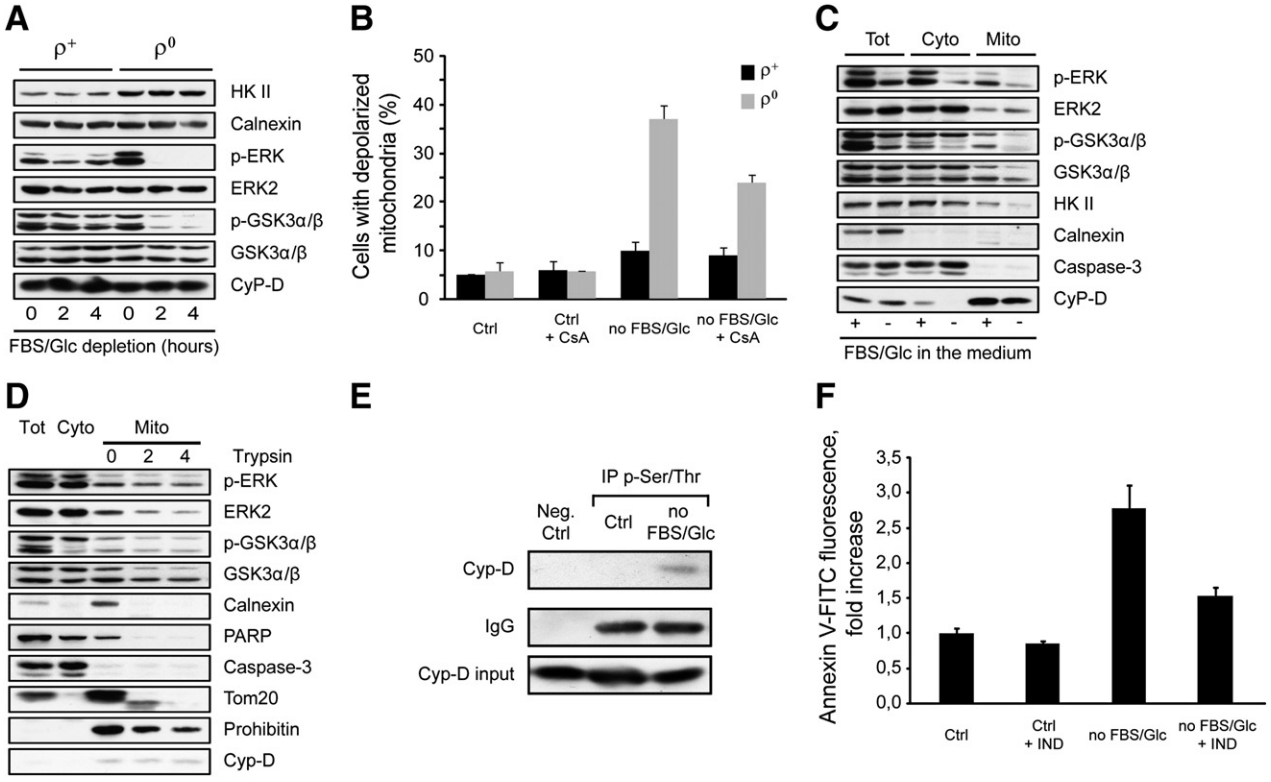

Fig. 4. FBS/glucose depletion of 206 human osteosarcoma ρ^0 cells triggers PTP opening and cell death through the phosphorylation of CyP-D. A, immunoblot analysis of total lysates of 143B ρ^+ and 206 ρ^0 cells before (lanes marked *0*) and after the indicated times of FBS/glucose depletion. B, FACS analysis of the number of cells with depolarized mitochondria (as determined on the lack of staining with TMRM, see Fig. 3C) under basal conditions (Ctrl) or after 1 h of FBS/glucose depletion with or without 1.6 μM CsA. C, immunoblot analysis of subcellular fractions of ρ^0 cells incubated for 2 h in the presence (+) or absence (−) of FBS/glucose. D, immunoblot analysis of the subcellular expression of ERK and GSK3α/β in total lysates (Tot), cytosolic (Cyto) or mitochondrial fractions (Mito) before (lanes marked *0*) or after treatment with 2 or 4 μg of trypsin every 70 μg of mitochondria. Endoplasmic reticulum, nucleus, cytosol and mitochondrial markers are as described in Fig. 1. E, Phospho-Ser/Thr immunoprecipitations on lysates from ρ^0 cells kept in medium with or without FBS and glucose for 2 h. Blot probing with CyP-D is shown, and IgG and input of CyP-D are reported as loading controls. F, FACS analysis of annexin V-FITC staining of ρ^0 cells depleted or not for 6 hours of FBS and glucose; IND is the GSK3α/β inhibitor indirubin-3′-oxime. Mean fluorescence is plotted as fold change compared to control.

devoid of mtDNA, suggesting that a functional respiratory chain is dispensable for PTP induction.

The observation that ρ^0 cells are more sensitive than ρ^+ cells to the PTP-inducing effects of HK II detachment could find a reasonable explanation within the framework of the PTP voltage-dependence [55] and in the light of previous studies on the genesis of the $\Delta\psi_m$ in ρ^0 cells [9,11]. Although the F_1F_0 ATP synthase of ρ^0 cells does not pump protons it is catalytically active as an ATP hydrolase, and this activity is essential to maintain a gradient of ATP between the cytosol and the matrix allowing the electrogenic exchange of extramitochondrial ATP for matrix ADP, which generates the $\Delta\psi_m$ [9]. Sensitive isotope distribution techniques allowed to determine the $\Delta\psi_m$ of ρ^0 cells to ≈ -67 mV, which is about half of that maintained by parental ρ^+ cells under the same experimental conditions [11]. This means that the resting potential of ρ^0 cells is closer to the voltage threshold for PTP opening, which is therefore easily activated as soon as HK II is removed from the outer membrane. Remarkably, in ρ^0 cells binding of HK II to the outer membrane of mitochondria is upregulated and contributes to inhibition of outer membrane permeabilization via either the Bax pathway or the permeability transition [47,56]. Thus, increased mitochondrial HK II in ρ^0 cells appears as a protective mechanism meant to counteract PTP opening, which is rapidly induced when HK II is detached from mitochondria with either CTM or a HK II-derived peptide.

Why should PTP opening be detrimental in mitochondria that do not pump protons across the inner mitochondrial membrane? The very existence of a $\Delta\psi_m$ implies that the inner membrane permeability of ρ^0 cells is low enough for charge separation to occur. It has been calculated that mitochondria in ρ^0 cells utilize $\approx$13% of the total glycolytic flux to maintain $\Delta\psi_m$; and that this flux is $\approx$18% of the maximal ATP hydrolytic capacity of mitochondria as measured after permeabilization [11]. This means that PTP opening can increase the mitochondrial ATP hydrolytic rate up to five fold, thus drawing an increased fraction of the glycolytic ATP flux and contributing to ATP depletion.

It is becoming increasingly clear that the PTP is the terminal effector of several signal transduction modules, including organelle-restricted kinases and phosphatases [29]. We and others have recently shown that signalling through mitochondrial ERK and GSK3 contributes to the anti-apoptotic phenotype of tumor cells through PTP inhibition conveyed by modulation of Ser/Thr CyP-D phosphorylation [48,49]. Our present findings of a similar regulatory pattern of CyP-D in ρ^0 cells further extend the interest in this model to understand the antiapoptotic defence mechanisms of highly glycolytic tumor cells.

Acknowledgements

This manuscript is in partial fulfilment of the requirements for the PhD of IM. We would like to thank Lodovica Vergani for providing the cells used in this study, Valeria Petronilli, Marco Sciacovelli and Luca Azzolin for helpful discussions, Oriano Marin for peptide synthesis and Marco Ardina for invaluable assistance with informatics. This work was supported by Telethon-Italy (Program Project *Therapeutic Strategies to Combat Mitochondrial Disorders*) and the University of Padova (Progetto Strategico *Models of mitochondrial diseases*).

References

[1] M.P. King, G. Attardi, Human cells lacking mtDNA: repopulation with exogenous mitochondria by complementation, Science 246 (1989) 500–503.
[2] M.P. King, G. Attardi, Isolation of human cell lines lacking mitochondrial DNA, Methods Enzymol. 264 (1996) 304–313.
[3] D. Pye, D.S. Kyriakouli, G.A. Taylor, R. Johnson, M. Elstner, B. Meunier, Z.M. Chrzanowska-Lightowlers, R.W. Taylor, D.M. Turnbull, R.N. Lightowlers, Production of transmitochondrial cybrids containing naturally occurring pathogenic mtDNA variants, Nucleic Acids Res. 34 (2006) e95.
[4] I.A. Trounce, C.A. Pinkert, Cybrid models of mtDNA disease and transmission, from cells to mice, Curr. Top. Dev. Biol. 77 (2007) 157–183.
[5] M.D. Jacobson, J.F. Burne, M.P. King, T. Miyashita, J.C. Reed, M.C. Raff, Bcl-2 blocks apoptosis in cells lacking mitochondrial DNA, Nature 361 (1993) 365–369.
[6] P. Marchetti, S.A. Susin, D. Decaudin, S. Gamen, M. Castedo, T. Hirsch, N. Zamzami, J. Naval, A. Senik, G. Kroemer, Apoptosis-associated derangement of mitochondrial function in cells lacking mitochondrial DNA, Cancer Res. 56 (1996) 2033–2038.
[7] L.R. Cavalli, M. Varella-Garcia, B.C. Liang, Diminished tumorigenic phenotype after depletion of mitochondrial DNA, Cell Growth Differ. 8 (1997) 1189–1198.
[8] M. Higuchi, B.B. Aggarwal, E.T. Yeh, Activation of CPP32-like protease in tumor necrosis factor-induced apoptosis is dependent on mitochondrial function, J. Clin. Invest. 99 (1997) 1751–1758.
[9] K. Buchet, C. Godinot, Functional F1-ATPase essential in maintaining growth and membrane potential of human mitochondrial DNA-depleted ρ° cells, J. Biol. Chem. 273 (1998) 22983–22989.
[10] B.C. Liang, E. Ullyatt, Increased sensitivity to cis-diamminedichloroplatinum induced apoptosis with mitochondrial DNA depletion, Cell Death Differ. 5 (1998) 694–701.
[11] R.D. Appleby, W.K. Porteous, G. Hughes, A.M. James, D. Shannon, Y.H. Wei, M.P. Murphy, Quantitation and origin of the mitochondrial membrane potential in human cells lacking mitochondrial DNA, Eur. J. Biochem. 262 (1999) 108–116.
[12] S. Jiang, J. Cai, D.C. Wallace, D.P. Jones, Cytochrome c-mediated apoptosis in cells lacking mitochondrial DNA. Signaling pathway involving release and caspase 3 activation is conserved, J. Biol. Chem. 274 (1999) 29905–29911.
[13] R. Dey, C.T. Moraes, Lack of oxidative phosphorylation and low mitochondrial membrane potential decrease susceptibility to apoptosis and do not modulate the protective effect of Bcl-x(L) in osteosarcoma cells, J. Biol. Chem. 275 (2000) 7087–7094.
[14] J.Y. Kim, Y.H. Kim, I. Chang, S. Kim, Y.K. Pak, B.H. Oh, H. Yagita, Y.K. Jung, Y.J. Oh, M.S. Lee, Resistance of mitochondrial DNA-deficient cells to TRAIL: role of Bax in TRAIL-induced apoptosis, Oncogene 21 (2002) 3139–3148.
[15] S.Y. Park, I. Chang, J.Y. Kim, S.W. Kang, S.H. Park, K. Singh, M.S. Lee, Resistance of mitochondrial DNA-depleted cells against cell death: role of mitochondrial superoxide dismutase, J. Biol. Chem. 279 (2004) 7512–7520.
[16] G. Biswas, M. Guha, N.G. Avadhani, Mitochondria-to-nucleus stress signaling in mammalian cells: nature of nuclear gene targets, transcription regulation, and induced resistance to apoptosis, Gene 354 (2005) 132–139.
[17] G. Biswas, H.K. Anandatheerthavarada, N.G. Avadhani, Mechanism of mitochondrial stress-induced resistance to apoptosis in mitochondrial DNA-depleted C2C12 myocytes, Cell Death Differ. 12 (2005) 266–278.
[18] J.Q. Kwong, M.S. Henning, A.A. Starkov, G. Manfredi, The mitochondrial respiratory chain is a modulator of apoptosis, J. Cell Biol. 179 (2007) 1163–1177.
[19] R.C. Taylor, S.P. Cullen, S.J. Martin, Apoptosis: controlled demolition at the cellular level, Nat. Rev. Mol. Cell Biol. 9 (2008) 231–241.
[20] W.-X. Zong, C.B. Thompson, Necrotic death as a cell fate, Genes Dev. 20 (2006) 1–15.
[21] A. Rasola, P. Bernardi, Mitochondrial permeability transition in Ca^{2+}-dependent apoptosis and necrosis, Cell Calcium 50 (2011) 222–233.
[22] R.A. Altschuld, C.M. Hohl, L.C. Castillo, A.A. Garleb, R.C. Starling, G.P. Brierley, Cyclosporin inhibits mitochondrial calcium efflux in isolated adult rat ventricular cardiomyocytes, Am. J. Physiol. 262 (1992) H1699–H1704.
[23] P. Bernardi, V. Petronilli, The permeability transition pore as a mitochondrial calcium release channel: a critical appraisal, J. Bioenerg. Biomembr. 28 (1996) 131–138.
[24] J.W. Elrod, R. Wong, S. Mishra, R.J. Vagnozzi, B. Sakthievel, S.A. Goonasekera, J. Karch, S. Gabel, J. Farber, T. Force, J.H. Brown, E. Murphy, J.D. Molkentin, Cyclophilin D controls mitochondrial pore-dependent Ca^{2+} exchange, metabolic flexibility, and propensity for heart failure in mice, J. Clin. Invest. 120 (2010) 3680–3687.
[25] A. Barsukova, A. Komarov, G. Hajnoczky, P. Bernardi, D. Bourdette, M. Forte, Activation of the mitochondrial permeability transition pore modulates Ca^{2+} responses to physiological stimuli in adult neurons, Eur. J. Neurosci. 33 (2011) 831–842.
[26] S. von Stockum, E. Basso, V. Petronilli, P. Sabatelli, M.A. Forte, P. Bernardi, Properties of Ca^{2+} transport in mitochondria of *Drosophila melanogaster*, J. Biol. Chem. 286 (2011) 41163–41170.
[27] P. Bernardi, V. Petronilli, F. Di Lisa, M. Forte, A mitochondrial perspective on cell death, Trends Biochem. Sci. 26 (2001) 112–117.
[28] A. Rasola, P. Bernardi, The mitochondrial permeability transition pore and its involvement in cell death and in disease pathogenesis, Apoptosis 12 (2007) 815–833.
[29] A. Rasola, M. Sciacovelli, B. Pantic, P. Bernardi, Signal transduction to the permeability transition pore, FEBS Lett. 584 (2010) 1989–1996.
[30] V. Giorgio, E. Bisetto, M.E. Soriano, F. Dabbeni-Sala, E. Basso, V. Petronilli, M.A. Forte, P. Bernardi, G. Lippe, Cyclophilin D modulates mitochondrial F0F1-ATP synthase by interacting with the lateral stalk of the complex, J. Biol. Chem. 284 (2009) 33982–33988.
[31] A.M. Porcelli, A. Angelin, A. Ghelli, E. Mariani, A. Martinuzzi, V. Carelli, V. Petronilli, P. Bernardi, M. Rugolo, Respiratory complex I dysfunction due to mitochondrial DNA mutations shifts the voltage threshold for opening of the permeability transition pore toward resting levels, J. Biol. Chem. 284 (2009) 2045–2052.
[32] D.R. Johns, M.J. Neufeld, R.D. Park, An ND-6 mitochondrial DNA mutation associated with Leber hereditary optic neuropathy, Biochem. Biophys. Res. Commun. 187 (1992) 1551–1557.
[33] S.I. Zhadanov, V.V. Atamanov, N.I. Zhadanov, O.V. Oleinikov, L.P. Osipova, T.G. Schurr, A novel mtDNA ND6 gene mutation associated with LHON in a Caucasian family, Biochem. Biophys. Res. Commun. 332 (2005) 1115–1121.

[34] A. Zielke, S. Tezelman, G.H. Jossart, M. Wong, A.E. Siperstein, Q.Y. Duh, O.H. Clark, Establishment of a highly differentiated thyroid cancer cell line of Hurthle cell origin, Thyroid 8 (1998) 475–483.
[35] E. Bonora, A.M. Porcelli, G. Gasparre, A. Biondi, A. Ghelli, V. Carelli, A. Baracca, G. Tallini, A. Martinuzzi, G. Lenaz, M. Rugolo, G. Romeo, Defective oxidative phosphorylation in thyroid oncocytic carcinoma is associated with pathogenic mitochondrial DNA mutations affecting complexes I and III, Cancer Res. 66 (2006) 6087–6096.
[36] O. Warburg, On the origin of cancer cells, Science 123 (1956) 309–314.
[37] P.P. Hsu, D.M. Sabatini, Cancer cell metabolism: Warburg and beyond, Cell 134 (2008) 703–707.
[38] C. Frezza, E. Gottlieb, Mitochondria in cancer: not just innocent bystanders, Semin. Cancer Biol. 19 (2009) 4–11.
[39] M. Brandon, P. Baldi, D.C. Wallace, Mitochondrial mutations in cancer, Oncogene 25 (2006) 4647–4662.
[40] P.H. Yin, H.C. Lee, G.Y. Chau, Y.T. Wu, S.H. Li, W.Y. Lui, Y.H. Wei, T.Y. Liu, C.W. Chi, Alteration of the copy number and deletion of mitochondrial DNA in human hepatocellular carcinoma, Br. J. Cancer 90 (2004) 2390–2396.
[41] Y. Wang, V.W. Liu, W.C. Xue, A.N. Cheung, H.Y. Ngan, Association of decreased mitochondrial DNA content with ovarian cancer progression, Br. J. Cancer 95 (2006) 1087–1091.
[42] M. Yu, Y. Zhou, Y. Shi, L. Ning, Y. Yang, X. Wei, N. Zhang, X. Hao, R. Niu, Reduced mitochondrial DNA copy number is correlated with tumor progression and prognosis in Chinese breast cancer patients, IUBMB Life 59 (2007) 450–457.
[43] R.L. Correia, S.M. Oba-Shinjo, M. Uno, N. Huang, S.K. Marie, Mitochondrial DNA depletion and its correlation with TFAM, TFB1M, TFB2M and POLG in human diffusely infiltrating astrocytomas, Mitochondrion 11 (2011) 48–53.
[44] H. Cheon, H.E. Moon, M.S. Lee, S.S. Kim, Loss of mitochondrial DNA enhances angiogenic and invasive potential of hepatoma cells, Oncol. Rep. 23 (2010) 779–786.
[45] K.K. Singh, V. Ayyasamy, K.M. Owens, M.S. Koul, M. Vujcic, Mutations in mitochondrial DNA polymerase-gamma promote breast tumorigenesis, J. Hum. Genet. 54 (2009) 516–524.
[46] A. Naito, J. Carcel-Trullols, C.H. Xie, T.T. Evans, T. Mizumachi, M. Higuchi, Induction of acquired resistance to antiestrogen by reversible mitochondrial DNA depletion in breast cancer cell line, Int. J. Cancer 122 (2008) 1506–1511.
[47] F. Chiara, D. Castellaro, O. Marin, V. Petronilli, W.S. Brusilow, M. Juhaszova, S.J. Sollott, M. Forte, P. Bernardi, A. Rasola, Hexokinase II detachment from mitochondria triggers apoptosis through the permeability transition pore independent of voltage-dependent anion channels, PLoS One 3 (2008) e1852.
[48] A. Rasola, M. Sciacovelli, F. Chiara, B. Pantic, W.S. Brusilow, P. Bernardi, Activation of mitochondrial ERK protects cancer cells from death through inhibition of the permeability transition, Proc. Natl. Acad. Sci. U. S. A. 107 (2010) 726–731.
[49] J. Traba, A. del Arco, M.R. Duchen, G. Szabadkai, J. Satrustegui, SCaMC-1 promotes cancer cell survival by desensitizing mitochondrial permeability transition via ATP/ADP-mediated matrix Ca2+ buffering, Cell Death Differ. 19 (2012) 650–660.
[50] P. Bernardi, L. Scorrano, R. Colonna, V. Petronilli, F. Di Lisa, Mitochondria and cell death. Mechanistic aspects and methodological issues, Eur. J. Biochem. 264 (1999) 687–701.
[51] A. Nicolli, E. Basso, V. Petronilli, R.M. Wenger, P. Bernardi, Interactions of cyclophilin with the mitochondrial inner membrane and regulation of the permeability transition pore, a cyclosporin A-sensitive channel, J. Biol. Chem. 271 (1996) 2185–2192.
[52] D.G. Nicholls, M.W. Ward, Mitochondrial membrane potential and neuronal glutamate excitotoxicity: mortality and millivolts, Trends Neurosci. 23 (2000) 166–174.
[53] S.P. Mathupala, Y.H. Ko, P.L. Pedersen, Hexokinase II: cancer's double-edged sword acting as both facilitator and gatekeeper of malignancy when bound to mitochondria, Oncogene 25 (2006) 4777–4786.
[54] P. Bernardi, A. Krauskopf, E. Basso, V. Petronilli, E. Blachly-Dyson, F. Di Lisa, M.A. Forte, The mitochondrial permeability transition from in vitro artifact to disease target, FEBS J. 273 (2006) 2077–2099.
[55] P. Bernardi, Modulation of the mitochondrial cyclosporin A-sensitive permeability transition pore by the proton electrochemical gradient. Evidence that the pore can be opened by membrane depolarization, J. Biol. Chem. 267 (1992) 8834–8839.
[56] J.G. Pastorino, N. Shulga, J.B. Hoek, Mitochondrial binding of hexokinase II inhibits Bax-induced cytochrome c release and apoptosis, J. Biol. Chem. 277 (2002) 7610–7618.

REFERENCES

Acin-Perez, R., Fernandez-Silva, P., Peleato, M.L., Perez-Martos, A., and Enriquez, J.A. (2008). Respiratory active mitochondrial supercomplexes. Mol. Cell *32,* 529-539.

Adam, J., Hatipoglu, E., O'Flaherty, L., Ternette, N., Sahgal, N., Lockstone, H., Baban, D., Nye, E., Stamp, G.W., Wolhuter, K.*, et al.* (2011). Renal cyst formation in Fh1-deficient mice is independent of the Hif/Phd pathway: roles for fumarate in KEAP1 succination and Nrf2 signaling. Cancer. Cell. *20,* 524-537.

Akerfelt, M., Morimoto, R.I., and Sistonen, L. (2010). Heat shock factors: integrators of cell stress, development and lifespan. Nat. Rev. Mol. Cell Biol. *11,* 545-555.

Aravind, L., Neuwald, A.F., and Ponting, C.P. (1999). Sec14p-like domains in NF1 and Dbl-like proteins indicate lipid regulation of Ras and Rho signaling. Curr. Biol. *9,* R195-7.

Ars, E., Serra, E., Garcia, J., Kruyer, H., Gaona, A., Lazaro, C., and Estivill, X. (2000). Mutations affecting mRNA splicing are the most common molecular defects in patients with neurofibromatosis type 1. Hum. Mol. Genet. *9,* 237-247.

Arun, V., Worrell, L., Wiley, J.C., Kaplan, D.R., and Guha, A. (2013). Neurofibromin interacts with the cytoplasmic Dynein Heavy Chain 1 in melanosomes of human melanocytes. FEBS Lett. *587,* 1466-1473.

Baines, C.P., Kaiser, R.A., Purcell, N.H., Blair, N.S., Osinska, H., Hambleton, M.A., Brunskill, E.W., Sayen, M.R., Gottlieb, R.A., Dorn, G.W., Robbins, J., and Molkentin, J.D. (2005). Loss of cyclophilin D reveals a critical role for mitochondrial permeability transition in cell death. Nature *434,* 658-662.

Ballester, R., Marchuk, D., Boguski, M., Saulino, A., Letcher, R., Wigler, M., and Collins, F. (1990). The NF1 locus encodes a protein functionally related to mammalian GAP and yeast IRA proteins. Cell *63,* 851-859.

Baracca, A., Chiaradonna, F., Sgarbi, G., Solaini, G., Alberghina, L., and Lenaz, G. (2010). Mitochondrial Complex I decrease is responsible for bioenergetic dysfunction in K-ras transformed cells. Biochim. Biophys. Acta *1797,* 314-323.

Bardella, C., Pollard, P.J., and Tomlinson, I. (2011). SDH mutations in cancer. Biochim. Biophys. Acta *1807,* 1432-1443.

Basso, E., Fante, L., Fowlkes, J., Petronilli, V., Forte, M.A., and Bernardi, P. (2005). Properties of the permeability transition pore in mitochondria devoid of Cyclophilin D. J. Biol. Chem. *280,* 18558-18561.

Baysal, B.E., Ferrell, R.E., Willett-Brozick, J.E., Lawrence, E.C., Myssiorek, D., Bosch, A., van der Mey, A., Taschner, P.E., Rubinstein, W.S., Myers, E.N*., et al.* (2000). Mutations in SDHD, a mitochondrial complex II gene, in hereditary paraganglioma. Science *287,* 848-851.

Bernardi, P. (2013). The mitochondrial permeability transition pore: a mystery solved? Front. Physiol. *4,* 95.

Bernardi, P., Krauskopf, A., Basso, E., Petronilli, V., Blachly-Dyson, E., Di Lisa, F., and Forte, M.A. (2006). The mitochondrial permeability transition from in vitro artifact to disease target. FEBS J. *273,* 2077-2099.

Bertout, J.A., Patel, S.A., and Simon, M.C. (2008). The impact of O2 availability on human cancer. Nat. Rev. Cancer. *8,* 967-975.

Boland, M.L., Chourasia, A.H., and Macleod, K.F. (2013). Mitochondrial Dysfunction in Cancer. Front. Oncol. *3,* 292.

Brandon, M., Baldi, P., and Wallace, D.C. (2006). Mitochondrial mutations in cancer. Oncogene *25,* 4647-4662.

Brannan, C.I., Perkins, A.S., Vogel, K.S., Ratner, N., Nordlund, M.L., Reid, S.W., Buchberg, A.M., Jenkins, N.A., Parada, L.F., and Copeland, N.G. (1994). Targeted disruption of the neurofibromatosis type-1 gene leads to developmental abnormalities in heart and various neural crest-derived tissues. Genes Dev. *8,* 1019-1029.

Briere, J.J., Favier, J., Benit, P., El Ghouzzi, V., Lorenzato, A., Rabier, D., Di Renzo, M.F., Gimenez-Roqueplo, A.P., and Rustin, P. (2005). Mitochondrial succinate is instrumental for HIF1alpha nuclear translocation in SDHA-mutant fibroblasts under normoxic conditions. Hum. Mol. Genet. *14,* 3263-3269.

Brossier, N.M., and Carroll, S.L. (2012). Genetically engineered mouse models shed new light on the pathogenesis of neurofibromatosis type I-related neoplasms of the peripheral nervous system. Brain Res. Bull. *88,* 58-71.

Buchet, K., and Godinot, C. (1998). Functional F1-ATPase essential in maintaining growth and membrane potential of human mitochondrial DNA-depleted rho degrees cells. J. Biol. Chem. *273,* 22983-22989.

Cairns, R.A., Harris, I.S., and Mak, T.W. (2011). Regulation of cancer cell metabolism. Nat. Rev. Cancer. *11,* 85-95.

Chiara, F., Castellaro, D., Marin, O., Petronilli, V., Brusilow, W.S., Juhaszova, M., Sollott, S.J., Forte, M., Bernardi, P., and Rasola, A. (2008). Hexokinase II detachment from mitochondria triggers apoptosis through the permeability transition pore independent of voltage-dependent anion channels. PLoS One *3,* e1852.

Chiara, F., Gambalunga, A., Sciacovelli, M., Nicolli, A., Ronconi, L., Fregona, D., Bernardi, P., Rasola, A., and Trevisan, A. (2012). Chemotherapeutic induction of mitochondrial oxidative stress activates GSK-3alpha/beta and Bax, leading to permeability transition pore opening and tumor cell death. Cell. Death Dis. *3,* e444.

Chiara, F., and Rasola, A. (2013). GSK-3 and mitochondria in cancer cells. Front. Oncol. *3,* 16.

Chiaradonna, F., Gaglio, D., Vanoni, M., and Alberghina, L. (2006). Expression of transforming K-Ras oncogene affects mitochondrial function and morphology in mouse fibroblasts. Biochim. Biophys. Acta *1757,* 1338-1356.

Chiaradonna, F., Sacco, E., Manzoni, R., Giorgio, M., Vanoni, M., and Alberghina, L. (2006). Ras-dependent carbon metabolism and transformation in mouse fibroblasts. Oncogene *25,* 5391-5404.

Chomyn, A., and Attardi, G. (2003). MtDNA mutations in aging and apoptosis. Biochem. Biophys. Res. Commun. *304,* 519-529.

Christofk, H.R., Vander Heiden, M.G., Harris, M.H., Ramanathan, A., Gerszten, R.E., Wei, R., Fleming, M.D., Schreiber, S.L., and Cantley, L.C. (2008). The M2 splice isoform of pyruvate kinase is important for cancer metabolism and tumour growth. Nature *452,* 230-233.

Cichowski, K., and Jacks, T. (2001). NF1 tumor suppressor gene function: narrowing the GAP. Cell *104,* 593-604.

Cichowski, K., Santiago, S., Jardim, M., Johnson, B.W., and Jacks, T. (2003). Dynamic regulation of the Ras pathway via proteolysis of the NF1 tumor suppressor. Genes Dev. *17,* 449-454.

Ciscato, F., Sciacovelli, M., Villano, G., Turato, C., Bernardi, P., Rasola, A., & Pontisso, P. (2013). SERPINB3 protects from oxidative damage by chemotherapeutics through inhibition of mitochondrial respiratory Complex I. Oncotarget, 4(9).

Costa, R.M., Federov, N.B., Kogan, J.H., Murphy, G.G., Stern, J., Ohno, M., Kucherlapati, R., Jacks, T., and Silva, A.J. (2002). Mechanism for the learning deficits in a mouse model of neurofibromatosis type 1. Nature *415,* 526-530.

Costantino, E., Maddalena, F., Calise, S., Piscazzi, A., Tirino, V., Fersini, A., Ambrosi, A., Neri, V., Esposito, F., and Landriscina, M. (2009). TRAP1, a novel mitochondrial chaperone responsible for multi-drug resistance and protection from apoptotis in human colorectal carcinoma cells. Cancer Lett. *279,* 39-46.

Crabtree, H.G. (1928). The carbohydrate metabolism of certain pathological overgrowths. Biochem. J. *22,* 1289-1298.

Dang, C.V., Le, A., and Gao, P. (2009). MYC-induced cancer cell energy metabolism and therapeutic opportunities. Clin. Cancer Res. *15,* 6479-6483.

Dang, L., White, D.W., Gross, S., Bennett, B.D., Bittinger, M.A., Driggers, E.M., Fantin, V.R., Jang, H.G., Jin, S., Keenan, M.C*., et al.* (2009). Cancer-associated IDH1 mutations produce 2-hydroxyglutarate. Nature *462,* 739-744.

Daston, M.M., Scrable, H., Nordlund, M., Sturbaum, A.K., Nissen, L.M., and Ratner, N. (1992). The protein product of the neurofibromatosis type 1 gene is expressed at highest abundance in neurons, Schwann cells, and oligodendrocytes. Neuron *8,* 415-428.

DeBerardinis, R.J., Mancuso, A., Daikhin, E., Nissim, I., Yudkoff, M., Wehrli, S., and Thompson, C.B. (2007). Beyond aerobic glycolysis: transformed cells can engage in glutamine metabolism that exceeds the requirement for protein and nucleotide synthesis. Proc. Natl. Acad. Sci. U. S. A. *104,* 19345-19350.

Deberardinis, R.J., Sayed, N., Ditsworth, D., and Thompson, C.B. (2008). Brick by brick: metabolism and tumor cell growth. Curr. Opin. Genet. Dev. *18,* 54-61.

Dilworth, J.T., Kraniak, J.M., Wojtkowiak, J.W., Gibbs, R.A., Borch, R.F., Tainsky, M.A., Reiners, J.J.,Jr, and Mattingly, R.R. (2006). Molecular targets for emerging anti-tumor therapies for neurofibromatosis type 1. Biochem. Pharmacol. *72,* 1485-1492.

Downward, J. (2003). Targeting RAS signalling pathways in cancer therapy. Nat. Rev. Cancer. *3,* 11-22.

Elgendy, M., Sheridan, C., Brumatti, G., and Martin, S.J. (2011). Oncogenic Ras-induced expression of Noxa and Beclin-1 promotes autophagic cell death and limits clonogenic survival. Mol. Cell *42,* 23-35.

Frezza, C. (2014). The role of mitochondria in the oncogenic signal transduction. Int. J. Biochem. Cell Biol. *48C,* 11-17.

Frezza, C., and Gottlieb, E. (2009). Mitochondria in cancer: not just innocent bystanders. Semin. Cancer Biol. *19,* 4-11.

Frezza, C., Zheng, L., Folger, O., Rajagopalan, K.N., MacKenzie, E.D., Jerby, L., Micaroni, M., Chaneton, B., Adam, J., Hedley, A*., et al.* (2011). Haem oxygenase is synthetically lethal with the tumour suppressor fumarate hydratase. Nature *477,* 225-228.

Gaglio, D., Metallo, C.M., Gameiro, P.A., Hiller, K., Danna, L.S., Balestrieri, C., Alberghina, L., Stephanopoulos, G., and Chiaradonna, F. (2011). Oncogenic K-Ras decouples glucose and glutamine metabolism to support cancer cell growth. Mol. Syst. Biol. *7,* 523.

Giorgio, V., von Stockum, S., Antoniel, M., Fabbro, A., Fogolari, F., Forte, M., Glick, G.D., Petronilli, V., Zoratti, M., Szabo, I., Lippe, G., and Bernardi, P. (2013). Dimers of mitochondrial ATP synthase form the permeability transition pore. Proc. Natl. Acad. Sci. U. S. A. *110,* 5887-5892.

Gottfried, O.N., Viskochil, D.H., Fults, D.W., and Couldwell, W.T. (2006). Molecular, genetic, and cellular pathogenesis of neurofibromas and surgical implications. Neurosurgery *58,* 1-16; discussion 1-16.

Guertin, D.A., and Sabatini, D.M. (2007). Defining the role of mTOR in cancer. Cancer. Cell. *12,* 9-22.

Guo, H.F., The, I., Hannan, F., Bernards, A., and Zhong, Y. (1997). Requirement of Drosophila NF1 for activation of adenylyl cyclase by PACAP38-like neuropeptides. Science *276,* 795-798.

Guo, H.F., Tong, J., Hannan, F., Luo, L., and Zhong, Y. (2000). A neurofibromatosis-1-regulated pathway is required for learning in Drosophila. Nature *403,* 895-898.

Guo, J.Y., Chen, H.Y., Mathew, R., Fan, J., Strohecker, A.M., Karsli-Uzunbas, G., Kamphorst, J.J., Chen, G., Lemons, J.M., Karantza, V*., et al.* (2011). Activated Ras requires autophagy to maintain oxidative metabolism and tumorigenesis. Genes Dev. *25,* 460-470.

Gutmann, D.H., Aylsworth, A., Carey, J.C., Korf, B., Marks, J., Pyeritz, R.E., Rubenstein, A., and Viskochil, D. (1997). The diagnostic evaluation and multidisciplinary management of neurofibromatosis 1 and neurofibromatosis 2. JAMA *278,* 51-57.

Gutmann, D.H., Geist, R.T., Wright, D.E., and Snider, W.D. (1995). Expression of the neurofibromatosis 1 (NF1) isoforms in developing and adult rat tissues. Cell Growth Differ. *6,* 315-323.

Gutmann, D.H., Wood, D.L., and Collins, F.S. (1991). Identification of the neurofibromatosis type 1 gene product. Proc. Natl. Acad. Sci. U. S. A. *88,* 9658-9662.

Hanahan, D., and Weinberg, R.A. (2011). Hallmarks of cancer: the next generation. Cell *144,* 646-674.

Hanahan, D., and Weinberg, R.A. (2000). The hallmarks of cancer. Cell *100,* 57-70.

Hiatt, K.K., Ingram, D.A., Zhang, Y., Bollag, G., and Clapp, D.W. (2001). Neurofibromin GTPase-activating protein-related domains restore normal growth in Nf1-/- cells. J. Biol. Chem. *276,* 7240-7245.

Hollstein, P.E., and Cichowski, K. (2013). Identifying the Ubiquitin Ligase complex that regulates the NF1 tumor suppressor and Ras. Cancer. Discov. *3,* 880-893.

Horton, T.M., Petros, J.A., Heddi, A., Shoffner, J., Kaufman, A.E., Graham, S.D.,Jr, Gramlich, T., and Wallace, D.C. (1996). Novel mitochondrial DNA deletion found in a renal cell carcinoma. Genes Chromosomes Cancer *15,* 95-101.

Hu, Y., Lu, W., Chen, G., Wang, P., Chen, Z., Zhou, Y., Ogasawara, M., Trachootham, D., Feng, L., Pelicano, H*., et al.* (2012). K-ras(G12V) transformation leads to mitochondrial dysfunction and a metabolic switch from oxidative phosphorylation to glycolysis. Cell Res. *22,* 399-412.

Hunter, T. (1997). Oncoprotein networks. Cell *88,* 333-346.

Ishii, T., Yasuda, K., Akatsuka, A., Hino, O., Hartman, P.S., and Ishii, N. (2005). A mutation in the SDHC gene of complex II increases oxidative stress, resulting in apoptosis and tumorigenesis. Cancer Res. *65,* 203-209.

Jacks, T., Shih, T.S., Schmitt, E.M., Bronson, R.T., Bernards, A., and Weinberg, R.A. (1994). Tumour predisposition in mice heterozygous for a targeted mutation in Nf1. Nat. Genet. *7,* 353-361.

Jacobson, M.D., Burne, J.F., King, M.P., Miyashita, T., Reed, J.C., and Raff, M.C. (1993). Bcl-2 blocks apoptosis in cells lacking mitochondrial DNA. Nature *361,* 365-369.

Jiang, S., Cai, J., Wallace, D.C., and Jones, D.P. (1999). Cytochrome c-mediated apoptosis in cells lacking mitochondrial DNA. Signaling pathway involving release and caspase 3 activation is conserved. J. Biol. Chem. *274,* 29905-29911.

Jones, R.G., and Thompson, C.B. (2009). Tumor suppressors and cell metabolism: a recipe for cancer growth. Genes Dev. *23,* 537-548.

Jope, R.S., and Johnson, G.V. (2004). The glamour and gloom of glycogen synthase kinase-3. Trends Biochem. Sci. *29,* 95-102.

Joseph, N.M., Mosher, J.T., Buchstaller, J., Snider, P., McKeever, P.E., Lim, M., Conway, S.J., Parada, L.F., Zhu, Y., and Morrison, S.J. (2008). The loss of Nf1 transiently promotes self-renewal but not tumorigenesis by neural crest stem cells. Cancer. Cell. *13,* 129-140.

Joseph, N.M., Mukouyama, Y.S., Mosher, J.T., Jaegle, M., Crone, S.A., Dormand, E.L., Lee, K.F., Meijer, D., Anderson, D.J., and Morrison, S.J. (2004). Neural crest stem cells undergo multilineage differentiation in developing peripheral nerves to generate endoneurial fibroblasts in addition to Schwann cells. Development *131,* 5599-5612.

Kang, B.H., and Altieri, D.C. (2009). Compartmentalized cancer drug discovery targeting mitochondrial Hsp90 chaperones. Oncogene *28,* 3681-3688.

Kang, B.H., Plescia, J., Dohi, T., Rosa, J., Doxsey, S.J., and Altieri, D.C. (2007). Regulation of tumor cell mitochondrial homeostasis by an organelle-specific Hsp90 chaperone network. Cell *131,* 257-270.

Karnoub, A.E., and Weinberg, R.A. (2008). Ras oncogenes: split personalities. Nat. Rev. Mol. Cell Biol. *9,* 517-531.

Kim, H.A., Ling, B., and Ratner, N. (1997). Nf1-deficient mouse Schwann cells are angiogenic and invasive and can be induced to hyperproliferate: reversion of some phenotypes by an inhibitor of farnesyl protein transferase. Mol. Cell. Biol. *17,* 862-872.

Kim, I., and He, Y.Y. (2013). Targeting the AMP-Activated Protein Kinase for Cancer Prevention and Therapy. Front. Oncol. *3,* 175.

Kim, J.W., Tchernyshyov, I., Semenza, G.L., and Dang, C.V. (2006). HIF-1-mediated expression of pyruvate dehydrogenase kinase: a metabolic switch required for cellular adaptation to hypoxia. Cell. Metab. *3,* 177-185.

King, M.P., and Attardi, G. (1996). Isolation of human cell lines lacking mitochondrial DNA. Methods Enzymol. *264,* 304-313.

Knight, Z.A., Lin, H., and Shokat, K.M. (2010). Targeting the cancer kinome through polypharmacology. Nat. Rev. Cancer. *10,* 130-137.

Knudson, A.G. (2002). Cancer genetics. Am. J. Med. Genet. *111,* 96-102.

Koppenol, W.H., Bounds, P.L., and Dang, C.V. (2011). Otto Warburg's contributions to current concepts of cancer metabolism. Nat. Rev. Cancer. *11,* 325-337.

Kwong, J.Q., Henning, M.S., Starkov, A.A., and Manfredi, G. (2007). The mitochondrial respiratory chain is a modulator of apoptosis. J. Cell Biol. *179,* 1163-1177.

Le, L.Q., and Parada, L.F. (2007). Tumor microenvironment and neurofibromatosis type I: connecting the GAPs. Oncogene *26,* 4609-4616.

Le, L.Q., Shipman, T., Burns, D.K., and Parada, L.F. (2009). Cell of origin and microenvironment contribution for NF1-associated dermal neurofibromas. Cell. Stem Cell. *4,* 453-463.

Lemarie, A., and Grimm, S. (2011). Mitochondrial respiratory chain complexes: apoptosis sensors mutated in cancer? Oncogene *30,* 3985-4003.

Li, W., Cui, Y., Kushner, S.A., Brown, R.A., Jentsch, J.D., Frankland, P.W., Cannon, T.D., and Silva, A.J. (2005). The HMG-CoA reductase inhibitor lovastatin reverses the learning and attention deficits in a mouse model of neurofibromatosis type 1. Curr. Biol. *15,* 1961-1967.

Lunt, S.Y., and Vander Heiden, M.G. (2011). Aerobic glycolysis: meeting the metabolic requirements of cell proliferation. Annu. Rev. Cell Dev. Biol. *27,* 441-464.

Majewski, N., Nogueira, V., Bhaskar, P., Coy, P.E., Skeen, J.E., Gottlob, K., Chandel, N.S., Thompson, C.B., Robey, R.B., and Hay, N. (2004). Hexokinase-mitochondria interaction mediated

by Akt is required to inhibit apoptosis in the presence or absence of Bax and Bak. Mol. Cell *16,* 819-830.

Malumbres, M., and Barbacid, M. (2003). RAS oncogenes: the first 30 years. Nat. Rev. Cancer. *3,* 459-465.

Mangoura, D., Sun, Y., Li, C., Singh, D., Gutmann, D.H., Flores, A., Ahmed, M., and Vallianatos, G. (2006). Phosphorylation of neurofibromin by PKC is a possible molecular switch in EGF receptor signaling in neural cells. Oncogene *25,* 735-745.

Mathupala, S.P., Ko, Y.H., and Pedersen, P.L. (2006). Hexokinase II: cancer's double-edged sword acting as both facilitator and gatekeeper of malignancy when bound to mitochondria. Oncogene *25,* 4777-4786.

McCubrey, J.A., Steelman, L.S., Chappell, W.H., Abrams, S.L., Wong, E.W., Chang, F., Lehmann, B., Terrian, D.M., Milella, M., Tafuri, A*., et al.* (2007). Roles of the Raf/MEK/ERK pathway in cell growth, malignant transformation and drug resistance. Biochim. Biophys. Acta *1773,* 1263-1284.

Mirsky, R., Woodhoo, A., Parkinson, D.B., Arthur-Farraj, P., Bhaskaran, A., and Jessen, K.R. (2008). Novel signals controlling embryonic Schwann cell development, myelination and dedifferentiation. J. Peripher. Nerv. Syst. *13,* 122-135.

Muir, D., Neubauer, D., Lim, I.T., Yachnis, A.T., and Wallace, M.R. (2001). Tumorigenic properties of neurofibromin-deficient neurofibroma Schwann cells. Am. J. Pathol. *158,* 501-513.

Onnis, B., Rapisarda, A., and Melillo, G. (2009). Development of HIF-1 inhibitors for cancer therapy. J. Cell. Mol. Med. *13,* 2780-2786.

Papandreou, I., Cairns, R.A., Fontana, L., Lim, A.L., and Denko, N.C. (2006). HIF-1 mediates adaptation to hypoxia by actively downregulating mitochondrial oxygen consumption. Cell. Metab. *3,* 187-197.

Parrinello, S., and Lloyd, A.C. (2009). Neurofibroma development in NF1--insights into tumour initiation. Trends Cell Biol. *19,* 395-403.

Pollard, P.J., Briere, J.J., Alam, N.A., Barwell, J., Barclay, E., Wortham, N.C., Hunt, T., Mitchell, M., Olpin, S., Moat, S.J*., et al.* (2005). Accumulation of Krebs cycle intermediates and over-expression of HIF1alpha in tumours which result from germline FH and SDH mutations. Hum. Mol. Genet. *14,* 2231-2239.

Porcelli, A.M., Angelin, A., Ghelli, A., Mariani, E., Martinuzzi, A., Carelli, V., Petronilli, V., Bernardi, P., and Rugolo, M. (2009). Respiratory complex I dysfunction due to mitochondrial DNA mutations shifts the voltage threshold for opening of the permeability transition pore toward resting levels. J. Biol. Chem. *284,* 2045-2052.

Pridgeon, J.W., Olzmann, J.A., Chin, L.S., and Li, L. (2007). PINK1 protects against oxidative stress by phosphorylating mitochondrial chaperone TRAP1. PLoS Biol. *5,* e172.

Rasola, A., and Bernardi, P. (2007). The mitochondrial permeability transition pore and its involvement in cell death and in disease pathogenesis. Apoptosis *12,* 815-833.

Rasola, A., Sciacovelli, M., Chiara, F., Pantic, B., Brusilow, W.S., and Bernardi, P. (2010). Activation of mitochondrial ERK protects cancer cells from death through inhibition of the permeability transition. Proc. Natl. Acad. Sci. U. S. A. *107,* 726-731.

Rasola, A., Sciacovelli, M., Pantic, B., and Bernardi, P. (2010). Signal transduction to the permeability transition pore. FEBS Lett. *584,* 1989-1996.

Robey, R.B., and Hay, N. (2009). Is Akt the "Warburg kinase"?-Akt-energy metabolism interactions and oncogenesis. Semin. Cancer Biol. *19,* 25-31.

Schaap, F.G., French, P.J., and Bovee, J.V. (2013). Mutations in the isocitrate dehydrogenase genes IDH1 and IDH2 in tumors. Adv. Anat. Pathol. *20,* 32-38.

Schubbert, S., Shannon, K., and Bollag, G. (2007). Hyperactive Ras in developmental disorders and cancer. Nat. Rev. Cancer. *7,* 295-308.

Schubert, A., and Grimm, S. (2004). Cyclophilin D, a component of the permeability transition-pore, is an apoptosis repressor. Cancer Res. *64,* 85-93.

Sciacovelli, M., Guzzo, G., Morello, V., Frezza, C., Zheng, L., Nannini, N., Calabrese, F., Laudiero, G., Esposito, F., Landriscina, M.*, et al.* (2013). The mitochondrial chaperone TRAP1 promotes neoplastic growth by inhibiting succinate dehydrogenase. Cell. Metab. *17,* 988-999.

Selak, M.A., Armour, S.M., MacKenzie, E.D., Boulahbel, H., Watson, D.G., Mansfield, K.D., Pan, Y., Simon, M.C., Thompson, C.B., and Gottlieb, E. (2005). Succinate links TCA cycle dysfunction to oncogenesis by inhibiting HIF-alpha prolyl hydroxylase. Cancer. Cell. *7,* 77-85.

Semenza, G.L. (2010). HIF-1: upstream and downstream of cancer metabolism. Curr. Opin. Genet. Dev. *20,* 51-56.

Shackelford, D.B., and Shaw, R.J. (2009). The LKB1-AMPK pathway: metabolism and growth control in tumour suppression. Nat. Rev. Cancer. *9,* 563-575.

Shakya, A., Cooksey, R., Cox, J.E., Wang, V., McClain, D.A., and Tantin, D. (2009). Oct1 loss of function induces a coordinate metabolic shift that opposes tumorigenicity. Nat. Cell Biol. *11,* 320-327.

Shapira, S., Barkan, B., Friedman, E., Kloog, Y., and Stein, R. (2007). The tumor suppressor neurofibromin confers sensitivity to apoptosis by Ras-dependent and Ras-independent pathways. Cell Death Differ. *14,* 895-906.

Shaw, R.J., and Cantley, L.C. (2006). Ras, PI(3)K and mTOR signalling controls tumour cell growth. Nature *441,* 424-430.

Shulga, N., Wilson-Smith, R., and Pastorino, J.G. (2010). Sirtuin-3 deacetylation of cyclophilin D induces dissociation of hexokinase II from the mitochondria. J. Cell. Sci. *123,* 894-902.

Solaini, G., Sgarbi, G., and Baracca, A. (2011). Oxidative phosphorylation in cancer cells. Biochim. Biophys. Acta *1807,* 534-542.

Tait, S.W., and Green, D.R. (2010). Mitochondria and cell death: outer membrane permeabilization and beyond. Nat. Rev. Mol. Cell Biol. *11,* 621-632.

Tennant, D.A., Duran, R.V., Boulahbel, H., and Gottlieb, E. (2009). Metabolic transformation in cancer. Carcinogenesis *30,* 1269-1280.

Tennant, D.A., Duran, R.V., and Gottlieb, E. (2010). Targeting metabolic transformation for cancer therapy. Nat. Rev. Cancer. *10,* 267-277.

The, I., Hannigan, G.E., Cowley, G.S., Reginald, S., Zhong, Y., Gusella, J.F., Hariharan, I.K., and Bernards, A. (1997). Rescue of a Drosophila NF1 mutant phenotype by protein kinase A. Science *276,* 791-794.

Tomlinson, I.P., Alam, N.A., Rowan, A.J., Barclay, E., Jaeger, E.E., Kelsell, D., Leigh, I., Gorman, P., Lamlum, H., Rahman, S*., et al.* (2002). Germline mutations in FH predispose to dominantly inherited uterine fibroids, skin leiomyomata and papillary renal cell cancer. Nat. Genet. *30,* 406-410.

Tong, J., Hannan, F., Zhu, Y., Bernards, A., and Zhong, Y. (2002). Neurofibromin regulates G protein-stimulated adenylyl cyclase activity. Nat. Neurosci. *5,* 95-96.

Trovo-Marqui, A.B., and Tajara, E.H. (2006). Neurofibromin: a general outlook. Clin. Genet. *70,* 1-13.

Ulivieri, C. (2010). Cell death: insights into the ultrastructure of mitochondria. Tissue Cell *42,* 339-347.

Vandenbroucke, I., Van Oostveldt, P., Coene, E., De Paepe, A., and Messiaen, L. (2004). Neurofibromin is actively transported to the nucleus. FEBS Lett. *560,* 98-102.

Vander Heiden, M.G., Cantley, L.C., and Thompson, C.B. (2009). Understanding the Warburg effect: the metabolic requirements of cell proliferation. Science *324,* 1029-1033.

Viskochil, D.H. (2003). It takes two to tango: mast cell and Schwann cell interactions in neurofibromas. J. Clin. Invest. *112,* 1791-1793.

Vousden, K.H., and Ryan, K.M. (2009). P53 and Metabolism. Nat. Rev. Cancer. *9,* 691-700.

Wallace, D.C. (2012). Mitochondria and cancer. Nat. Rev. Cancer. *12,* 685-698.

Wallace, M.R., Marchuk, D.A., Andersen, L.B., Letcher, R., Odeh, H.M., Saulino, A.M., Fountain, J.W., Brereton, A., Nicholson, J., and Mitchell, A.L. (1990). Type 1 neurofibromatosis gene: identification of a large transcript disrupted in three NF1 patients. Science *249,* 181-186.

Wang, W., and Guan, K.L. (2009). AMP-activated protein kinase and cancer. Acta Physiol. (Oxf) *196,* 55-63.

WARBURG, O. (1956). On respiratory impairment in cancer cells. Science *124,* 269-270.

WARBURG, O. (1956). On the origin of cancer cells. Science *123,* 309-314.

Warburg, O., Wind, F., and Negelein, E. (1927). The Metabolism of Tumors in the Body. J. Gen. Physiol. *8,* 519-530.

Ward, P.S., Patel, J., Wise, D.R., Abdel-Wahab, O., Bennett, B.D., Coller, H.A., Cross, J.R., Fantin, V.R., Hedvat, C.V., Perl, A.E*., et al.* (2010). The common feature of leukemia-associated IDH1 and IDH2 mutations is a neomorphic enzyme activity converting alpha-ketoglutarate to 2-hydroxyglutarate. Cancer. Cell. *17,* 225-234.

Ward, P.S., and Thompson, C.B. (2012). Metabolic reprogramming: a cancer hallmark even warburg did not anticipate. Cancer. Cell. *21,* 297-308.

Wittig, I., and Schagger, H. (2008). Features and applications of blue-native and clear-native electrophoresis. Proteomics *8,* 3974-3990.

Wong, K.K., Engelman, J.A., and Cantley, L.C. (2010). Targeting the PI3K signaling pathway in cancer. Curr. Opin. Genet. Dev. *20,* 87-90.

Wu, J., Williams, J.P., Rizvi, T.A., Kordich, J.J., Witte, D., Meijer, D., Stemmer-Rachamimov, A.O., Cancelas, J.A., and Ratner, N. (2008). Plexiform and dermal neurofibromas and pigmentation are caused by Nf1 loss in desert hedgehog-expressing cells. Cancer. Cell. *13,* 105-116.

Wu, M., Wallace, M.R., and Muir, D. (2005). Tumorigenic properties of neurofibromin-deficient Schwann cells in culture and as syngrafts in Nf1 knockout mice. J. Neurosci. Res. *82,* 357-367.

Xu, G.F., O'Connell, P., Viskochil, D., Cawthon, R., Robertson, M., Culver, M., Dunn, D., Stevens, J., Gesteland, R., and White, R. (1990). The neurofibromatosis type 1 gene encodes a protein related to GAP. Cell *62,* 599-608.

Xu, H., and Gutmann, D.H. (1997). Mutations in the GAP-related domain impair the ability of neurofibromin to associate with microtubules. Brain Res. *759,* 149-152.

Yang, F.C., Ingram, D.A., Chen, S., Zhu, Y., Yuan, J., Li, X., Yang, X., Knowles, S., Horn, W., Li, Y.*, et al.* (2008). Nf1-dependent tumors require a microenvironment containing Nf1+/-- and c-kit-dependent bone marrow. Cell *135,* 437-448.

Yang, M., Soga, T., and Pollard, P.J. (2013). Oncometabolites: linking altered metabolism with cancer. J. Clin. Invest. *123,* 3652-3658.

Yang, W., Zheng, Y., Xia, Y., Ji, H., Chen, X., Guo, F., Lyssiotis, C.A., Aldape, K., Cantley, L.C., and Lu, Z. (2012). ERK1/2-dependent phosphorylation and nuclear translocation of PKM2 promotes the Warburg effect. Nat. Cell Biol. *14,* 1295-1304.

Ying, H., Kimmelman, A.C., Lyssiotis, C.A., Hua, S., Chu, G.C., Fletcher-Sananikone, E., Locasale, J.W., Son, J., Zhang, H., Coloff, J.L.*, et al.* (2012). Oncogenic Kras maintains pancreatic tumors through regulation of anabolic glucose metabolism. Cell *149,* 656-670.

Zhang, J., Yang, P.L., and Gray, N.S. (2009). Targeting cancer with small molecule kinase inhibitors. Nat. Rev. Cancer. *9,* 28-39.

Zheng, H., Chang, L., Patel, N., Yang, J., Lowe, L., Burns, D.K., and Zhu, Y. (2008). Induction of abnormal proliferation by nonmyelinating schwann cells triggers neurofibroma formation. Cancer. Cell. *13,* 117-128.

Zhu, Y., Ghosh, P., Charnay, P., Burns, D.K., and Parada, L.F. (2002). Neurofibromas in NF1: Schwann cell origin and role of tumor environment. Science *296,* 920-922.